Int J Cardiovasc Imaging (2022) 38:2513–2579
https://doi.org/10.1007/s10554-022-02733-6

ABSTRACT

# ESCR Abstracts 2022

Published online: 28 October 2022


## A-109

### Reproducibility of radiomics features extracted from late gadolinium enhancement imaging in patients with acute myocarditis

C. Monti[1], D. Capra[1], M. Zanardo[1], G. Lastella[2], F. Sardanelli[1,3], F. Secchi[1,3]

[1]Università degli Studi di Milano, Dipartimento di Scienze Biomediche per la Salute, Milano, Italy, [2]ASST Nord Milano, Milano, Italy, [3]IRCCS Policlinico San Donato, San Donato Milanese, Italy.

**Purpose/Objectives** To review the inter-reader reproducibility of various radiomics features extracted from late gadolinium enhancement (LGE) sequences at cardiac magnetic resonance (CMR) in patients with acute myocarditis.

**Methods & Materials** We retrospectively included all patients with acute myocarditis who underwent CMR at our institution between March 2014 and December 2020. From each CMR examination two readers segmented the epicardium and endocardium of the left ventricle on all short-axis slices from LGE sequences. Afterwards we performed a radiomics extraction from 5 individual classes using 7 image filters, totalling 1320 individual features. Features were deemed reproducible when their inter-reader intra-class correlation coefficient (ICC) was $\geq 0.8$. Data were reported as median and interquartile range (IQR).

**Results** Our final study population counted 66 patients with acute myocarditis, with a median age of 28 years (IQR 20–44 years), 56 (85%) of whom were males. Patients' median left ventricular ejection fraction was 67% (IQR 37–67%). Out of 1320 features, 820 appeared reproducible, with an ICC $\geq 0.8$. The most reproducible features were the minimums of the original image and the logarithm and square root filtered image (all ICC = 0.99), whereas the least reproducible features were the grey level non uniformity of the exponential and gradient filtered image (both ICC = 0.00). Overall, features extracted from the original image showed the highest ICC, with a median of 0.91 (IQR 0.86–0.95), whereas features extracted from the exponential filtered image yielded the lowest ICC with a median of 0.82 (IQR 0.74–0.89).

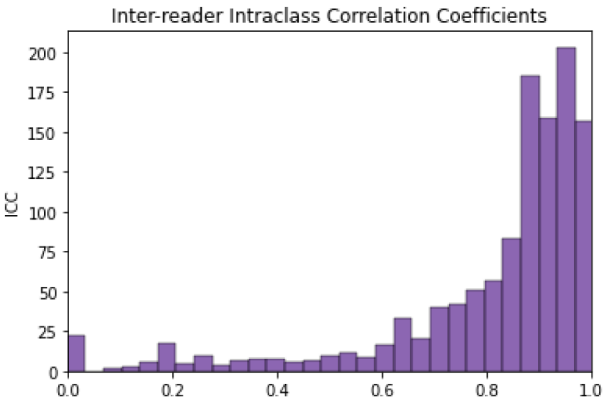

Inter-reader intraclass correlation coefficients for different radiomics features

**Conclusion** A considerable number of radiomics feature extracted from LGE sequences in patients with acute myocarditis could be used for further clinical models, as they present with a satisfactory reproducibility. Radiomics analyses on LGE imaging may offer a potential source of novel insight for the assessment of patients with acute myocarditis.

## A-110

### Associations between left atrial volumetric and blood flow-parameters: the multi-ethnic study of atherosclerosis

M. Pradella[1,2], J. J. Baraboo[1], A. Maroun[1], S. Z. Liu[1], A. L. DiCarlo[1], R. Passman[3,4], S. R. Heckbert[5], P. Greenland[3,4], M. Markl[1]

[1]Northwestern University, Department of Radiology, Chicago, United States of America, [2]University Hospital Basel, Department of Radiology, Basel, Switzerland, [3]Northwestern University, Department of Medicine, Division of Cardiology, Chicago, United States of America, [4]Northwestern University, Department of Preventive Medicine,

Chicago, United States of America, [5]University of Washington, Department of Epidemiology, Seattle, United States of America.

**Purpose/Objectives** Imaging of the left atrium (LA) identified associations of LA volume (LAV) and function with stroke and outcome after myocardial infarction (1,2). LAV including maximum and minimum LAV ($LAV_{max}$, $LAV_{min}$) as well as LA emptying fractions (LAEF) can be measured on time-resolved (CINE) MRI. Ideally, these measurements are performed on short axis (SAX) planes covering the whole LA allowing 3D-based assessment.
4D-flow MRI enables measurements of LA hemodynamics and has the ability to characterize LA myopathy. Higher stasis and lower peak velocity are thereby hypothesized to be associated with thrombus formation (3). The associations between LAV, function and 3D blood flow dynamics have not been systematically investigated in a general population cohort. The aim of this study was to investigate these associations in the Multi-Ethnic Study of Atherosclerosis (MESA), a study of middle-age and older adults in the USA free of clinically-recognized cardiovascular disease at enrollment in 2000–2002.
**Methods & Materials** Participants underwent 1.5 T MRI in 2018–2020 including 4D-flow and CINE imaging. Retrospectively ECG-gated, free breathing 4D-flow MRI with full coverage of the heart was acquired in coronal orientation. After data pre-processing, a radiologist segmented LA and LA appendage (LAA) on 3D phase-contrast MRA derived from 4D-flow MRI. Those were used to calculate parametric maps of peak velocity and mean blood stasis (%voxels < 0.1 m/s) for both LA and LAA.

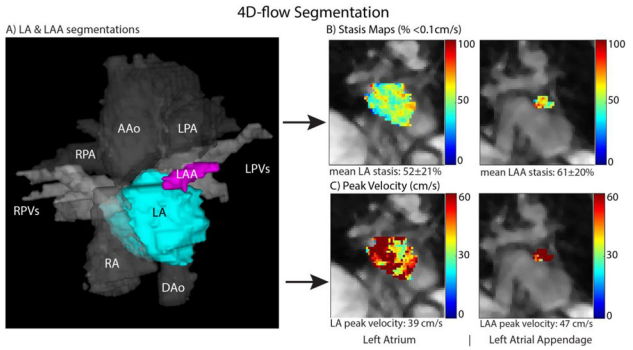


**Fig. 1** After pre-processing the 4D-flow data, (A) left atrium (LA) and LA appendage (LAA) were segmented on phase-contrast magnetic resonance angiographies excluding the pulmonary veins. These segmentations were used to calculate parametric maps for stasis (B) and peak velocity (C) in the LA and LAA

**Table 1** Correlations for the four 4D-flow parameters with the volumetric and functional LA and LV parameters. * = $p < 0.05$, ** = $p < 0.01$, *** = $p < 0.001$.

| Pearson correlation | LA stasis | LA peak velocity | LAA stasis | LAA peak velocity |
|---|---|---|---|---|
| $LAEF_{total}$ | **-0.53*** ** | **0.56*** ** | -0.37*** | 0.46*** |
| $LAEF_{active}$ | -0.41*** | 0.50*** | -0.22** | 0.38*** |
| $LAEF_{passive}$ | -0.20* | 0.12 | -0.18* | 0.12 |
| $LAV_{max}$ | 0.14 | -0.22** | 0.18* | -0.36*** |
| $LAV_{min}$ | 0.39*** | -0.46*** | 0.36** | -0.56*** |
| $LAV_{preA}$ | 0.13 | -0.16* | 0.16* | -0.32*** |
| $LAVI_{max}$ | 0.27*** | -0.32*** | 0.32*** | -0.44*** |
| $LAVI_{min}$ | 0.45*** | -0.51*** | **0.43*** ** | **-0.59*** ** |
| $LAVI_{preA}$ | 0.23** | -0.24** | 0.29** | -0.39*** |
| LV_EDVi | -0.23** | 0.14 | -0.14 | 0.00 |
| LV_ESVi | -0.12 | 0.04 | -0.07 | -0.07 |
| LV_SVi | -0.24** | 0.18* | -0.15 | 0.05 |
| LVEF | -0.07 | 0.12 | -0.06 | 0.12 |

LA – left atrial, LAA – LA appendage, LAEF – LA emptying fraction, LAVI – LA volume indexed, LV – left ventricular, LVEF – LV ejection fraction, LV_EDVi – LV end-diastolic volume indexed, LV_ESVi – LV end-systolic volume indexed, LV_SVi – LV stroke volume indexed

(4). LA was also segmented on all cardiac time points on balanced steady-state free precession SAX series; $LAV_{min}$, $LAV_{max}$ and LAV before atrial contraction ($LAV_{preA}$) were extracted and used to calculate $LAEF_{total}$, $LAEF_{active}$ and $LAEF_{passive}$;

**Results** 158 participants were included (age: 73 ± 7 years, 52% female). For the LA, the highest correlation was found for $LAEF_{total}$ with both LA stasis ($r = -0.53$, $p < 0.001$) and LA peak velocity ($p = 0.56$, $p < 0.001$). This was primarily based on $LAV_{min}$ rather than $LAV_{max}$ ($LAV_{min}$ & LA stasis: $r = 0.39$, $p < 0.001$; $LAV_{min}$ & LA peak velocity: $r = -0.46$, $p < 0.001$); see.

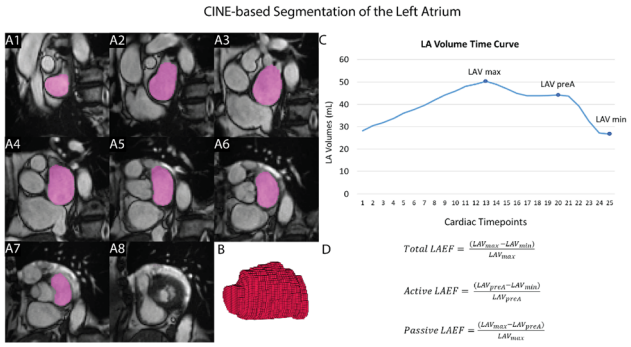


**Fig. 2** LA segmentation on all SAX slices (A1-A8) and cardiac time points (images represent a single time point). Those segmentations were combined into a 3D object for each time point (B) and the respective volumes were extracted to generate volume-time curves (C). Based of those curves, LAEFtotal, LAEFactive and LAEFpassive were calculated (D). Left ventricular (LV) assessment was also performed on SAX series. All volumes were also indexed to body surface area. Pearson correlations were calculated between each flow parameter with all LA and LV parameters
$LAVI_{min}$ was the parameter which correlated best with LAA stasis ($r = 0.43$, $p < 0.001$) and LAA peak velocity ($r = -0.59$, $p < 0.001$). We only found weak correlations between the LV and LA/LAA flow.

**Conclusion** Higher $LAV_{min}$, indexed and absolute, was associated with impaired flow characteristics (higher stasis, lower peak velocity) in the LAA and LA (the latter via $LAEF_{total}$). These findings support the importance of $LAV_{min}$ assessment and potentially contributing to thrombus formation.

## References

1 Leng S, Ge H, He J et al. Long-term Prognostic Value of Cardiac MRI Left Atrial Strain in ST-Segment Elevation Myocardial Infarction. Radiology 2020;296:299–309

2 Habibi M, Zareian M, Ambale Venkatesh B et al. Left Atrial Mechanical Function and Incident Ischemic Cerebrovascular Events Independent of AF: Insights From the MESA Study. JACC Cardiovasc Imaging 2019;12:2417–242

3 Shen MJ, Arora R, Jalife J. Atrial Myopathy. JACC Basic Transl Sci 2019;4:640–654

4 Markl M, Lee DC, Ng J, Carr M, Carr J, Goldberger JJ. Left Atrial 4-Dimensional Flow Magnetic Resonance Imaging: Stasis and Velocity Mapping in Patients With Atrial Fibrillation. Invest Radiol 2016;51:147–54

## A-114

### Subendocardial involvement as an underrecognized LGE subtype related to adverse outcomes in hypertrophic cardiomyopathy

S. Yang, S. Zhao

Fuwai Hospital, Beijing, China.

**Purpose/Objectives** Late gadolinium enhancement (LGE) has been established as an independent predictor for adverse outcomes in hypertrophic cardiomyopathy (HCM). However, the prevalence and clinical significance of some LGE subtypes have not been well demonstrated. Hence, this study aims to investigate the prognostic value of subendocardium-involved LGE pattern and right ventricle insertion points (RVIP) LGE location in HCM patients.

**Methods & Materials** In this single-center retrospective study, 497 consecutive HCM patients with LGE confirmed by cardiac MR (CMR) were included. Subendocardium-involved LGE was defined as LGE involving subendocardium not corresponding to a coronary vascular distribution. Subjects with ischemic heart disease that would contribute to subendocardial LGE were excluded. Endpoints included a composite of heart failure events, arrhythmic events, and stroke.

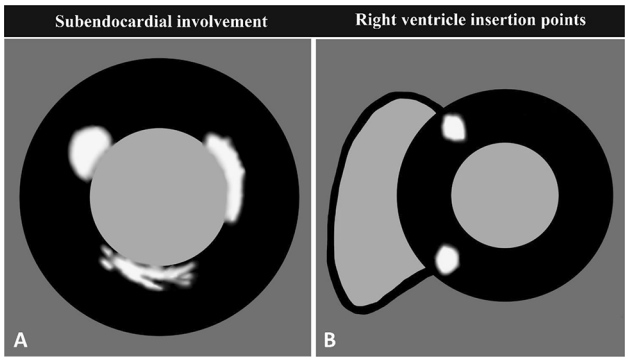


Diagram illustrating the subendocardium-involved late gadolinium enhancement pattern (A) and right ventricle insertion points late gadolinium enhancement position (B) in hypertrophic cardiomyopathy.

**Results** Of the 497 patients, subendocardium-involved LGE and RVIP LGE were observed in 184 (37.0%) and 414 (83.3%), respectively. Extensive LGE (≥ 15% of LV mass) was detected in 135 patients. During follow-up of 57.9 months, 66 of 497 patients (13.3%) experienced composite endpoints. Patients with extensive LGE had a significantly higher annual incidence of adverse events (5.1%/year vs. 1.9%/year, $P < 0.0001$). However, spline analysis showed a non-linear association between LGE extent with hazard ratios for adverse outcomes: the risk of composite endpoint increased with per percentage increase in LGE extent in patients with extensive LGE, while a similar trend was not observed in patients with non-extensive LGE. In patients with extensive LGE, LGE extent significantly correlated to composite endpoints (HR, 1.05; $P = 0.03$) after adjusting for left ventricular (LV) ejection fraction, age, sex, LV outflow tract obstruction, and maximum LV wall thickness, while in patients with non-extensive LGE, subendocardium-involved LGE rather than LGE extent was independently associated with adverse outcomes (HR, 2.87; $P = 0.003$). RVIP LGE was not significantly associated with poor outcomes in both groups.

| Variable | LGE < 15% (n = 362) Crude Hazard Ratio (95% CI) | P value | Adjusted Hazard Ratio (95% CI) | P value | LGE ≥ 15% (n = 135) Crude Hazard Ratio (95% CI) | P value | Adjusted Hazard Ratio (95% CI) | P value |
|---|---|---|---|---|---|---|---|---|
| LGE% | 1.03(0.94,1.12) | 0.57 | | | 1.1(1.05,1.15) | < 0.001 | 1.05(1.0,1.1) | 0.03 |
| Right ventricular insertion point LGE | 1.63(0.63,4.20) | 0.31 | | | 0.44(0.1,1.86) | 0.27 | | |
| Ischemia-like LGE | 2.36(1.21,4.60) | 0.01 | 2.87(1.42, 5.81) | 0.003 | 1.41(0.63,3.16) | 0.41 | | |

Univariable and Multivariable Analyses of Association between LGE and Outcome(Adjusted for LVEF, Age, Sex, LVOTO, Maximum LV wall thickness)

**Conclusion** In HCM patients with non-extensive LGE, the presence of subendocardium-involved LGE rather than LGE extent is associated with unfavorable outcomes. Given the prognostic value of extensive LGE has been broadly recognized, subendocardial involvement as an underrecognized LGE pattern shows the potential to improve risk stratification in HCM patients with non-extensive LGE.

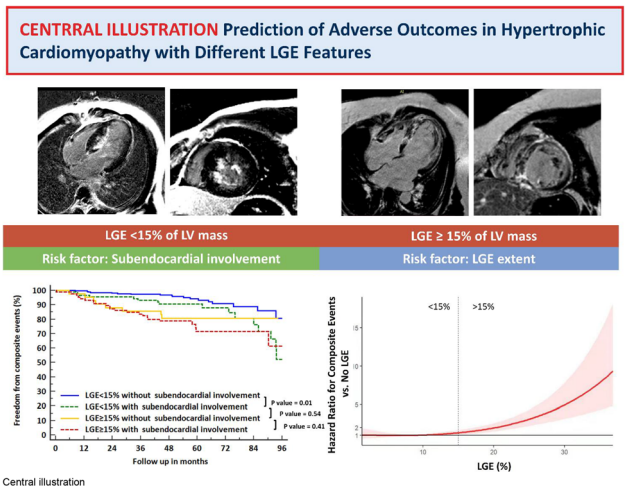


Central illustration

## A-115

### First in-vivo plaque characterization with ultra-high resolution coronary photon-counting CT angiography

V. Mergen, M. Eberhard, A. Euler, H. Alkadhi

University Hospital Zurich, Institute of Diagnostic and Interventional Radiology, Zurich, Switzerland.

**Purpose/Objectives** To assess the effect of ultra-high-resolution (UHR) coronary computed tomography angiography (CCTA) with photon-counting detector (PCD) CT on quantitative plaque characterization.

**Methods & Materials** In this IRB-approved study, 20 plaques of 18 patients (6 women; age 75 ± 7 years, BMI 26.3 ± 3.6 kg/m$^2$) undergoing ECG-gated UHR PCD-CCTA were included. Images were reconstructed with a smooth (Bv40) and a sharp (Bv64) vascular kernel, quantum iterative reconstruction (strength level 4), and with a slice thickness of 0.6, 0.4, and 0.2 mm, respectively. Reconstructions with the Bv40 kernel and slice thickness of 0.6 mm served as the reference. After identification of a plaque in the proximal coronary arteries, plaque composition was determined using a dedicated, semi-

automated, plaque quantification software. Calcified, fibrotic, and lipid rich components of the plaque were quantified.
**Results** Mean plaque volume was highest (28.1 ± 11.9 $mm^3$) for reconstructions with the reference standard and lowest for reconstructions with the Bv64 kernel at a slice thickness of 0.2 mm (21.9 ± 9.8 $mm^3$, $p < 0.001$). Both for reconstructions with the Bv40 and Bv64 kernel, plaque volume continuously decreased at thinner slice thicknesses (Bv40 kernel, 28.1 ± 11.9 $mm^3$ vs 25.1 ± 10.8 $mm^3$ and Bv64 kernel, 25.6 ± 11.6 $mm^3$ vs 21.9 ± 9.8 $mm^3$ for slice thickness 0.6 and 0.2 mm, respectively). Reconstructions with the reference standard showed largest calcified (80.1 ± 18.1%) and lowest lipid rich plaque components (1.2 ± 1.5%). Smallest calcified plaque components (74.0 ± 3.8%) and largest lipid rich components (7.0 ± 3.8%) were found for the Bv64 kernel at a slice thickness of 0.2 mm.

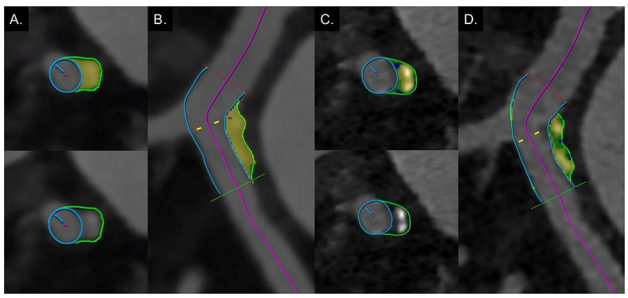


Images of an ultra-high-resolution coronary CTA with photon-counting CT show a mixed plaque reconstructed with the Bv40 kernel (slice thickness 0.6 mm, A, B) and with the Bv64 kernel (0.2 mm, C,D). Note the improved visualization of non-calcified components (blue = lipid rich, green = fibrotic) at a slice thickness of 0.2 mm with the Bv64 kernel (C,D).

At an identical slice thickness, volume of calcified components was always lower and lipid rich components always higher for the Bv64 compared with the Bv40 kernel (all, $p < 0.001$).

**Conclusion** Ultra-high-resolution coronary CT angiography with photon-counting detector CT using reconstructions with a slice thickness of 0.2 mm and a sharp vascular kernel yield smallest calcified and largest non-calcified plaque components, which indicates reduced blooming artifacts and better visualization of non-calcified plaque components, the latter being considered important for risk prediction.

## A-171

### High risk coronary plaque features are common in a general population examined with cardiac computed tomography angiography: results from an annotated dataset designed for deep learning

**E. Fagman[1,2], J. Alvén[3,4], J. Westerbergh[5], P. Kitslaar[6], M. Kercsik[2], K. Cederlund[7,8], O. Duvernoy[9], J. Engvall[10], I. Gonçalves[11], H. Markstad[11], E. Ostenfeld[12], G. Bergström[4], O. Hjelmgren[4]**

[1]Sahlgrenska University Hospital, Department of Radiology, Gothenburg, Sweden, [2]University of Gothenburg, Department of Radiology, Gothenburg, Sweden, [3]Chalmers University of Technology, Computer Vision and Medical Image Analysis, Dept. of Electrical Engineering, Gothenburg, Sweden, [4]University of Gothenburg, Department of Molecular and Clinical Medicine, Gothenburg, Sweden, [5]Uppsala University, Uppsala Clinical Research Center, Uppsala, Sweden, [6]Leiden University Medical Center/Medis Medical Imaging Systems, Leiden, The Netherlands, [7]Karolinska institutet, Department of Clinical Science, Intervention and Technology, Stockholm, Sweden, [8]Södertälje Hospital, Department of radiology, Södertälje, Sweden, [9]Uppsala University Hospital, Department of Radiology, Uppsala, Sweden, [10]Linköping University, Department of Clinical Physiology, Linköping, Sweden, [11]Lund University, Department of Clinical Sciences in Malmö, Malmö, Sweden, [12]Lund University, Department of Clinical Sciences in Lund, Lund, Sweden.

**Purpose/Objectives** Comprehensive analysis of coronary plaques with coronary computed tomography angiography (CCTA) is a promising tool to identify high risk of future coronary artery disease. However, the analysis process is time-consuming, and automation of analyses is needed. Development of deep learning analysis tools requires suitable data. The aims of this study were to generate a large, high-quality annotated CCTA dataset derived from a general population study with no previous coronary artery disease (Swedish CArdioPulmonary BioImage Study, SCAPIS), describe the plaque characteristics and their association with established risk factors and report the reproducibility of the analysis.
**Materials & Methods**
CCTA was performed on dual source CT scanners and the coronary artery tree was manually segmented using semi-automatic software by four primary and one senior secondary reader.

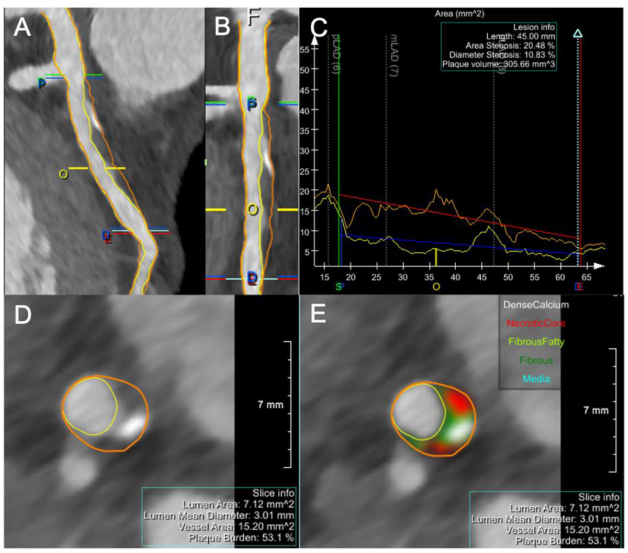


Semiautomated plaque analysis. Curved (A) and straightened (B) MPR show a mixed plaque in proximal LAD. Vessel wall and lumen contours are automatically detected and manually corrected. (C) is a graphic representation of the plaque area. (D) and (E) show a representative cross section of the plaque where plaque components are color coded in E.

A randomly selected sample of 469 subjects, all with coronary plaques and stratified for cardiovascular risk using the Systematic Coronary Risk Evaluation (SCORE), were analyzed. A reproducibility analysis was performed on 78 subjects (42 with plaques and 36 without plaques).
**Results** High-risk plaque (HRP) features (positive remodeling and low attenuation plaque) were common with 16% of subjects having plaques with two simultaneous HRP features. The number of HRP

features in each subject increased significantly ($p < 0.05$) across strata of SCORE. There was a positive correlation between SCORE and total plaque volume (rho = 0.30, $p < 0.001$) and total low attenuation plaque volume (rho = 0.29, $p < 0.001$).

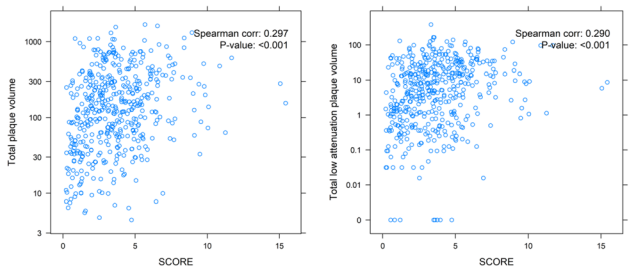


Total plaque volume and total low attenuation plaque volume versus SCORE. Spearman correlation and test of Spearman correlation included.

Total calcium volume showed strong positive correlation to coronary artery calcium score reported from the non-enhanced CT scan in the SCAPIS study (rho = 0.94, $p < 0.001$).

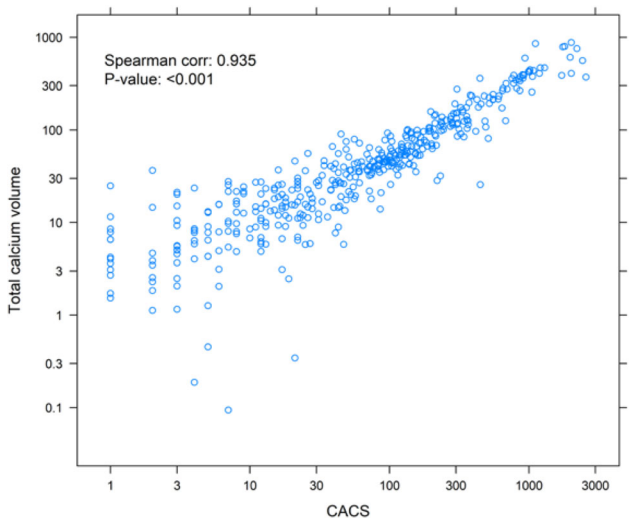


Total calcium volume versus CACS, Spearman correlation included.

The reproducibility study (68 subjects) showed an agreement for plaque detection of 0.91 (0.84—0.97) with a kappa of 0.82 (0.68–0.96). The mean percentage difference for volume of plaques was -0.6%, the mean absolute percentage difference 19.4% (18.2 CV%, ICC 0.98).

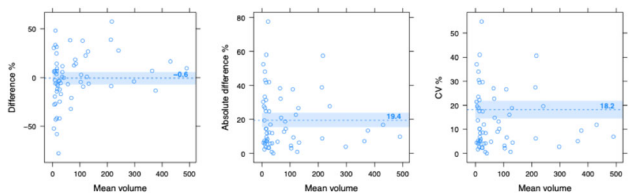


Difference and absolute difference in percent and variation in CV% for plaque volume in matched plaques between analysis 1 and analysis 2, 95% confidence intervals included.

**Conclusion** High-risk plaque features are common in a general population and plaque characteristics that signal vulnerability correlate with SCORE. The CCTA analysis showed high reproducibility indicating high quality of the dataset, that is well suited as training and validation data for supervising a fully automatic analysis tool based on deep learning.

## A-174

### Multiparametric assessment of Fabry Disease Cardiomyopathy at pre-hypertrophic stage: a cardiac magnetic resonance study

**L. Dominici[1], G. Pambianchi[1], L. Marchitelli[1], C. Roberti[1], M. Francone[2], C. Catalano[1], N. Galea[1]**

[1]Sapienza University of Rome, Department of Radiological, Oncological and Pathological Sciences, Rome, Italy, [2]Humanitas University, Department of Biomedical Sciences, Pieve Emanuele, Italy.

**Purpose/Objectives** Fabry Disease (FD) is a rare hereditary X-linked lysosomal storage disorder determined by mutations in the α-galactosidase A gene (GLA). The enzyme deficit causes a progressive accumulation of glycosphingolipids in multiple organs, including the heart typically causing hypertrophy. However, cardiac involvement in FD may precede left ventricular hypertrophy (LVH). We investigated the spectrum of cardiac magnetic resonance (CMR) features in non-hypertrophic FD subjects in terms of contractile dysfunction and myocardial relaxometry changes.

**Methods & Materials** Twenty-nine GLA gene mutation carriers (6 males, age 35.5 years) with pre-hypertrophic phenotype and biopsy-proven glycosphingolipid myocardial accumulation underwent CMR examination at 1.5 T (Avanto, Siemens Healthcare, Erlangen, Germany) which included STIR T2-w, cineMR, late enhancement and Modified Look Locker inversion recovery (MOLLI) sequences. CMR image analysis and FT was performed using dedicated software (Cvi42, Circle Cardiovascular Imaging) and LV volumes, maximal wall thickness, nT1, T2 mapping, LV global longitudinal (GLS and GLSR) and circumferential (GCS and GCSR) strain and strain rate, diastolic GLSR and GCSR were measured.

**Results** Native T1 values were abnormal (increased or reduced) in 13 FD patients (48%), whereas only 4 patients showing decreased nT1 values (941 ± 20.7 [ms, mean ± SD]). The remaining population had nT1 in normal range (n = 16; 1012.14 ± 21.52 [ms, mean ± SD]). Patients with abnormal nT1 showed significant impairment of GLS, GCS and GLSR in comparison to the normal T1 group (GLS: -15.72 ± 2.9 vs -19.46 ± 2.7 [%, p = 0.002]; GCS: -17.58 ± 1.64 vs 19.29 ± 1.86 [%, p = 0.018]; GLSR: -0.79 ± 0.11 vs -0.98 ± 0.17 [%, p = 0.013]). However, FD patients with reduced nT1 didn't show any significative difference in strain and strain rate values in comparison to the other patients. Statistical analysis showed low correlation between GLS, GCS and nT1 values (r = 0.4 and r = 0.49 respectively; $p < 0.04$ for both).

**Conclusion** Most patients with pre-hypertrophic FD had normal nT1, reflecting the low sensitivity of this CMR technique to detect subclinical stage of FD. Abnormal nT1 is associated to contractile impairment in FD, even in absence of hypertrophy.

Although T1 mapping technique offers a formidable tool in the non-invasive diagnosis of FD, its sensitivity is reduced in patients at pre-hypertrophic stage. Therefore the nT1 values in normal range in patients with familiarity or carriers of mutation does not exclude myocardial FD involvement.

## A-186

### MRI validated myocardial characterization with extracellular volume quantification on a first-generation, dual-source photon-counting detector CT

A. Varga-Szemes, G. Aquino, U. J. Schoepf, J. O'Doherty, T. Emrich

Medical University of South Carolina, Charleston, United States of America.

**Purpose/Objectives** To compare extracellular volume (ECV) quantification by using a first-generation, photon counting-detector CT (PCD-CT) against MRI reference.
**Methods & Materials** In this single-center, prospective study, subjects (n = 30) underwent same day cardiac PCD-CT and MRI with pre- and post-contrast T1 mapping and late gadolinium enhancement (LGE) for various clinical indications between July 2021 and January 2022. Global and midventricular ECV was assessed using three methods: single-energy CT (CT-$ECV_{SE}$), dual-energy CT (CT-$ECV_{DE}$), and MRI T1 mapping (MRI-ECV). Quantitative comparisons between all techniques, and qualitative comparison of CT-ECV maps and LGE-MRI were performed.
**Results** The final cohort included 29 subjects (mean age 54 ± 17 years; 15 men). There was an excellent correlation between global CT-$ECV_{SE}$ and CT-$ECV_{DE}$ (r = 0.91), but the single-energy method required a higher radiation dose (mean CTDIvol 28.0 vs 21.4; $P < 0.001$). In comparison to MRI-ECV, CT-$ECV_{DE}$ showed excellent correlation (global ECV, r = 0.91; midventricular ECV, r = 0.82; both $P < 0.001$), but slightly overestimated ECV by 1.9 ± 2.5% on global analysis and 2.3 ± 3.2% on midventricular analysis. Whole-heart, volumetric CT-$ECV_{DE}$ maps detected various patterns of myocardial involvement in comparison to LGE-MRI. Representative cases are shown in the image below.

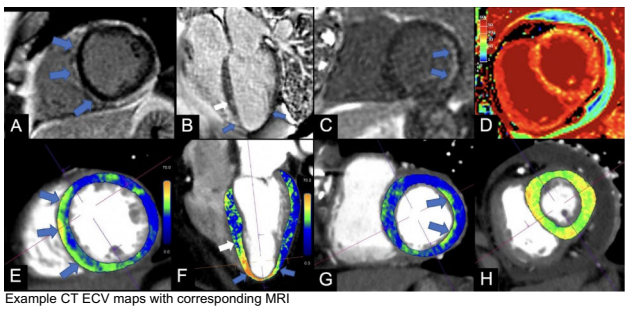

Example CT ECV maps with corresponding MRI

**Conclusion** Quantitative and qualitative analysis of ECV maps for myocardial tissue characterization was obtained on a PCD-CT with excellent correlation to MRI as reference standard.

## A-193

### Papillary muscles abnormalities and arrhythmic events: the prognostic role of early post contrast dark papillary muscles at Magnetic resonance

G. D. Aquaro[1], C. De Gori[2], R. Licordari[3], U. Ianni[4], L. Restivo[5], M. Parollo[6], M. Adami[2], G. Di Bella[3], E. Neri.[2]

[1]G. Monasterio CNR-Tuscany Foundation, Pisa, Italy, [2]University of Pisa, Academic Radiology, Department of Translational Research, Pisa, Italy, [3]Rare Cardiac Disease Centre, University of Messina, Department of Clinical and Experimental Medicine, Messina, Italy, [4]University of Chieti, Chieti, Italy, [5]Azienda Sanitaria Universitaria Giuliano Isontina, Cardiovascular Department, Trieste, Italy, [6]University of Pisa, Pisa, Italy.

**Purpose/Objectives** The prognostic role of papillary muscle abnormalities in patients with preserved left ventricular systolic ejection fraction (LVEF) is unknown.
We sought to evaluate the prognosis role of different papillary muscle abnormalities in a cohort of patients with ventricular arrhythmias, preserved LVEF and without a definite diagnosis of cardiac disease.
**Methods & Materials** 350 patients with frequent (> 500/24 h) premature ventricular complexes and/or non-sustained ventricular tachycardia (NSVT), preserved LVEF and no history of cardiac disease were enrolled. The following characteristic of papillary muscles were considered: supernumerary muscles, papillary dimension, the type of attachment, the angle of attachment, the angle between muscles, the presence of late gadolinium enhancement (LGE) of papillary muscles, and the signal intensity (SI) of papillary muscle in early post-contrast cine images. Dark-PAP was defined when both anterolateral and posterolateral papillary muscles had lower SI than interventricular septum in the end-systolic frame of early post-contrast short axis cine images. Other parameters as mitral prolapse, mitral annular disjunction (MAD), myocardial LGE were considered.
**Results** Dark-PAP was found in 65% of patients and was associated with MAD, LGE of papillary muscle and of LV walls. During a median follow-up of 2534 days, 22 hard cardiac events occurred. At Kaplan–Meier curve analysis patients with Dark-PAP were at higher risk of events than those without ($p < 0.0001$). Dark-PAP was the only papillary muscle parameter resulting an independent predictor of hard cardiac events in all the multivariate models. In stepwise models, Dark-PAP improved prognostic estimation when added to NSVT (p = 0.0006), to LGE of LV walls (p = 0.005) and to a model including NSVT + LGE (p = 0.014). Dark-PAP allowed a significant net reclassification when add to NSVT (NRI 0.30, p = 0.03), to LGE (NRI 0.25, p = 0.04), and to NSVT + LGE (NRI 0.32, p = 0.02).
**Conclusion** Dark-PAP is a novel prognostic marker in patients with ventricular arrhythmias and preserved ejection fraction.

## A-202

### Coronary CTA-based calcium scoring: in-vitro and in-vivo validation of a novel virtual non-iodine reconstruction algorithm on a clinical, first generation photon counting-detector system

T. Emrich[1,2], G. Aquino[2], U. J. Schoepf[2], J. O'Doherty[3], A. Varga-Szemes[2]

[1]University Medical Center Mainz, Radiology, Mainz, Germany, [2]Medical University of South Carolina, Charleston, United States of America, [3]Siemens Healthcare, Malvern, United States of America.

**Purpose/Objectives** To evaluate coronary CTA (CCTA)-based in-vitro and in-vivo coronary artery calcium scoring (CACS) using a novel virtual non-iodine (VNI) reconstruction on a clinical, first-generation Photon Counting Detector (PCD)-CT system compared to virtual non-contrast (VNC) and true non-contrast (TNC) acquisitions.
**Methods & Materials** While CACS and CCTA are well established techniques for the assessment of coronary artery disease, they are complementary acquisitions, translating into increased scan time and radiation dose. Hence, accurate CACS derived from a single CCTA acquisition would be highly desirable. In this study, CACS based on VNI, VNC and TNC reconstructions were evaluated in a CACS phantom (QRM, Moehrendorf, Germany) and in 32 prospectively recruited patients (59.4 ± 14.1 years, 59.3% male) undergoing CCTA with a first generation PCD-CT system (NAEOTOM Alpha,

Siemens Healthineers, Germany). CACS were quantified for the three reconstructions and compared using Wilcoxon's test. Agreement was evaluated by Spearmen's correlation and Bland-Altmann analysis. Classification of CACS categories (CACS 0, 1–100, 101–400 and > 400) were compared using Cohen's kappa.

**Results** Phantom studies demonstrated strong agreement between VNI and TNC (60.7 ± 90.6 vs 67.3 ± 88.3,p = 0.01, r = 0.98, mean bias: 6.6), while VNC showed a significant underestimation of CACS (42.4 ± 75.3 vs 67.3 ± 88.3, $p < 0.001$, r = 0.94, mean bias: 24.9). In-vivo comparison confirmed the high correlation, but revealed a slight underestimation of CACS based on VNI (Median(IQR): 21.7 (0/472.5) vs 9.0 (0/364.6), $p < 0.001$; r = 0.99; mean bias: -113.5). In comparison, VNC showed weaker correlation and a larger underestimation (21.7(0/472.5) vs 0.8(0/86.6), $p < 0.001$, r = 0.93; mean bias -372.4). VNI showed superior agreement of CACS classification (kappa = 0.93), compared to that of VNC (kappa = 0.69).

**Conclusion** Accuracy of CACS quantification and classification based on VNI reconstruction of CCTA outperforms CACS derived from VNC. VNI reconstructions could be used to acquire CACS based on CCTA while saving radiation and examination time.

## A-217

### Detection of papillary muscles involvement in subacute STEMI using T1 mapping and Cine sequences

**G. Pambianchi[1], M. Giannetti[2], G. Cundari[2], L. Ruoli[3], M. Francone[4], C. Catalano[2], N. Galea[2]**

[1]Sapienza policlinico Umberto I, Department of Radiological, Oncological and Pathological Sciences, Roma, Italy, [2]Sapienza policlinico Umberto I, Department of Radiological, Oncological and Pathological Sciences, Rome, Italy, [3]Sapienza policlinico Umberto I, Dipartimento di Scienze Radiologiche Oncologiche e Anatomo Patologiche, Rome, Italy, [4]Humanitas University, Milan, Italy.

**Purpose/Objectives** Left ventricular papillary muscles (PPMs) involvement in acute myocardial infarction (AMI) is a negative prognostic factor, in fact, it can increase the risk of secondary mitral valve regurgitation during follow-up.

Cardiac magnetic resonance (CMR) is the reference standard for the in vivo assessment of myocardial damage in AMI, nT1-mapping combined with a morphodynamical assessment could be promising in identifying the PPMs infarction (IPPMs), also in view of avoiding CA administration. The aim of this study was to assess the diagnostic performance of nativeT1 (nT1) in identifying PPMs involvement in AMI, combining the results with their morphological analysis.

**Methods & Materials** CMR protocol included MOLLI T1 mapping sequences, STIR T2 sequences, and PSIR-GRE sequences for late gadolinium enhancement (LGE) assessment. 48 Patients with subacute AMI (onset 14- 30 days) were enrolled and analyzed, 18 pts showed PMMs enhancement in LGE sequences, and 30 didn't demonstrate any PPM involvement in LGE images. In MOLLI sequences nT1 values were measured within the infarcted myocardium (IM), remote myocardium (RM), blood pool (BP), anterolateral (AL), and posteromedial (PM) papillary muscles. Contrast-to-noise ratio (CNR) was calculated for the nT1-IA and nT1-PPMs values in the mapping sequences. We measured the PPMs systo-diastolic lenght and calculated the the percentage of shortening in Cine-SSFP images, for all the patients.

**Results** Most of the patients were male (82.6%), nT1 values of IA and IPPMs (LGE +) were significantly higher than those obtained in non-infarcted ones (LGE-), as follows: nT1-AL-PPM:1205.1 ± 66.9 vs 1057.8 ± 88.1 ($p < 0001$), nT1-PM-PPM:1200 ± 129.8 vs 1100.5 ± 87.5 (p:0.014), nT1-IA:1264.5 ± 98.5 vs nT1-RM:1034.7 ± 41.4 ($p < 0.001$).

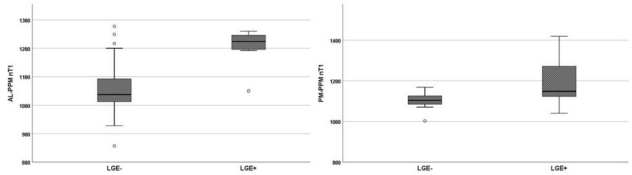


Box Plot comparing infarcted and non-infarcted AL-PPM and PM-PPM nT1 values.

The IA and PPMs CNR-values were further analyzed with Bland–Altman plot that confirmed the diagnostic performance of nT1 in recognizing infarcted PPMs (mean-difference: 1.9 and 1.7, for AL and PM PPMs respectively).

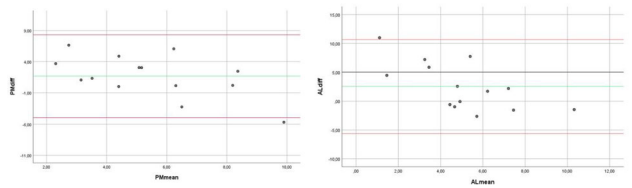


Bland–Altman plot showing the agreement between PPMs and IA CNR values in patients who demonstrated PPMs infarction in LGE sequences.

Patients with IPPMs showed reduced LVEF (35.9 ± 11.8 vs 44.4 ± 9.4; p:0.016) and an impaired shortening of the IPPM when compared with the non-infarcted PPMs (AL-PPM%: 16.3 ± 6.4 vs 23 ± 4.8; PM-PPM%: 15.3 ± 5.2 vs 21.7 ± 5.2; $p < 0.013$).

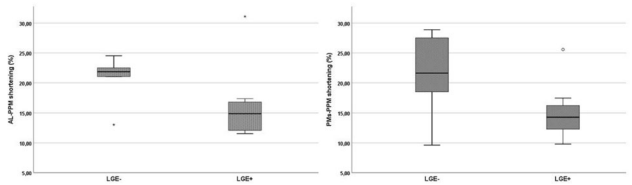


Box Plot comparing infarcted and non-infarcted AL-PPM and PM-PPM shortening (%).

**Conclusion** Papillary muscle involvement in AMI is identifiable in T1 maps with similar values to infarcted myocardium and sufficient contrast resolution. Furthermore, IPPMs show impaired shortening when compared with non-infarcted ones. A complete assessment of myocardial damage following AMI using nT1 mapping and Cine sequences is desirable and could allow an overall reduction of CMR examination time, by avoiding the administration of the contrast agent, with benefits in the patient management.

## A-250

### Characterization of microvascular injury with parametric mapping in reperfused acute myocardial infarction: correlation with vascular physiology at invasive coronary angiography

A. Bettinelli, A. Palmisano, D. Vignale, S. Barbieri, M. Gramegna, P. Camici, M. Montorfano, A. Esposito

IRCCS Ospedale San Raffaele, Milan, Italy.

**Purpose/Objectives** Cardiac Magnetic Resonance (CMR) is the standard of reference for the non-invasive characterization of myocardial damage and several CMR parameters are considered predictors of major cardiac events. Recently introduced mapping parameters showed the possibility to characterized microstructural myocardial alteration in quantitative fashion. Despite their currently established role in the setting of inflammatory and infiltrative cardiomyopathies, their value in the setting of ischemic cardiomyopathy remain to be established.
Aim of the present study was to investigate the association between parametric mapping alteration and invasive parameter of vascular physiology.
**Methods & Materials** From November 2020 to January 2022 a total of 30 patients with STEMI underwent CMR within 5 days after the event. In the same 30 patients the Index of Microcirculatory Resistance (IMR), as marker of coronary microvascular function (normal values $< / = 25$), and the coronary flow reserve (normal $> 2$) were measured during the Invasive coronary angiography (ICA). All of patients underwent CMR including native T1 mapping, T2 mapping and post-contrast T1 mapping to measure native T1, T2 and ECV values. Additionally conventional parameters were measured: infarct size (IS) using FWHM method, edema burden at + 2SD, myocardial salvage index using a dedicated software (Circle, CVI 42).
**Results** Patients were mainly man [25] with a median age of 61 [IQR = 15]. Native T1, T2 and ECV values were 1045[IQR = 112], 62 [IQR = 9.6] and 35.8 [IQR = 8.6] respectively. Comparing patients with increased versus normal IMR, the only parameters significantly different were the ECV of the area at risk (34.8% [33.2%-40%] vs 29.9% [28.9%-33%]; p = 0.001) and in the remote myocardium (27% [26.2%-29.6%] vs 25%[24.6%-27%]; p = 0.008). Patients with reduced CFR showed significantly increased ECV values in infarct core (52.9% vs 41.3%; p = 0.025) and in remote myocardium (27.0% vs 25.0%; p = 0.007) and lower ejection fraction (53.9% vs 44.4%). IMR correlates positively with ECV of the area at risk (p = 0.013) and of the remote myocardium ($p < 0.001$). CRF correlated negatively with ECV of the infarct core (p = 0.022).

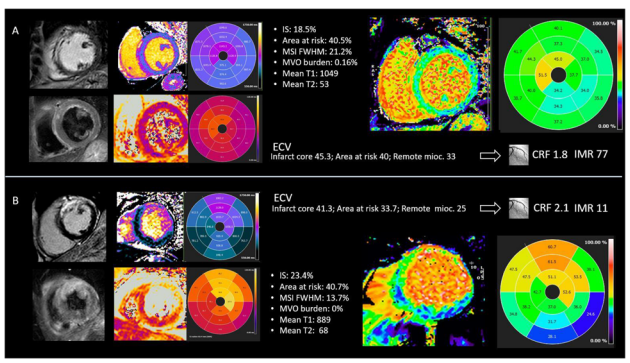


(A)Male [61yo] with acute chest pain, ST elevation in D1, D2, D3 AVL. Peak troponin 7295. (B)Male [53yo] with acute chest pain, ST elevation in D1, D2, D4, D5, D6, AVL. Peak troponin 3242. Patient A with higher area at risk and remote myocardium ECV values showed worst physiological parameters during coronarography compared to patient B.

**Conclusion** Our results suggest a value of ECV to provide a deeper characterization of infarcted and non-infarcted myocardium impacting on altered coronary physiology.

## A-261

### Comparison of conventional and spectral images for the discrimination of myocarditis late enhancement areas with dual-energy dual-layer CT

S. Boccalini[1], R. Wiemker[2], R. Dessouky[3], S. Si-Mohamed[4], L. Boussel[4], P. Douek[4]

[1]Hospices Civils de Lyon, Radiology, Lyon, France, [2]PHilips research, Hambourg, Germany, [3]Zagazig University Hospital, Zagazig, Egypt, [4]Hospices Civils de Lyon, Lyon, France.

**Purpose/Objectives** To compare the performance of conventional versus spectral images for the discrimination of late enhancement areas (LE-A) using a dual-energy dual-layer CT (DL-CT) in patients with myocarditis.
**Methods & Materials** We retrospectively evaluated images of 42 patients undergoing a DL-CT scan to demonstrate clinically suspected myocarditis, later confirmed on MRI. Retrospectively ECG-gated acquisitions were performed 7 min after the injection of 1.2 mL/kg of iodinated contrast media. Conventional (Conv), virtual mono-energetic at 40 keV (VME).

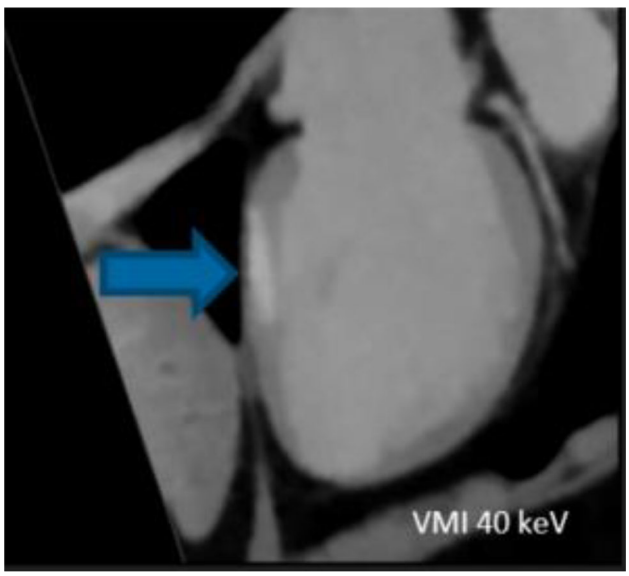


Example of late enhancement area on virtual mono-energy image (40 keV)

and iodine-density images (IoD) were reconstructed. An experienced reader segmented the entire myocardium of the left ventricle and of LE-A. Contrast-to-noise ratios (CNR) of the LE-A were determined with respect to the remote myocardium, for Conv, VME and IoD. Receiver-operating curves (ROC) were computed for the values of the voxels (HU for Conv and VME images, iodine concentration [mg/mL] for iodine maps) contained in the LE-A in respect

to remote myocardium in three ways: based on absolute voxels' values, on voxels' values normalized to the median value of the left ventricular cavity and on voxels' values normalized to the median value of the myocardium. Areas under the curve (AUC) were calculated and compared.

## Results

Compared to Conv images (median = 0.42, IQR = 0.30–0.53), CNR was higher in VMI-40 keV (0.84, 057–1.04) and IDM (1.34, 0.90–1.76, all $p < 0.001$).

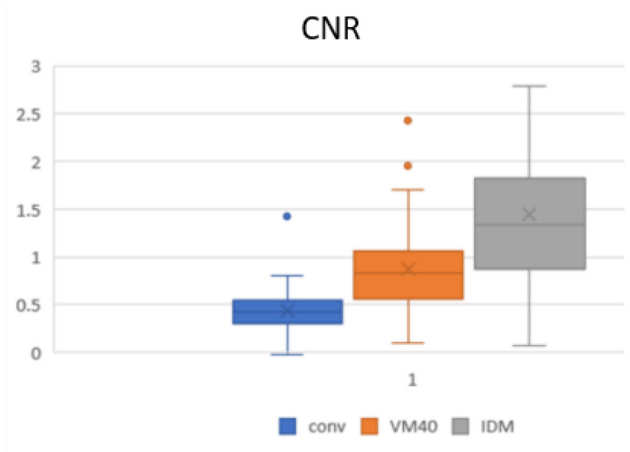


CNR box plots.

As compared to Conv images (AUC = 0.64), discrimination of LE-A based on absolute voxels' values was higher for VME (AUC = 0.70) and IoD images (AUC = 0.73, all $p < 0.001$). Compared to absolute values, normalization to the median of the left ventricle cavity yielded improved discrimination for all reconstructions (AUC = 0.70, 0.78, 0.82; all $p < 0.001$). Compared to normalization to the left ventricle, normalization to the median value of the myocardium showed higher AUC values (AUC = 0.70, 0.81, 0.86; all $p < 0.001$).

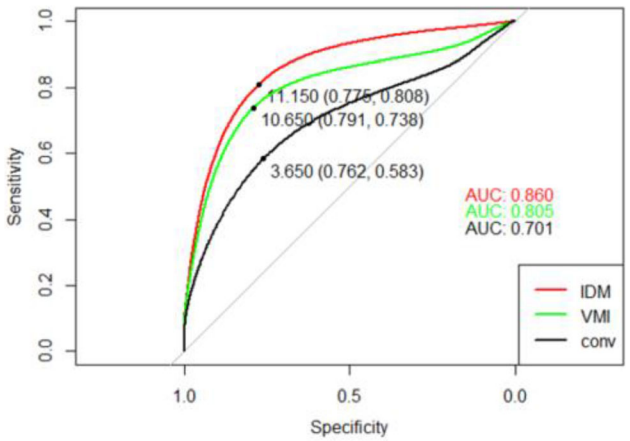


ROC curves comparing conventional vs mono-energy vs iodine-density based on voxels' values normalized to the median of the myocardium.

**Conclusion** Contrast and discrimination of LE-A in patients with myocarditis were significantly improved by DL-CT spectral reconstructions in comparison to conventional images. Normalization to the myocardium yielded the best results, in good agreement with manual segmentation.

## A-265

### CMR FT ventricular strain assessment in individuals with corrected Tetralogy of Fallot (TOF). A case–control study of patients with pulmonary valve replacement versus patients with primary TOF correction

**M. Pop[1,2], E. Nagy[3], E. Sorantin[3]**

[1]IUBCvT Tirgu Mures, Radiology, Tirgu Mures, Romania, [2]UMFST GE Palade, ME1, Tirgu Mures, Romania, [3]Medical University of Graz, Division of Pediatric Radiology, Department of Radiology, Graz, Austria.

**Purpose/Objectives** To investigate the impact of pulmonary valve replacement (PVR) on ventricular strain for patients with corrected of tetralogy of Fallot (TOF) versus matched TOF patients without PVR.
**Methods & Materials** This retrospective study included 24 TOF patients who underwent CMR before and after pulmonary valve replacement (PVR group) and 24 matched TOF patients (age, gender, BSA) with primary correction who underwent serial cardiac MRI (CMR) examinations (control group).
Demographic data (age, gender, body-surface area- BSA) and CMR data (biventricular volumes and function, valvular regurgitation) were collected from institutional database.

Feature tracking ventricular strain analysis was performed using Circle cvi42 5.12, using short axis cine slices, four chamber and three chamber cine slices.

Data analysis was performed using Kolmogorov–Smirnov for normality assessment, T-test for normal distributed data, and Mann–Whitney for unpaired data.

All calculations were performed using a statistical significance of 0.05.
**Results** The average age of the patients at the first examination was 21.13 years for patch group and 20.83 years for the PVR group (non-significant difference, $p = 0.918$).

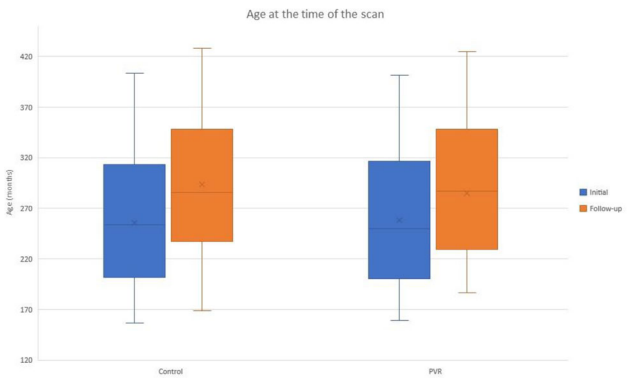


Age at the time of scan

In both groups the M:F ratio was 1.18.

For both initial and follow-up scan we found no statistically significant differences between groups in terms of age, time between scans, BSA, LV volumes and function. The initial RVEDV-BSA indexed differed significantly, between groups, with median values decreasing between scans with 10% in the control group (from 145.19 ml/m$^2$ to 131.06 ml/m$^2$) and 35% in the PVR group (form 162.55 to 106.42 ml/m$^2$).

Long axis peak global longitudinal strain (GLS), when comparing PVR vs control group, was similar for the initial scan ($p = 0.364$ for LV and $p = 0.298$ for RV) but significantly different in the follow-up scan ($p = 0.03$ for LV and $p = 0.004$ for RV).

The left ventricle GLS change from initial to follow-up scan was significant, with a relative increase of 17.44% ($p = 0.01$) for the control group and non-significant for the PVR patients ($p = 0.57$).

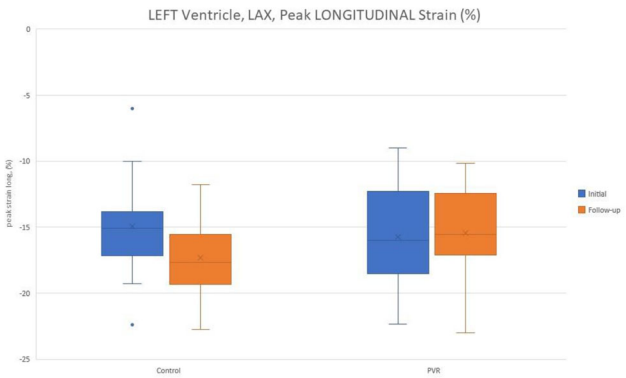


LV Longitudinal strain

For the right ventricle, the GLS change between examinations was non-significant in both groups (p-value of 0.07 for control and $p = 0.967$ for PVR).

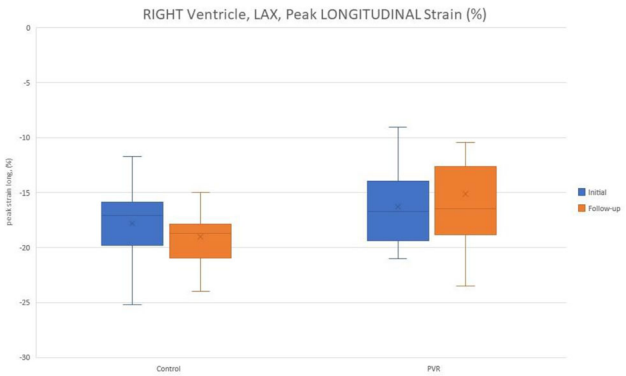


Right ventricle peak global longitudinal strain.

Peak global circumferential strain (GCS) showed no statistically significant difference between controls vs PVR nor when comparing the order of the scans within the groups (p values consistent $> 0.05$).

**Conclusion** Following PVR the change in cardiac function is reflected by decreased RVEDV-BSA indexed and an increase of the left ventricular longitudinal strain, while the circumferential strain showed no change, regardless of ventricular remodeling or functional change.

## A-284

### Comparison of statin-treated versus statin-naive individuals undergoing coronary computed tomography angiography

O. Furmaga[1], G. Tsiaousis[2], E. Delaveridou[1], T. Floros[3], A. Kallifatidis[4], K. Michailidis[5], M. Vlychou[6]

[1]Papanikolaou General hospital, Radiology, Thessaloniki, Greece, [2]Private Cardiology Practice, Cardiology, Kastoria, Greece, [3]General Hospital Larisa, Radiology, Larisa, Greece, [4]St Lukes Hospital, Radiology, Thessaloniki, Greece, [5]Cardiac Intelligence, Ptolemaida, Greece, [6]University of Thessaly, Radiology, Larisa, Greece.

**Purpose/Objectives** To clarify the potential effect of statin treatment on the coronary arteries. Coronary artery calcium (CAC) score is considered to be representative of the involvement of the vessel wall, while the percentile stenosis is representative of the effect on the lumen.

**Methods & Materials** We retrospectively enrolled 3966 consecutive individuals who had undergone coronary computed tomography angiography (CCTA) in our institution. For all patients, traditional risk factors were assessed, along with the causes of referral (symptoms or other). The sample was divided in statin-naive and statin-treated participants and the duration of statin treatment was recorded. Group comparisons were performed and multivariate analysis was applied to check the statistical importance of statin treatment in predicting CAC and stenosis severity.

**Results** Out of 3966 participants, 28% (1409) were receiving a statin and displayed a statistically higher median CAC score (66, range 0–5942) than statin-naive patients (median CAC 5, range 0–4378, $p < 0.0005$). When CAC was grouped into 4 categories (0, 1–99, 100–399, and CAC $>=$ 400), statin-treated patients appeared to be represented more frequently in the highest CAC groups than patients not on statins ($p < 0.0005$). As for coronary stenosis severity (4 groups: no, mild, moderate and critical stenosis), statin-treated patients were again more frequently represented in the highest coronary stenosis groups ($p < 0.0005$). Years of statin-treatment were positively correlated both with CAC score and stenosis severity. In multivariate models including well-established risk factors (e.g. age, male gender, hypertension, diabetes), statin treatment independently predicted both CAC score and stenosis severity.

**Conclusion** The widely accepted increase of coronary calcium by statins, which results in more stable plaques, albeit more lumen-narrowing, was confirmed in our study. However, statin treatment remained an independent predictor of coronary stenosis severity, meaning that CAC score and CCTA remain useful/meaningful primary prevention tools, even for the statin-treated patient.

## Scientific poster presentations

Abstracts appear as submitted to the system and have not been checked for correctness and completeness.

## A-113

### Reverse remodeling of left atrium assessed by cardiac MR feature tracking in hypertrophic obstructive cardiomyopathy after septal myectomy

S. Yang, S. Zhao

Fuwai Hospital, Beijing, China.

**Purpose/Objectives** Assessing the structure and function of left atrial (LA) is crucial in hypertrophic obstructive cardiomyopathy (HOCM)

because LA remodeling correlates to atrial fibrillation. However, there is little evidence showing the effect of myectomy on LA phasic remodeling in patients with hypertrophic obstructive cardiomyopathy using cardiac MR (CMR) feature tracking (FT). This study aimed to evaluate the effect of septal myectomy on left atrial (LA) structural and functional remodeling in patients with hypertrophic obstructive cardiomyopathy (HOCM) by using CMR-FT and to further investigate the determinants of postoperative LA strains.

**Methods & Materials** We retrospectively studied 88 patients with HOCM who received pre- and postmyectomy CMR between January 2011 and June 2021 in this single-center study. Pre- and postmyectomy left atrial (LA) parameters derived from CMR-FT were compared, including LA reservoir function (total ejection fraction [EF], total strain [εs], peak positive strain rate [SRs]), conduit function (passive EF, passive strain [εe], peak early negative strain rate [SRe]) and booster function (booster EF, active strain [εa], late peak negative strain rate [SRa]). Eighty-six healthy participants were collected for comparison. Univariate and multivariate linear regression determined the variables associated with postoperative LA strains.

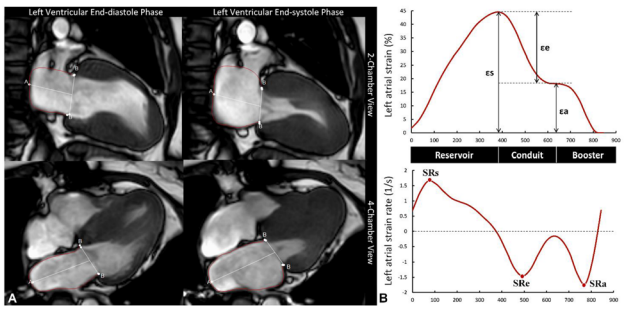


Example of measurement of left atrial phasic deformation by feature tracking.

**Results** Compared with preoperative parameters, LA reservoir function (total EF, εs, SRs), booster function (booster EF, εa, SRa), and SRe were significantly improved (all $P < 0.05$) after myectomy, while no significant difference was observed in passive EF and εe. However, postoperative patients with HOCM still had larger LA and worse LA phasic function than healthy controls (all $P < 0.05$). On multivariable regression analysis, LV maximal wall thickness ≥ 30 mm and minimum LA volume index were significantly associated with postoperative εs and εa.

| Parameter | Pre-myectomy (n = 88) | Post-myectomy (n = 88) | Healthy controls (n = 86) | P value for premyectomy vs postmyectomy |
|---|---|---|---|---|
| LA total EF (%) | 42.5 ± 12.5† | 49.4 ± 11.7† | 64.0 ± 5.4 | < 0.001 |
| εs (%) | 21.0 ± 9.8† | 25.6 ± 9.5† | 43.0 ± 9.0 | < 0.001 |
| SRs (1/s) | 0.84 ± 0.39† | 0.95 ± 0.40† | 1.58 ± 0.37 | 0.005 |
| LA passive EF (%) | 18.5 ± 9.1† | 19.6 ± 8.7† | 33.8 ± 8.7 | 0.21 |
| εe (%) | 10.4 ± 6.6† | 11.0 ± 5.9† | 23.3 ± 7.8 | 0.37 |
| SRe (1/s) | -0.55 ± 0.30† | -0.62 ± 0.33† | -1.42 ± 0.49 | 0.02 |
| LA booster EF (%) | 29.7 ± 11.7† | 37.5 ± 10.8† | 45.4 ± 6.4 | < 0.001 |
| εa (%) | 10.5 ± 5.6† | 14.7 ± 6.1† | 19.8 ± 4.0 | < 0.001 |
| SRa (1/s) | -0.93 ± 0.53† | -1.20 ± 0.52† | 1.78 ± 0.43 | < 0.001 |

LA deformation parameters in study groups

| | Univariate | | | | Multivariate | | | |
|---|---|---|---|---|---|---|---|---|
| | Postoperative εs | | Postoperative εa | | Postoperative εs | | Postoperative εa | |
| Preoperative variables | r | P | P | P | β | P | β | P |
| History of atrial fibrillation | -0.35 | 0.001 | -0.27 | 0.01 | -2.68 | 0.22 | -3.37 | 0.26 |
| LAVmin index (ml/m2) | -0.47 | < 0.001 | -0.24 | 0.02 | -0.07 | 0.03 | -0.19 | < 0.001 |
| LV maximal wall thickness ≥ 30 mm | -0.24 | 0.03 | -3.68 | 0.007 | -4.85 | 0.003 | -6.85 | < 0.001 |
| LV mass index | -0.21 | 0.048 | 0.10 | 0.18 | 0.008 | 0.56 | | |

Univariate and multivariate analysis showing preoperative factors associated with postoperative εs and εa

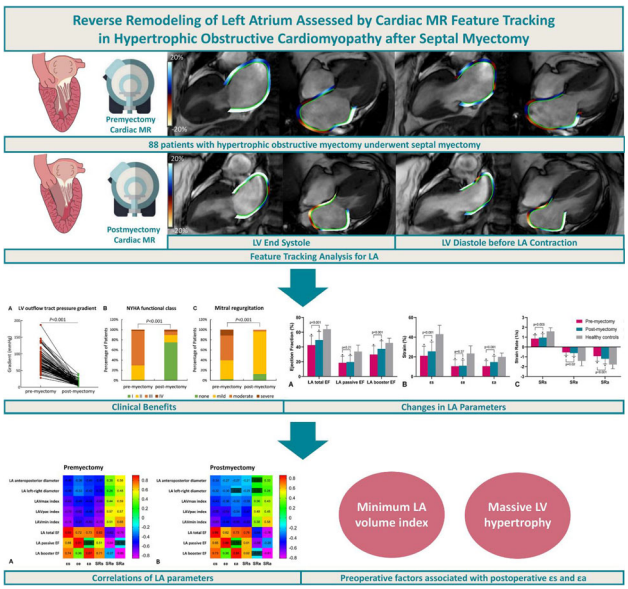


**Conclusion** In patients with HOCM, septal myectomy leads to the LA reverse remodeling with a reduction in LA size and improvement in LA reservoir and booster function, but unchanged LA conduit function. Besides, patients with massive LV hypertrophy and larger minimum LA volume index before myectomy may have poor LA deformation function postoperatively.

## A-120

### Cine cardiovascular magnetic resonance imaging using a prototype sequence on a commercially-available 0.55 T scanner: comparison with 1.5 T

**D. Winkel[1], M. Segeroth[1], J. Vosshenrich[1], H.-C. Breit[1], D. Giese[2], P. Haaf[3], M. Zellweger[3], J. Bremerich[1], F. Santini[1]**

[1]University Hospital Basel, Clinic of Radiology & Nuclear Medicine, Basel, Switzerland, [2]Magnetic Resonance, Siemens Healthcare GmbH, Erlangen, Germany, [3]University Hospital Basel, Clinic of Cardiology, Basel, Switzerland.

**Purpose/Objectives** To assess feasibility of cine cardiovascular magnetic resonance (CMR) imaging at 0.55 T by comparing volume and function parameters as well as measures of subjective and objective image quality to a standard 1.5 T scanner.
**Methods & Materials** 11 healthy volunteers underwent cine imaging at a 0.55 T (MAGNETOM Free.Max, Siemens Shenzhen Magnetic Resonance Ltd.) using a prototype sequence with external ECG and a 1.5 T scanner system (MAGNETOM Avanto Fit, Siemens Healthcare GmbH) using the product sequence within a time slot of two hours. Two expert readers independently assessed biventricular volume and function parameters as well as valve insufficiencies. Subjective image quality was rated on a 5-point Likert scale (range: 1 = non-diagnostic to 5 = excellent image quality). Objective image quality was assessed by calculating the signal-to-noise (SNR) ratio in the left ventricle and myocardium, as well as the blood-myocardium contrast index (BMCI). Patient comfort was evaluated with a survey adjunct to the scanning procedure.
**Results** With regards to the volume and function parameters, no significant differences were found between 0.55 T and 1.5 T by both readers (all parameters: $p > 0.05$). Four tricuspid valve insufficiencies were detected at 1.5 T, of all which were similarly detected at 0.55 T. Both readers rated the diagnostic image quality at 0.55 T as diagnostic. 10/11 studies were rated as excellent image quality by both readers, 1/11 study was rated as good image quality (mean Likert-score: 4.9).

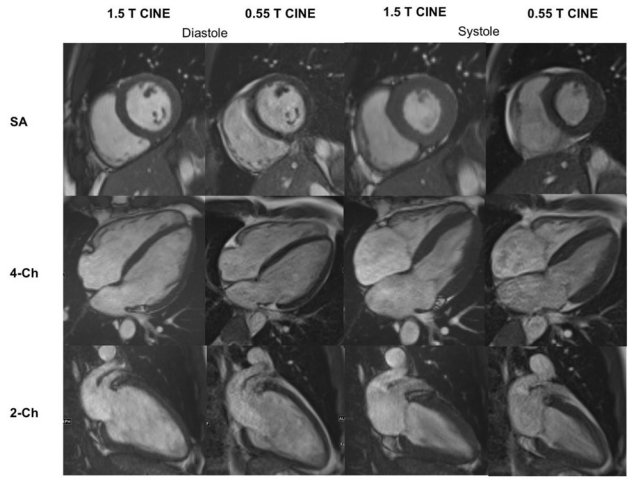


Comparison of Image Quality between the 0.55 T and 1.5 T Scanner in Diastole and Systole in Short Axis, 4-Chamber and 2-Chamber View.

Objective image quality assessment revealed a higher SNR in the left ventricle and myocardium at 1.5 T compared to 0.55 T (left ventricle: 3.6 vs. 3.3, $p = 0.04$; myocardium: 3.4 vs. 2.5, $p < 0.001$). BMCI was similar for 1.5 T and 0.55 T (2.03 vs. 2.05; $p = 0.97$). The participants rated the loudness and space perception much better at 0.55 T due to the wider bore of 80 cm. In a direct comparison, three participants rated the MRI set-up at 0.55 T "much better", seven "better" and one "equal".
**Conclusion** Cardiovascular cine imaging at 0.55 T yields similar results for quantitative function parameters and BMCI compared to imaging at 1.5 T, despite inferior SNR. Patient comfort was reported to be higher compared to imaging at 1.5 T.

## A-122

### What is the yield of iterative model-based reconstruction over hybrid iterative reconstruction in coronary CT-angiography when compared to the reference standard invasive coronary angiography?

A. Matuleviciute-Stojanoska[1], J. Sautier[1], V. Bauer[2], C. Stumpf[2], T. Klink[1]

[1]Klinikum Bayreuth, Radiology, Bayreuth, Germany, [2]Klinikum Bayreuth, Cardiology, Bayreuth, Germany.

**Purpose/Objectives** The hypothesis was to investigate whether iterative model-based reconstruction (IMR) can significantly improve image quality and diagnostic accuracy over hybrid iterative reconstruction (HIR) in the evaluation of coronary artery disease (CAD) in comparison to the reference standard invasive coronary angiography (ICA).
**Methods & Materials** This retrospective study includes 20 consecutive patients (4 female, 16 male). Mean age was 62,6 (43–76 years). All had low to intermediate risk of having coronary artery disease (CAD). All patients underwent coronary CTA and ICA. Indication for ICA was based on CTA results. CTA images were reconstructed using both HIR and IMR during 75/78% phase of the RR interval. ICA was used as reference standard. The coronary arteries were segmented according to the 18-segment model of the Society of Cardiovascular Computed Tomography (SCCT). In total, 774 segments (237 with HIR, 254 with IMR and 283 with ICA) were evaluated by two readers. The stenosis degree of each segment was classified according to CAD-RADS with a score $\geq 3$ for significant stenosis. Image quality of HIR and IMR was evaluated by using 5-point rating scale and by measuring the signal-to-noise ratio (SNR) in the ascending aorta.
**Results** Prevalence of significant stenosis ranged between 17.9 and 20.2%. HIR provided sensitivity of 75%, specificity of 92.78%, PPV of 68.18% and NPV of 94.74%. IMR yielded 80% sensitivity, 94.9% specificity, 76.2% PPV, and 95.8% NPV. Very strong positive correlation for both HIR/ICA (0.847) and IMR/ICA (0.921) were observed using Spearman's coefficient of rank correlation. Greater area under the ROC curve was measured for IMR than for HIR (0.933 vs. 0.907, $p = 0.226$). Image quality was higher on IMR than on HIR images (IMR 4.1, HIR 3.4, $p = 0.07$) with SNR of 19.25 and 11.79 ($p < 0.001$), respectively.

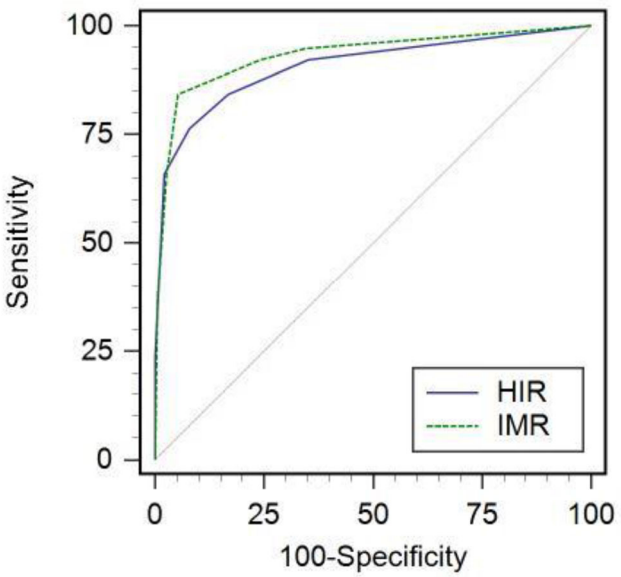


ROC curve

**Conclusion** IMR allows for slightly higher sensitivity than HIR in the diagnosis of significant CAD on CTA images, while no significant effect could be observed regarding overall diagnostic accuracy. The particular benefit of IMR is considered the superior image quality.

## A-125

### Combined coronary CT-angiography and TAVI planning: utility of CT-FFR in patients with morphologically ruled-out obstructive coronary artery disease

**R. Gohmann, P. Seitz, C. Luecke, M. Gutberlet**

Heart Center Leipzig at University of Leipzig, Department of Diagnostic and Interventional Radiology, Leipzig, Germany.

**Purpose/Objectives** To analyze the ability of machine learning (ML)-based CT-derived fractional flow reserve (CT-FFR) to correctly categorize coronary CT-angiography (cCTA) studies without obstructive coronary artery disease (CAD) acquired during pre-TAVI evaluation and to correlate recategorization to image quality and coronary artery calcium score (CAC).
**Methods & Materials** 116 patients without significant stenosis ($\geq$ 50% diameter) on cCTA as part of pre-TAVI CT were included. These patients were examined with an electrocardiogram-gated CT scan of the heart and high-pitch scan of the vascular access route. All patients were reevaluated with ML-based CT-FFR (threshold = 0.80) blinded to cCTA. Invasive coronary angiography served as the standard of reference.
**Results** ML-based CT-FFR was successfully performed in 94.0% (109/116) of all patients, including 436 vessels. With CT-FFR, 76 patients and 126 vessels were falsely reclassified as having significant CAD, respectively. With CT-FFR 2/2 patients but no vessels initially falsely classified by cCTA were correctly recategorized as having significant CAD. Reclassification occurred predominantly in distal segments. Virtually no correlation was found between image quality or CAC.
**Conclusion** Unselectively applied, CT-FFR may vastly increase the number of false positive ratings of CAD compared to morphological scoring. Recategorization was virtually independently from image quality or CAC and occurred predominantly in distal segments.

## A-126

### Multimodality assessment of early acute cardiac transplant rejection

**F. Lauriero[1], C. Loewe[2], P. Moser[2], A. Wielandner[2], A. Zuckermann[3], K. Uyanik-Uenal[3], D. Beitzke[2]**

[1]Catholic University of Sacred Heart, Department of Radiological and Hematological Sciences, Rome, Italy, [2]Medical University of Vienna, Department of Biomedical Imaging and Image guided Therapy, Vienna, Austria, [3]Medical University of Vienna, Department of Cardiac Surgery, Vienna, Austria.

**Purpose/Objectives** Acute cardiac allograft rejection (ACAR) is a severe complication of heart transplantation (HTx), responsible for 10% of deaths within the first three years after surgery. Furthermore, a history of ACAR is a risk factor for cardiac allograft vasculopathy (CAV) in the later course of HTx and confers higher mortality. Currently endomyocardial biopsy (EMB) is the gold standard screening technique performed to rule out rejection because of the lack of evidence on non-invasive diagnostic techniques. The presented data aims to identify cardiac magnetic resonance (CMR) and cardiac computed tomography angiography (CCTA) findings that could represent early changes occurring in ACAR focusing on the modifications of the epicardial and perivascular fat tissue.
**Methods & Materials** We present a subgroup analysis of patients included in an ongoing prospective cohort study for the evaluation of CMR in outcome prediction after HTx. Overall 93 patients were enrolled and were screened annually by CMR for five years. The CMR protocol included short tau inversion recovery (STIR) sequence, mapping and late gadolinium enhancement (LGE). Any CCTA performed during the same screening period was evaluated. Imaging findings were compared with histology results of screening EMBs based on the guidelines of the International Society for Heart and Lung Transplant (ISHLT).
**Results** Out of the cohort 7 patients were identified showing signs of epicardial fat inflammation as demonstrated by diffuse hyperintensity of fat tissue in STIR sequences and marked pericardial enhancement in LGE sequences. Mild subepicardial biventricular LGE was also evident in all the patients and two of them showed diffuse biventricular myocardial LGE. CCTAs of these patients showed diffuse changes in the perivascular fat in all the selected patients. ACAR was identified in at least one of the multiple screening EMBs in 6 patients, specifically 4 had a mild grade (1A/1R) and 2 had a severe grade (3A/3R). The latter corresponded to the patients with a diffuse biventricular myocardial LGE. Histology of the only patient without ACAR (0A/0R) was not completely negative as microvascular inflammation was described.


Severe acute cardiac allograft rejection (3A/3R): CMR shows "pericarditis-like " pattern with diffuse epicardial fat and biventricular subepicardial layer inflammation corresponding to high T2 signal intensity in STIR sequence (A) and marked delayed enhancement (B).

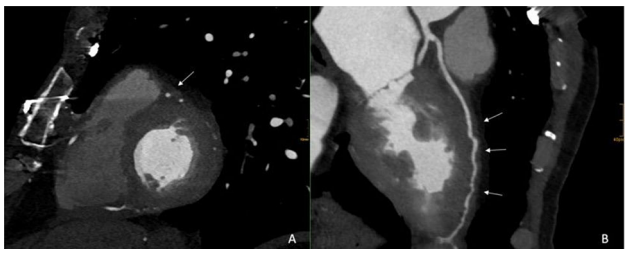


Severe acute cardiac allograft rejection (3A/3R): CT performed in the same patient shows perivascular inflammatory tissue along the course of LAD (arrows) replacing normal fat tissue.

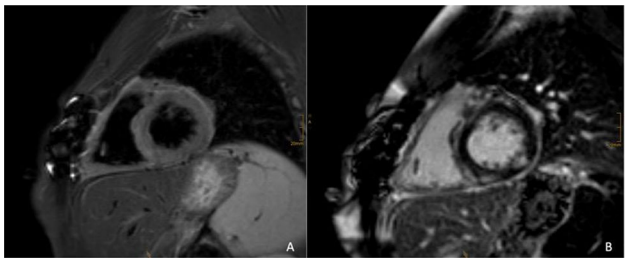

Mild acute cardiac allograft rejection (1A/1R): "pericarditis-like" pattern with a less prominent epicardial and biventricular myocardial inflammation as showed in STIR (A) and LGE (B) sequences.

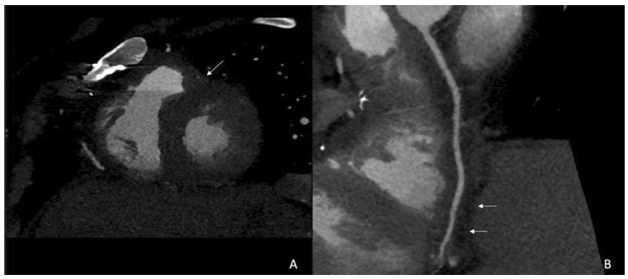

Mild acute cardiac allograft rejection (1A/1R): CT performed in the same patient shows increased attenuation values of the perivascular fat (arrows) around LAD (A) and along the course of RCA (B).

**Conclusion** Inflammation of epicardial and perivascular fat seems to be associated with ACAR. CMR shows a "pericarditis-like" pattern as demonstrated in STIR and LGE sequences. Involvement of biventricular myocardium also seems to correlate with more severe grades of rejection. CCTA, shows diffuse changes in the epicardial and perivascular fat due to the presence of inflammatory tissue. Overall, these imaging features should be considered as markers of ACAR, and if identified in an early stage may offer the possibility of further improving the course with a change of therapy.

## A-128

### Lipomatous hypertrophy of the atrial septum in cardiac magnetic resonance

**E. Schifano[1], M. Cè[1], D. Fazzini[2], M. Alì[2], S. Papa[2], F. Secchi.[1]**

[1]University of Milan, Diagnostic Imaging, Milan, Italy, [2]Centro Diagnostico Italiano, Unit of Diagnostic Imaging and Stereotactic Radiosurgery, Milano, Italy.

**Purpose/Objectives** Lipomatous hypertrophy of the atrial septum (LHAS) is a fatty infiltration, often found incidentally, dumbbell or hourglass shaped, of the interatrial septum sparing the fossa ovalis and is typically associated with elderly and obesity. LHAS has been reported to have not a clearly defined range of prevalence depending on diagnostic techniques used to detect this alteration. The aim of this retrospective study is to define prevalence of LHAS using cardiac magnetic resonance (CMR) and its correlation with age, sex or functional biventricular parameters.

**Methods & Materials** A total of 621 patients who underwent CMR from March 2020 to March 2022 were retrospectively evaluated. Inclusion criteria were the presence of a 4-chamber sequence and the presence of volume analysis. A reader reviewed all images to evaluate the presence of LHAS. For each patient with LHAS, atrial septum thickness was measured. Functional biventricular parameters of all patients were retrieved from the clinical report. Correlations between parameters were calculated using Spearman test.

**Results** Among the 619 patients included in the study, we found 241 (38.93%) patients with LHAS. 150 patients (24.23%) showed lipomatous deposition of the upper half of the atrial septum. The mean thickness of the atrial septum was 3 mm (range from 1 to 10 mm). In particular 147 (23.75%) patients present mild thickening (between 1–3 mm), 74 (11.95%) medium (4–6 mm) and 20 (3.23%) higher (7–10 mm). The mean age of patients with LHAS was 58 years old. The age distribution of patients with LHAS was: 9 patients (10,98%) under 30 years old, 121 (36.89%) between 31–59 years old and 111 (53.11%) over 60 years old. We found a significant negative correlation between the degree of LHAS and left ventricle end-diastolic volume ($r = -0.21$, $p < 0.001$) and systolic volume ($r = -0.20$, $p < 0.001$). We found a significant negative correlation between the degree of LHAS and right ventricle end-diastolic volume ($r = -0.25$, $p < 0.001$) and systolic volume ($r = -0.18$, $p < 0.001$).

**Conclusion** CMR is a useful method to detect LHAS, a benign disorder that in our series reached a 38.93% prevalence. A progressive increase of prevalence was seen with age in accordance with many studies. A significant negative correlation between LHAS and biventricular end-diastolic volumes according to a consecutive reduction of atrial and ventricular volumes in order to offset volumetric increase of atrial septum.

## A-130

### Augmenting double-rule-out CT to triple-rule-out CT through color mapping of the myocardium—development and validation in a multi-reader, multi-case study

**D. Winkel[1], M. Segeroth[1], S. Yang[1], J. Vosshenrich[1], H.-C. Breit[1], J. Wasserthal[1], J. Cyriac[1], P. Haaf[2], J. Bremerich[1]**

[1]University Hospital Basel, Clinic of Radiology & Nuclear Medicine, Basel, Switzerland, [2]University Hospital Basel, Clinic of Cardiology, Basel, Switzerland.

**Purpose/Objectives** Unexpected cases of acute coronary syndrome (ACS) may be encountered on double-rule-out CT performed to identify other causes of acute chest pain than ACS. We therefore aimed to assess, if additional attenuation-based myocardial color mapping improves the detectability of abnormalities in the sense of a triple-rule-out CT in patients with low-to-moderate ACS risk.

**Methods & Materials** 119 consecutive patients who underwent double-rule-out CT and invasive coronary angiogram (ICA, gold standard) within 48 h from 01/2016–10/2021 were included. CT and ICA reports were reviewed for presence/absence of vessel occlusion and myocardial ischemia/infarction. Using clinical information, patients were adjudicated to the presence of STEMI, NSTEMI or no evidence of ACS.

Following left ventricular myocardium segmentation by an in-house developed deep-learning algorithm, overlying color maps were created. Color-coding represented the difference in myocardial attenuation from the mean divided by the standard deviation on a voxel-level.

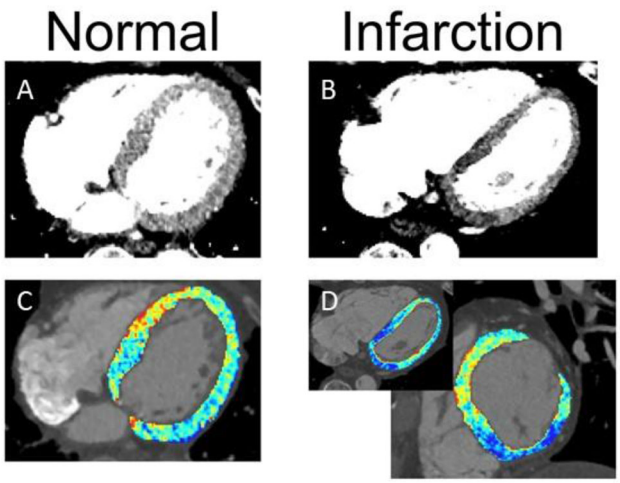


Figure showing a 4-chamber view of the heart from a double-rule out CT examinations without (A-B) and with (C-D) overlying colormaps (additional short axis view in D). A and C represent a case without myocardial abnormalities and a bland invasive coronary angiography (ICA), where B and C represent a case with transmural infarction of the inferior wall of the basis with a 100% occlusion of the RCA in the ICA.

Figure depicting the myocardium with and without overlying colormaps in two cases with and without a myocardial infarction.

CT examinations were re-assessed by two junior residents and two fellows blinded to reports and clinical information for the presence of myocardial abnormalities in a multi-reader, multi-case scenario with and without the use of additional color maps.

**Results** ICA confirmed vessel occlusion in 56% of patients (67/119; 22 STEMI, 45 NSTEMI). CT reports mentioned vessel occlusion or myocardial abnormalities in 32 cases (sensitivity: 43%; specificity: 94%). Myocardial ischemia/infarction was suspected in 77% of STEMI cases (17/22) and 27% of NSTEMI cases (12/45).

Re-assessment by the four readers showed an almost similar sensitivity for myocardial abnormalities compared to initial CT reports (40% vs. 43%). The use of color maps increased overall sensitivity to 53%. For STEMI cases, sensitivity increased from 41 to 60%, for NSTEMI cases from 39 to 45%. Mean overall specificity decreased from 76 to 67%, accuracy increased from 55 to 59%.

With regard to reader experience, color maps showed higher increases in sensitivity for fellows than for junior residents (STEMI: 23% vs. 14% increase; NSTEMI: 17% vs. 7% increase).

**Conclusion** The additional use of color maps improves the identification of myocardial infarction/ischemia when assessing double-rule-out CTs in patients with acute chest pain and a low-to-moderate pre-test probability for ACS.

## A-131

### High rate of identification of ruptured mitral valve prolapse on non-ECG gated chest CT

**S. M. Yoo, M. J. Son**

CHA University Bundang Medical center, Radiology, Bundang, South Korea.

**Purpose/Objectives** Primary imaging modality for mitral valve prolapse (MVP) is echocardiography supplemented by ECG-gated cardiac CT angiography. However, the authors have recently encountered multiple patients with ruptured MVP, initially indentified on non-ECG-gated chest CT (Image 1).

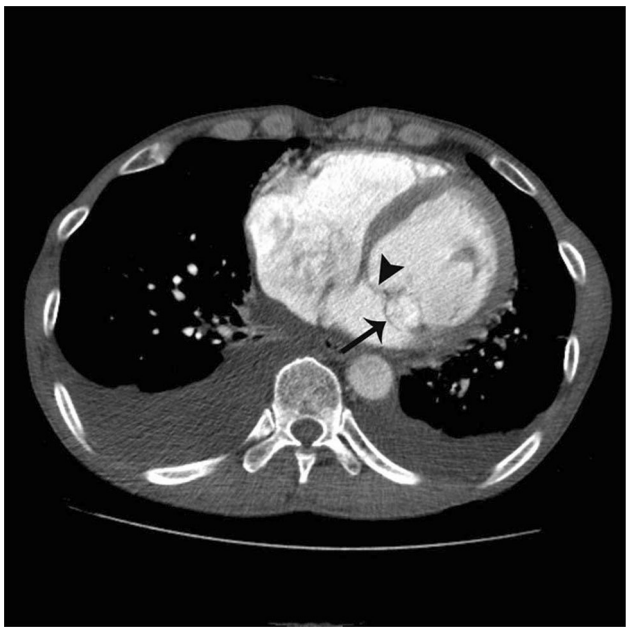

Typical asymmetrical double line sign on non-ECG gated chest CT in a 57-year-old male patient presented with acute heart failure. Initial diagnosis of MVP was made on the non-ECG-gated chest CT.

Notably, there has been no study regarding indentification of ruptured MVP on non-ECG-gated chest CT. Thus, the purpose of this study is to evaluate the diagnostic accuracy of non-ECG gated chest CT to identify MVP.

**Methods & Materials** We retrospectively evaluated non-ECG gated chest CT of 65 patients with surgically confirmed MVP [group 1 with chorda rupture (n = 50) and group 2 without (n = 15)]. Two blind readers analyzed CT findings of MVP [i.e., presence or absence of double-line sign (potential flailed leaflet) and localization for the culprit segment for MVP (i.e., A1, 2, 3 P1, 2, 3)] by consensus. Double line sign on axial CT (Image 2–4) was defined as presence of a linear valve structure, not located at the plane traversing the mitral annulus. Statistical analysis (SPSS Inc., Chicago, IL, USA) was performed using Fisher's exact or Chi-square, and Student's t-test for categorical and continuous variables, respectively. A statistically significant difference was defined as $p < 0.05$.

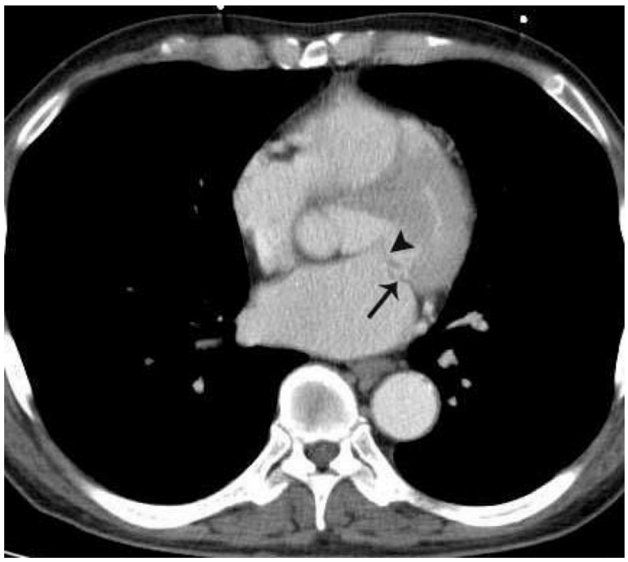

Typical asymmetrical double line sign is noted at the p1 mitral leaflet (arrow) on an axial non-ECG gated CT image. Note normal mitral leaflet (arrowhead) at the plane of mitral annulus.

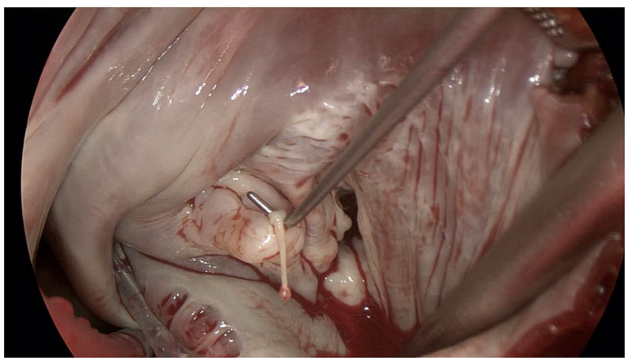

P1 chorda rupture is confirmed on operative field. This is the same patient with Image 1. Neochorda formation and mitral annuloplasty was performed in this patient.

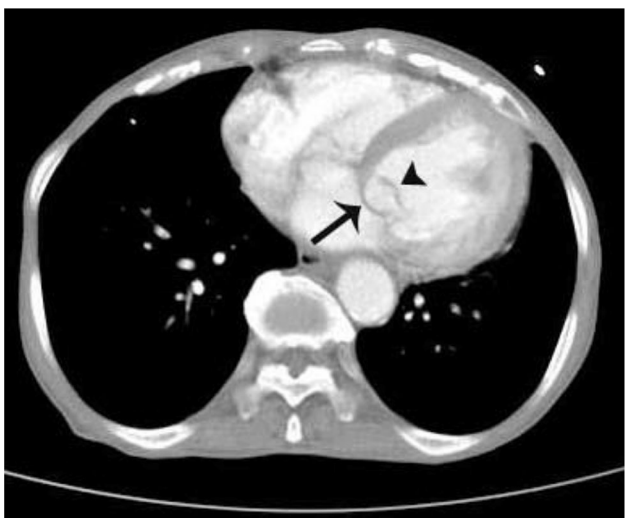

Typical asymmetrical double line sign is noted at the p3 mitral leaflet (arrow) on an axial non-ECG gated CT image. Note normal mitral leaflet (arrowhead) at the plane of mitral annulus.

**Results** Double line sign on non-ECG gated chest CT suggesting MVP was identified in 68% of group 1 (34/50) and 126.7% of group 2 (4/15) (p = 0.0068). Thus, presence of asymmetrical double line sign to identify rupture MVP on non-ECG-gated chest CT showed modest sensitivity [68% (34/50) and specificity 73.3% (11/15)], but high positive predictive value [89.5% (34/38)]. In contrast, discriminating power to localize culprit leaflet (i.e., A1, 2, 3 or P1, 2, 3) for MVP was poor (24.6%, 16/65) mainly due to motion blurring or overlapping anterior and posterior leaflet on axial CT images.
**Conclusion** Ruptured MVPs may be incidentally identified on non-ECG-gated chest CT. Thus, radiologists should check presence of asymmetrical double-line sign not to miss ruptured MVP on non-ECG-gated chest CT.

## A-132

### Cardiac motion detection using deep learning coronary artery segmentation and machine learning based feature extraction

**D. Winkel[1], M. Segeroth[1], J. Cyriac[1], S. Yang[1], J. Wasserthal[1], J. Vosshenrich[1], H.-C. Breit[1], P. Haaf[2], J. Bremerich.[1]**

[1]University Hospital Basel, Clinic of Radiology & Nuclear Medicine, Basel, Switzerland, [2]University Hospital Basel, Clinic of Cardiology, Basel, Switzerland.

**Purpose/Objectives** Motion artefacts are a possible cause for misinterpretation of coronary CTAs. Scans are therefore usually evaluated by a radiologist during image acquisition and, if necessary, repeated using a different acquisition mode.
We aimed to (semi-) automate this process through detection of motion artifacts using a deep learning-based coronary artery segmentation.
**Methods & Materials** All patients who had repeated coronary CT angiography acquisitions during one examination (n = 68) between 01/2010–10/2021 were included. An additional 74 negative controls were retrieved from the radiology information system. Cases were manually evaluated for motion artifacts.
Coronary arteries were manually segmented in 77 independent patients. Hereafter, a nnUNet was trained to automatically perform this task. All segmentations were reviewed for accuracy. The nnUNet was then applied to the study sample. Segmentation centerlines were extracted via skeleton algorithm from a python package (scikit-image). Number of connected volumes (CV), volumes of the CVs, centerline lengths, number of junctions and endpoints were extracted.

Diagnostic accuracy was assessed by receiver operating characteristics curves. Logistic regression analysis was used as a prediction model.
**Results** Automatic segmentation of coronary arteries worked well in patients without artifacts (training dice 0.89).

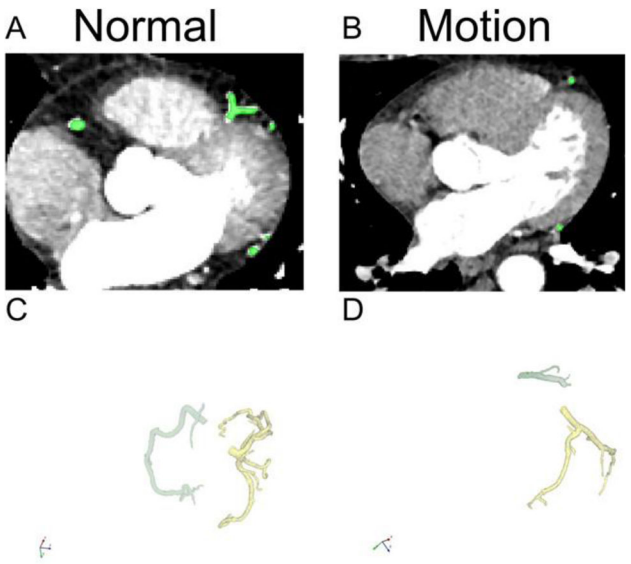


A) CTA without motion artefact and with segmentation of the coronary arteries. C) 3D visualization of the segmentation without motion. B) CTA with motion artefact and with failed segmentation in the right coronary artery. D) 3D visualization of the segmentation with motion disturbing the segmentation in the right coronary artery.

In cases with motion artifacts, segmentation was insufficient in the affected areas (n = 41).

Motion was confirmed in 54/142 of the cases (38%) partially in multiple areas. In 52 cases motion was described in the right coronary artery (96%), in 11 cases motion was detected in the left anterior descending artery (20%) and in 17 cases motion was observed in the ramus circumflexus (31%). With regard to cases classified as suffering from motion artifacts, the AUCs of mean centerline length and endpoint to endpoint were 0.58 (CI 0.67 to 0.49; p = 0.047) and 0.644 (CI 0.55 to 0.74; p = 0.001) compared to cases without motion. Number of CV and mean total volume of the segmentation amounted to an AUC of 0.69 (CI 0.59 to 0.78; $p < 0.001$) and 0.7 (CI 0.8 to 0.6; $p < 0.001$).

A logistic regression analysis combining the number of CVs, mean volume of the CVs, mean centerline length, number of junctions and number of endpoints revealed an AUC of 0.74 (CI 0.65 to 0.81; $p < 0.001$).

**Conclusion** The nnUNet is suitable for coronary artery segmentation and can be used to (semi)- automate the process of motion artifact detection in conjunction with a logistic regression analysis for predictive modelling.

## A-135

### High negative predictive value of pre-TAVI CT-based calculation of fractional flow reserve (FFRCT) compared to invasive catheter angiography

**N. Riedel[1], S. Klömpken[1], H. Brunner[1], S. Schmidt[1], C. Panknin[2], C. Buck[3], D. Buckert[3], M. Beer[4]**

[1]Ulm University Medical Center, Department of Diagnostic and Interventional Radiology, Ulm, Germany, [2]Siemens Healthineers, Scientific Collaborations, Erlangen, Germany, [3]Ulm University Medical Center, Department of Internal Medicine II, Ulm, Germany, [4]University Hospital Ulm, Department for Radiology, Ulm, Germany.

**Purpose/Objectives** Comparison of technical feasibility and diagnostic accuracy of fractional flow reserve from coronary computed tomographic angiography compared to invasive catheter angiography (ICA) in patients prior TAVI procedures.

**Methods & Materials** This retrospective analysis included 134 patients (63 male, 71 female; mean age 81.8 yrs). 33 patients had to be excluded due to image artefacts due to steps (36,4%) or mitral clipping (12,1%), due to system errors (6,1%), bypass grafts (18,2%), coronary anomalies (18,2%) or missing ICA reports (9,1%). $FFR_{CT}$ values were obtained using a deep learning based non-commercial research prototype (cFFR Version 3.5.1, Siemens Healthineers), which allows on site $FFR_{CT}$ computation with minimal interaction. The measurements were compared with ICA (stenosis definition in percent).

**Results** Technical success rate was overall 75,7%. In 25 randomly selected patients the mean processing time was 8.8 min (3–20 min). 91,6% of vessels could be analyzed (exclusion of 33/370 vessels due to stents (32) and to one stenosis that was visible but could not be measured. Sensitivity, specificity, PPV and NPV were 0.63, 0.89, 0.42, 0.95. Direct comparison between CTCA and ICA showed high significance.

**Conclusion** Non-invasive CTFFR allows to rule out obstructive coronary artery disease with a high NPV in patients prior TAVI. Thus, TAVI CT might be an integrative planning tool (one-stop-shop assessment) not only concerning aortic anatomy plus vessel access but also for coronary status.

## A-138

### Combined coronary CT-angiography and TAVI planning for ruling out significant coronary artery disease: added value of machine-learning–based CT-FFR

**R. Gohmann, P. Seitz, M. Gutberlet, C. Luecke**

Heart Center Leipzig at University of Leipzig, Department of Diagnostic and Interventional Radiology, Leipzig, Germany.

**Purpose/Objectives** The purpose of this study was to analyze the ability of machine-learning (ML)-based computed tomography (CT)-derived fractional flow reserve (CT-FFR) to further improve the diagnostic performance of coronary CT-angiography (cCTA) for ruling out significant coronary artery disease (CAD) during pre-transcatheter aortic valve implantation (TAVI) evaluation in patients with a high pre-test probability for CAD.

**Methods & Materials** Overall, 460 patients (age 79.6 ± 7.4 years) undergoing pre-TAVI CT were included and examined with an electrocardiogram-gated CT scan of the heart and high-pitch scan of the vascular access route. Images were evaluated for significant CAD. Patients routinely underwent ICA (388/460), which was omitted at the discretion of the local Heart Team if CAD could be effectively ruled out on cCTA (72/460). CT examinations in which CAD could not be ruled out ($CAD^{+}$) (n = 272) underwent additional ML-based CT-FFR.

**Results** ML-based CT-FFR was successfully performed in 79.4% (216/272) of all CADþ patients and correctly reclassified 17 patients as CAD negative. CT-FFR was not feasible in 20.6% because of reduced image quality (37/56) or anatomic variants (19/56). Sensitivity, specificity, positive predictive value, and negative predictive value were 94.9%, 52.0%, 52.2%, and 94.9%, respectively. The additional evaluation with ML-based CT-FFR increased accuracy by

Dþ3.4% ($CAD^+$: $\Delta + 6.0\%$) and raised the total number of examinations negative for CAD to 43.9% (202/460).
**Conclusion** ML-based CT-FFR may further improve the diagnostic performance of cCTA by correctly reclassifying a considerable proportion of patients with morphological signs of obstructive CAD on cCTA during pre-TAVI evaluation. Thereby, CT-FFR has the potential to further reduce the need for ICA in this challenging elderly group of patients before TAVI.

## A-140

### Changes of cardiac length and center along the z-axis in coronary CT-angiography: influence of cardiac phase and respiration

R. Gohmann, P. Seitz, C. Luecke, M. Gutberlet.
Heart Center Leipzig at University of Leipzig, Department of Diagnostic and Interventional Radiology, Leipzig, Germany.

**Purpose/Objectives** Precise knowledge of the position of the heart along the z-axis in addition to its influencing factors and their magnitude is of paramount importance during cardiac CT for any indication. Only with this, precise and yet robust planning of cardiac exams with optimal radiation dose efficiency is possible.
The objective was to quantify the influence of cardiac phase and breathing state on cardiac length and center during coronary CT-angiography.
**Methods & Materials** 1607 patients undergoing CT for pre-transcatheter aortic valve implantation evaluation were included retrospectively. All patients concomitantly received a retrospectively ECG-gated helical CTA of the heart in inspiration and a non-ECG gated high-pitch-CTA of the torso in free breathing.
For the ECG-gated scan, reconstructions at 70% of the RR-interval (diastole) and 350 ms post R (systole) were analyzed. In the non-ECG gated scan, the mitral valve was characterized as either open or closed as a surrogate for cardiac phase. In both scans the table positions of the most cranial and most caudal point of the coronary arteries were recorded for the analyzed phases. Cardiac length was calculated as the difference between table positions; cardiac center was calculated as the mean of both table positions.
**Results** Mean cardiac length differed significantly between diastole and systole (97.7 ± 9.1 mm, 92.3 ± 8.8 mm, $p < 0.0001$). The cardiac center shifted caudally from diastole to systole by 0.9 ± 1.7 mm ($p < 0.0001$).
In subgroup analysis of patients examined in diastole and systole in the high-pitch-scan, the cardiac center shifted cranially from inspiration to free breathing by 7.1 ± 7.5 mm ($p < 0.0001$) and by 7.2 ± 7.9 mm ($p < 0.0001$), respectively.
**Conclusion** Cardiac length was largest in diastole and smallest in systole and the cardiac center shifted minutely between cardiac phases. The influence of respiration on cardiac position along the z-axis was much larger than the change of position between cardiac phases, but respiration did not influence cardiac length.

## A-143

### Effect of papillary muscle and trabeculae on left ventricular function analysis using CT

D. Kang, M. Kim

Ajou University School of Medicine, Radiology, Suwon, South Korea.

**Purpose/Objectives** To obtain standard value of the proportion of papillary muscle and trabeculae using cardiac CT in normal adults, and to find out how the inclusion or exclusion of papillary muscle and trabeculae affect left ventricular (LV) functional parameters depending on the patient group.
**Methods & Materials** From September 2019 to March 2022, 288 normal controls were collected by balancing age and sex among cardiac CT performed with health check-up. Among the patients who underwent cardiac CT during the same period, 102 hypertrophic cardiomyopathy (HCMP) patients, 55 dilated cardiomyopathy (DCMP) patients, and 201 old myocardial infraction (MI) patients were collected as patient group. LV function was measured in two ways of standard (ST) Simpson's method and threshold-based blood volume (BV) method based on attenuation differences between contrast in the LV cavity and the myocardium. We compared LV functional parameters and LV mass index (LVMI) measured by two methods according to sex and age group in normal control group, and according to disease entities in patient group. A comparison of parameters according to sex and age group was performed using an independent t-test and one-way ANOVA, respectively. A comparison of parameters measured by two methods in each group was performed using a paired t-test.
**Results** In normal control group, LV ejection fraction (LVEF) measured by BV method was higher (73.2 ± 4.9 vs. 67.7 ± 6.8%, $p < 0.001$) than the LVEF measured by ST method. The proportion of papillary muscle and trabeculae to LV mass (LVM) was 20.2 ± 4.3%, and was not statistically different between male and female. LVMI in male group was higher compared with female group in both methods. LV end-diastolic volume index (LVEDVI) and LVMI measured by both methods were not statistically different according to age group.
In patient group, LVEF measured by BV method in DCMP and old MI patients were higher than the LVEF measured by ST method. However LVEF measured by both methods were not statistically different ($p = 0.435$) in HCMP patients. Diagnosis of LV systolic dysfunction and LV enlargement were significantly decreased (35.9% vs. 29.6%, $p < 0.001$ and 37.8% vs. 22.7%, $p < 0.001$, respectively) with BV method compared with ST method. The proportion of papillary muscle and trabeculae to LVM was not statistically different between normal control group and HCMP patients ($p = 0.706$), and between normal control group and LV hypertrophy patients ($p = 0.261$).
**Conclusion** The proportion of papillary muscle and trabeculae to LVM is 20.2 ± 4.3%, and significantly affects disease diagnosis. However, the proportion of papillary muscle and trabeculae to LVM was not statistically different in HCMP and LV hypertrophy patients compared with normal control group.

## A-147

### Role of cardiac magnetic resonance in detection of myocardial damage in COVID-19 and related cardiac complications

D. Filatova[1], V. Sinitsyn[1], E. Mershina[1], E. Pavlikova[1], M. Lisitskaya[1], R. Myasnikov[2]

[1]Lomonosov Moscow State University Hospital, Radiology, Moscow, Russian Federation, [2]National Medical Research Center for Therapy and Preventive Medicine, Moscow, Russian Federation.

**Purpose/Objectives** Acute myocardial damage is known as one of the clinical manifestations of the new coronavirus disease caused by SARS-CoV-2. It is reported that about 20% of hospitalized patients

show evidence of cardiac damage. However, many aspects of myocardial damage in COVID-19 remain unclear. Cardiac magnetic resonance (CMR) is one of the most important tools for detection and characterization of myocardial diseases.
The purpose of the study was to analyze the frequency of post-COVID-19 myocardial damage and associated cardiac pathology such as arrhythmias and cardiac remodeling.
**Methods & Materials** The retrospective study included 58 patients (mean age 50.9 ± 13.2 years, male/female ratio 1:1) recovered from COVID-19 infection. They underwent CMR with intravenous contrast enhancement with a referral diagnosis of possible COVID-related myocarditis. The period between the recovery and the CMR ranged from 1.3 to 17 months; the patients were divided into three groups: up to 3 months; 3 to 6 months; more than 6 months.
**Results** In the whole group of patients the CMR signs of COVID-related myocardial damage were found in 16 (27.5%) cases. The frequency of myocardial damage was highest (42.9%) in patients studied 3–6 months after recovery. There were no correlation between the severity of coronavirus infection and the frequency of myocarditis signs detected by CMR. The severity of the disease did not correlate with the incidence of supraventricular and ventricular arrhythmias and heart block in patients with COVID-19-induced myocardial damages. There was also no correlation between the severity of infection and signs of left ventricle remodelling and disfunction.
**Conclusion** The study confirms a relatively high incidence of myocardial damage after COVID-19. The severity of COVID-19 infection was not related to the occurrence of myocardial damage signs on CMR and associated cardiac arrhythmias. CMR is a principal diagnostic tool for diagnosis of COVID-associated myocardial damage.

## A-149

### Prognostic role of coronary-CT in the stratification of patients with hepatic steatosis

**L. Evangelista[1], A. Bracci[1], A. Cirella[2], C. Balsano[2], A. Arceri[1], C. Acanfora[1], F. Sgalambro[1], P. Palumbo[1], E. Di Cesare[1], C. Masciocchi[1]**

[1]University of L'Aquila, Department of Applied Clinical Sciences and Biotechnology, L'Aquila, Italy, [2]University of L'Aquila, Department of Clinical Medicine, Life, Health & Environmental Sciences-MESVA, L'Aquila, Italy.

**Purpose/Objectives** To evaluate the prognostic value of coronary Calcium Score in patients with hepatic steatosis undergoing cardiac CT.
**Methods & Materials** This is a retrospective analysis of 122 patients (47 females and 73 males) underwent cardiac CT in the period between 2017 and 2021. Images were acquired with a cardiosynchronized prospective technique on Toshiba Aquilion 320slices-CT scanner (100 kV, 46mAs, 0.35 s × 0.5 mm × 280). Examination were considered reclutable for the study if the acquisition volume included liver and spleen in lower edge of FOV. Calcium Score (CS) by Agatston score, severity of coronary lesion by coronary CT angiography (classified according to AHA), fatty liver (in terms of density in HU, and classified as minimal, mild, moderate, severe) and the degree of liver fibrosis (using FIB4, calculated with a special formula) were collected. Extent of CAD was classified according to the CS value in absent, minimal, mild, moderate, and severe. The extent of steatosis was calculated by the ratio of hepatic and splenic density (cut-off < 1).
**Results** Mean CS was 619.4 ± 886. Mean liver-to-splenic density ratio was 2.8 ± 2.9. 37 out of 122 pts showed a ratio < 1. Fifteen out of 122 patients showed severe CAD, 34 moderate CAD, 12 mild, and 7 minimal. According to the Pearson correlation index, Agatstone score has a very high correlation with the degree of steatosis ($p < 0.004$), while the severity of coronary lesion correlates with the degree of fibrosis only in males ($p < 0.05$).
**Conclusion** Hepatic steatosis could represent an easily identifiable marker which correlate with coronary calcium amount, and thus useful to define a potential additional risk of CAD. More data however need to clarify the correlation of CT-derived liver injury marker and CAD severity, especially in male patients.

## A-150

### Non-coronary cardiac findings in non-emergent CT coronary angiography—a pictorial review

**I. Sousa**

Hospital das Forças Armadas, Radiology Department, Lisboa, Portugal.

**Purpose/Objectives** To review the non-coronary cardiac findings depicted in non-emergent coronary CT performed to evaluate coronary anatomy or atherosclerotic disease: the anatomical variants or incidental findings without clinical significance and also the signs of pathologic processes.
**Methods & Materials** The examinations were performed in a 64-slice-MDCT, with iodinated contrast injection and ECG-gated prospective or retrospective acquisitions (depending on the heart rate control) after sublingual nitroglycerin and intravenous esmolol (when needed) and, in certain cases, after metoprolol *per os*. Images were collected from the PACS archive.
**Results** Several non-coronary cardiac findings were shown in these examinations, regarding: the valves (vegetation of the mitral valve; caseous mitral annular calcification; bicuspid aortic valves—calcified and non-calcified; biological aortic valve replacement); the myocardium (left ventricular hypertrophy with apical aneurysm in hypertrophic cardiomyopathy; diverticula of the interventricular septum; myocardial crypts; sequelae of ischemic disease, such as subendocardial lipomatous metaplasia and myocardial thinning and calcification); the interatrial septum (very frequent channel-like morphology), the left atrium (focal calcification of its walls and stenosis of the left lower lobe pulmonary vein following atrial fibrillation radiofrequency ablation; wall diverticula and accessory appendages), the pericardium (effusion; calcification); the deposition of fat (non-pathological—in the papillary muscles and chordae tendineae of the left ventricle, in the moderator band of the right ventricle, lipomatosis of the interatrial septum, patchy deposition of fat in the apex of the left ventricle; as sequela of ischemic disease in the left ventricle, as previously described; in possible context of ancient myocarditis with sub-epicardial and middle-wall distribution in the left ventricle).

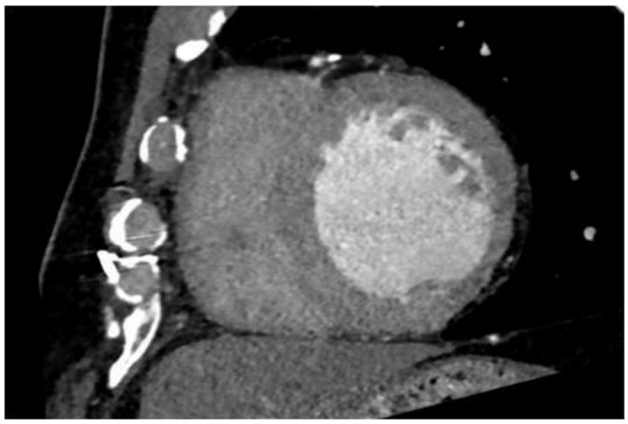

Short-axis view depicting thinning of the inferolateral wall of the left ventricle, post ancient myocardial infarction.

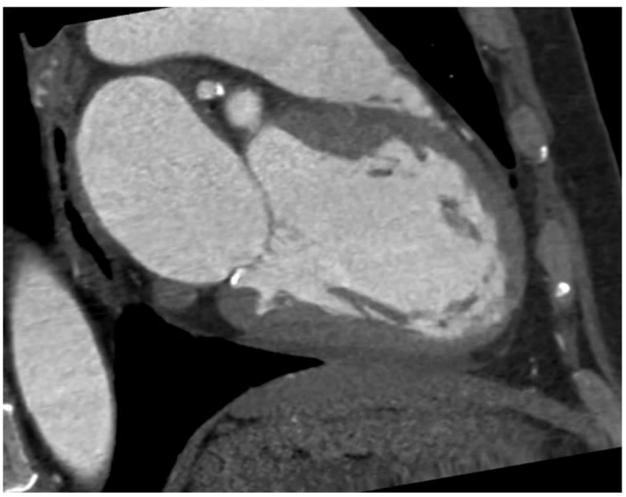

Long-axis angulated view showing a myocardial crypt in the basal segment of the inferior wall of the left ventricle.

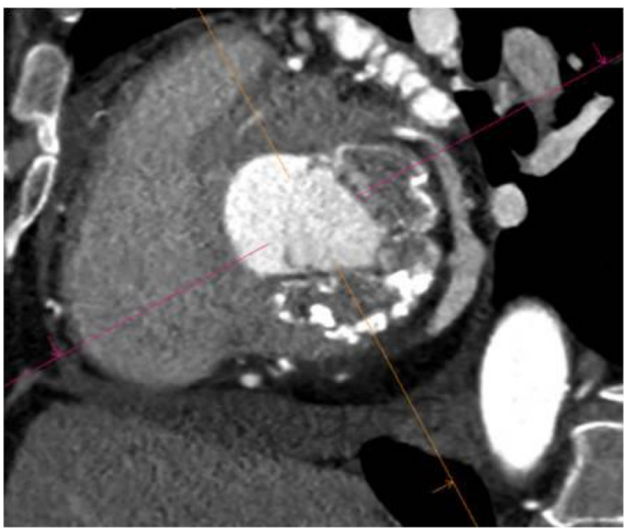

Short-axis view depicting caseous mitral annular calcification.

**Conclusion** It is important for radiologists performing coronary CT to recognize and be able to characterize, not only the coronary findings, but also the normal variants of cardiac anatomy or morphology without clinical implications and the non-coronary cardiac findings that might have clinical importance and prompt further investigation.

## A-152

### Preliminary evalutations impact of sarcopenia, muscolar and adipose masses in patients with cardiac transplantation, using pre-procedural CT scan images

**E. Bozzo, G. A. Strazzarino, D. Tore, A. Biondo, I. Landolfi, C. Centaro, F. Piroli, F. Ullo, S. Sara, A. Depaoli, R. Faletti, P. Fonio**

Città della Salute e della Scienza di Torino, Diagnostica per immagini, Torino, Italy.

**Purpose/Objectives** To evaluate the impact of sarcopenia, visceral and subcutaneous adipose tissue in patients undergoing cardiac transplantation, evaluated on pre-procedural CT scans.

**Methods & Materials** Monocentric retrospective study on 72 patients. The maximum time lapse between pre-procedural CT and transplantation was 12 months. Manual segmentations of abdominal skeletal muscles, subcutaneous adipose tissue (SAT), and visceral adipose tissue (VAT) were performed using the open-source software 3D Slicer on CT images at the level of the mid third (L3) and mid fourth (L4) lumbar vertebrae.

We adopted two radiologic sarcopenia definitions by the European Working Group on Sarcopenia in Older People (EWGSOP), namely psoas muscle area at the L4 vertebra level (PMA-sarcopenia) and indexed skeletal muscle area at the L3 vertebra level (SMI-sarcopenia).

The primary endpoint was long-term all-cause mortality; secondary endpoints were dialysis, mechanical circulatory support (MCS), early graft disfunction (EGD), primary graft disfunction (PGD).

**Results** SMI- and PMA-sarcopenia were present in 60 (82%) and 37 (52%) patients, respectively.

A statistically significant association was found between VAT and EGD ($p = 0.048$). No other statistically significant associations were found between muscular and adipose masses and outcomes.

**Conclusion** The only significant association found may be due to the relatively small sample size and high heterogeneous time lapses between pre-procedural CT and transplantation. Moreover, clinical conditions of such patients could change quickly leading cardiac cachexia making a CT scan acquired a few weeks before not representative of clinical conditions at the time of transplantation.

Multicentric studies on a bigger number of patients with a shorter time lapse between CT and transplant may highlight a prognostic role for sarcopenia and adipose tissue masses in the setting of heart transplant.

## A-154

### Dynamic myocardial perfusion CT: impact of different reconstruction algorithm

**A. Senatieri[1], G. Muscogiuri[2], G. Chierchia[1], E. Collaku[3], M. Tomaselli[4], D. Muraru[4], P. Marra[5], P. Bonaffini[5], D. Ippolito[6], S. Annibali[5], L. Badano[7], S. Sironi[8]**

[1]Università degli Studi di Milano Bicocca, Radiology, Milan, Italy, [2]Università degli Studi di Milano Bicocca—Istituto Auxologico

Italiano, Radiology, Milan, Italy, [3]Università degli Studi di Milano Bicocca, Radiology, Bergamo, Italy, [4]Istituto Auxologico Italiano, Cardiology, Milan, Italy, [5]ASST Ospedale Papa Giovanni XXIII, Radiology, Bergamo, Italy, [6]Ospedale San Gerardo—ASST Monza, Radiology, Monza, Italy, [7]Università degli Studi di Milano Bicocca—Istituto Auxologico Italiano, Cardiology, Milano, Italy, [8]Università degli Studi di Milano Bicocca—ASST Ospedale Papa Giovanni XXIII, Radiology, Bergamo, Italy.

**Purpose/Objectives** To evaluate the impact of different degrees of Adaptive Statistical Iterative Reconstruction (ASiR-V) algorithm on the reproducibility of myocardial blood flow (MBF) values in Dynamic Myocardial Perfusion CT (CTP).

**Methods & Materials** Twenty patients underwent dynamic CTP between January and May 2022. Images were reconstructed using ASiR-V 100%, 80%, 60%, 40%, 20%, 0%. In every patient, MBF values were analysed for every myocardial segment for every different degree of ASiR-V algorithm. Moreover, in eight patients relative MBF has been calculated for every different degree of ASiR-V algorithm. Statistical analysis was performed using Wilcoxon and Friedman tests. A p value less than 0,01 has been considered significant. Image noise of CTP and overall quality was evaluated through a four-point Likert score for every different degree of ASiR-V algorithm, subsequently data were analysed using paired samples t-test. A p value less than 0,01 has been considered significant.

**Results** Considering 100% ASiR-V as gold standard for CPT reconstruction and interpretation, no statistically significant difference was observed between MBF values obtained analysing images reconstructed using ASiR-V from 0 to 80% ($p > 0,01$) and MBF values obtained using ASiR-V 100%. Relative MBF calculated showed no significant differences between values obtained using ASiR-V algorithm from 0 to 80% and values obtained using 100% ASiR-V algorithm.

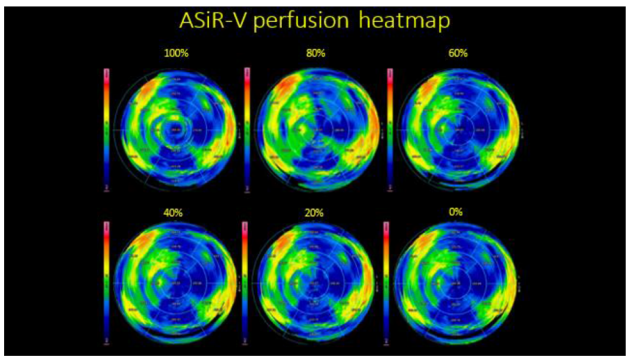


Perfusion bullseye heatmaps of the left ventricle obtained frome the same CTP acquisition reconstructed with different degrees of ASiR-V algorithm from 0% ASiR-V (only filtered back projection) to 100% ASiR-V.

A progressive increase of image quality due to noise reduction has been observed for images reconstructed through 0% to 60% ASiR-V ($p < 0,01$), although no qualitative difference has been noticed between 80 and 100% ASiR-V ($p > 0,01$).

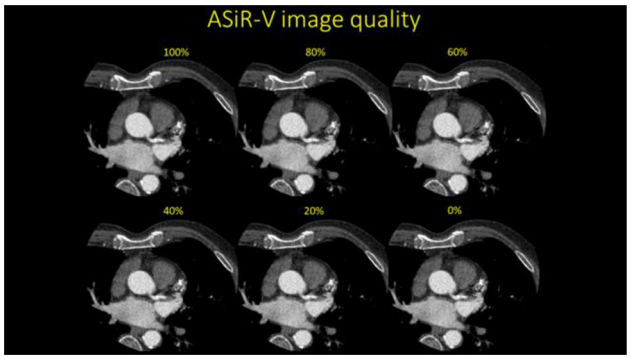


Same image obtained during CTP scan reconstructed with different degrees of ASiR-V algorithm. From 0% ASiR-V (only filtered back projection) to 100% ASiR-V there is a noticeable progressive improvement in subjective image quality due to image noise reduction.

**Conclusion** CTP obtained MBF values are not influenced by different degrees of ASiR-V algorithm used and ASiR-V proved to progressively increase image quality due to reduction of image noise. Moreover, relative MBF is preserved with every different degree of ASiR-V algorithm used. Those results, despite the small sample size, demonstrated that it would be feasible to reduce radiation dose increasing strength of iterative reconstruction.

## A-155

### Differences between systolic and diastolic phase in plaque characterization in patients with heart rate ≤ 80

**G. Chierchia[1], G. Muscogiuri[1], E. Collaku[1], A. Senatieri[1], D. Muraru[2], P. Marra[3], P. Bonaffini[3], D. Ippolito[4], S. Annibali[3], L. Badano[2], S. Sironi[3]**

[1]Ospedale Auxologico San Luca-Università degli Studi Milano-Bicocca, Radiology, Milano, Italy, [2]Ospedale Auxologico San Luca-Università degli Studi Milano-Bicocca, Cardiology, Milano, Italy, [3]ASST Ospedale Papa Giovanni Paolo XXIII, Bergamo-Università degli Studi Milano-Bicocca, Radiology, Bergamo, Italy, [4]Ospedale S. Gerardo-Università degli Studi Milano-Bicocca, Radiology, Monza, Italy.

**Purpose/Objectives** Evaluate the differences in plaque characterization between systolic and diastolic phase in patients with heart rate ≤ 80.

**Methods & Materials** 49 patients with cardiac frequency ≤ 80, BMI ≤ 28 and suspicion coronary artery disease have been recruited. They have been divided in two groups respectively of 23 patients with heart rate between 65 and 80 (group A) and of 26 patients with heart rate < 65 (group B). A plaque analysis has been performed in both the systolic (40–50% of the R-R interval) and diastolic phases (70–80% R-R), extracting volumes for total, non-calcific (NCP), calcific and lipid-rich plaques and the plaque remodeling index (PRI).

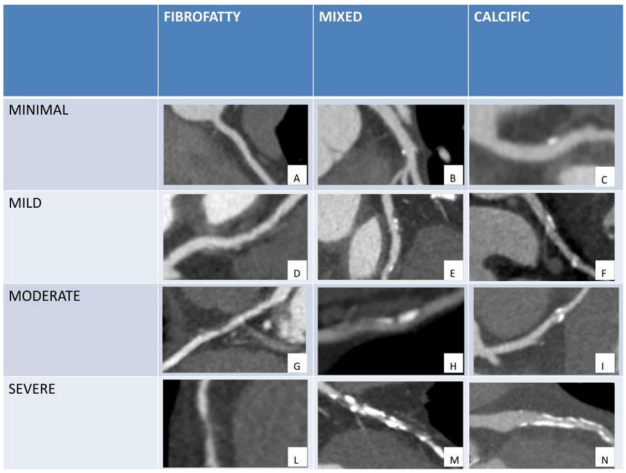


Examples of various degree of stenosis with different plaque composition; on the first row we can see minimal stenosis, on the second row mild stenosis, on the third one moderate stenosis and on the fourth one severe stenosis, each with an example of fibrofatty, mixed and calcific plaque. for each coronary segment and vessel (right coronary artery: RCA, left anterior descendant: LAD and circumflex artery: LCX), using a dedicated plaque assessment software (CVI42).

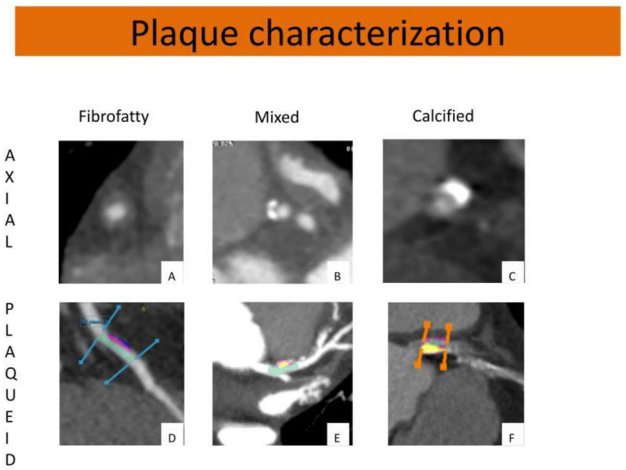


Plaques on axial view and examples of plaque assessment using post processing software: fibrofatty plaque in purple, low density plaque in blue, calcified plaque in yellow, green for viable vessel lumen.

Data were analyzed using Wilcoxon test. A p value $< 0,05$ has been considered significant.

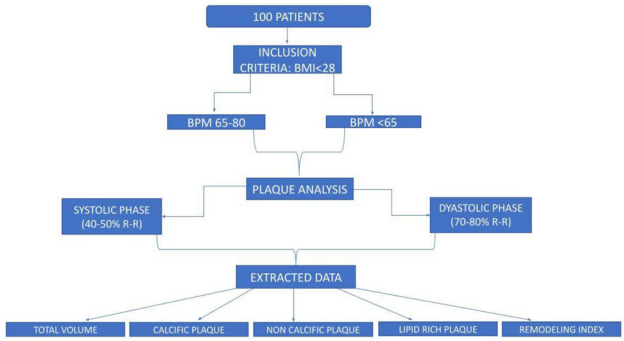


Flowchart showing inclusion criteria, group division of patients and information extracted with post-processing software.

**Results** The segmentary analysis has not shown significant differences in terms of plaque characteristics between systolic and diastolic phases, except for the first marginal branch in group A, in which a P = 0.02 for total volume, P = 0.01 for NCP and a P = 0.003 for lipid rich plaque has been found and for the PRI of the first diagonal branch of group B with P = 0.03. The vessel analysis hasn't shown any significant difference ($p > 0,05$) between phases of both group except for one significative difference in NCP volume of LAD of group B with $p = 0,02$.

**Conclusion** The plaque analysis in patients with bpm $\leq$ 80 has not t shown significant differences in terms of plaque characteristics except for the first marginal in group A and for NCP of LAD in group B. Those results, even if affected by the small sample size, underline how plaque characteristics are marginally influenced by different phases of the cardiac cycle, however a study with a huge numbers need to be performed.

## A-159

### Cardiac magnetic resonance in evaluation and differentiation of various left ventricular hypertrophy types

**M. Ishchenko, M. Tregubova, Y. Vitkovskyi**

Amosov national institute of cardiovascular surgery, Radiology department, Kyiv, Ukraine

**Purpose/Objectives** Left ventricular hypertrophy is defined as an increase in left ventricular myocardial mass or wall thickening. These changes are quite common in clinical practice and the differentiation of pathological left ventricular hypertrophy from physiological can be difficult, but it is crucial for further management.

The aim of the study was to describe the typical radiological features of various left ventricular hypertrophy types and to depict the diagnostic approach when you examine a patient with left ventricular hypertrophy.

**Methods & Materials** Left ventricular hypertrophy defined as a wall thickening > 11 mm measured in the end-diastolic phase of the cardiac cycle or an increase in left ventricular myocardial mass.
The main causes are presented below:

1. Hypertrophy can be the result of physiological adaptation to training (the so-called "athlete's heart").
2. Increased afterload (e.g., hypertension, aortic stenosis or coarctation).
3. Hypertrophic cardiomyopathy.
4. Storage diseases (amyloidosis, Fabry disease).

Hypertrophy can be symmetric (like in amyloidosis) and asymmetric (like in HCM).

Cardiac MRI is currently the gold standard for accurately assessing myocardial mass, volume, and function.

**Results Hypertrophic cardiomyopathy (HCM)** is the most common genetic disease of the heart muscle (prevalence ~ 1: 500 to 1: 200) and is the leading cause of sudden cardiac death in young people.

HCM is characterized by a thickening of the LV wall ≥ 15 mm in one or more segments of the myocardium, which is not explained solely by abnormal loading conditions.

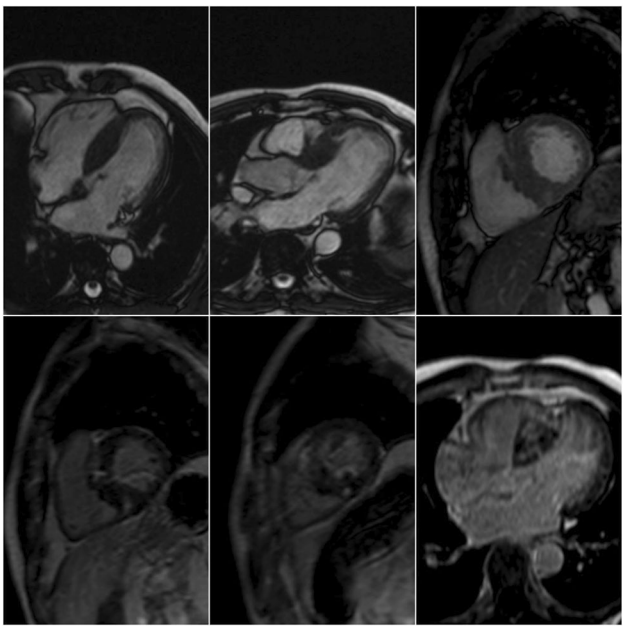

Hypertrophic cardiomyopathy in a man 40 years old. At MRI we see the pronounced asymmetric hypertrophy of a LV myocardium. Global LV function is good. Hypokinesia of IVS at the basal and middle levels was noted. Focal and cloud-like contrast enhancement is observed in the areas of greatest hypertrophy during LGE. Amosov NICVS/Kyiv, Ukraine.

**Athlete's heart** Physiological adaptation to regular, intense training can result in an increase in the size of the heart chambers and an increase in the mass of the LV myocardium or thickening of its walls. In athletes cardiac MRI helps to differentiate between HCM and the athlete's heart.

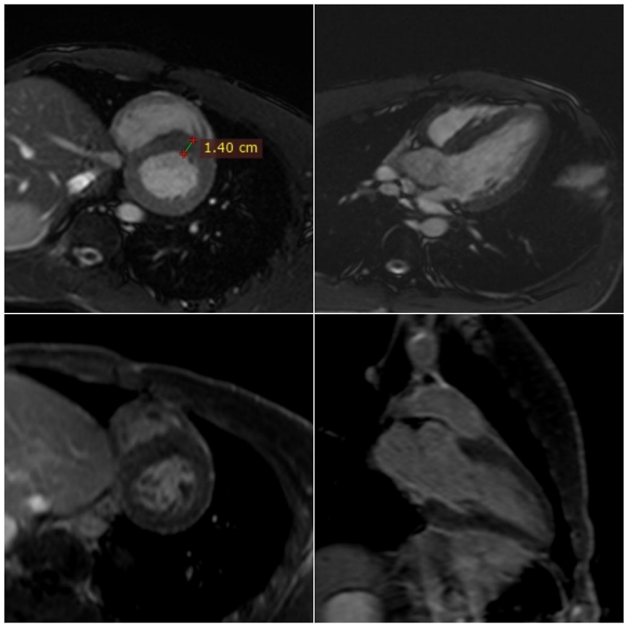


Athlete's heart in a 25-year-old man who is a professional football player. At cardiac MRI we see thickening of LV myocardium in a site of IVS to 14 mm. LV dysfunction was not detected. There was a slight dilatation of the LV. No signs of contrast enhancement were detected during LGE. Amosov NICVS/Kyiv, Ukraine.

**Cardiac Amyloidosis** Cardiac amyloidosis is a rare systemic disease characterized by progressive myocardial infiltration with amyloid deposits. As a result of this infiltration, there is a thickening of the myocardial wall and manifestations of heart failure.

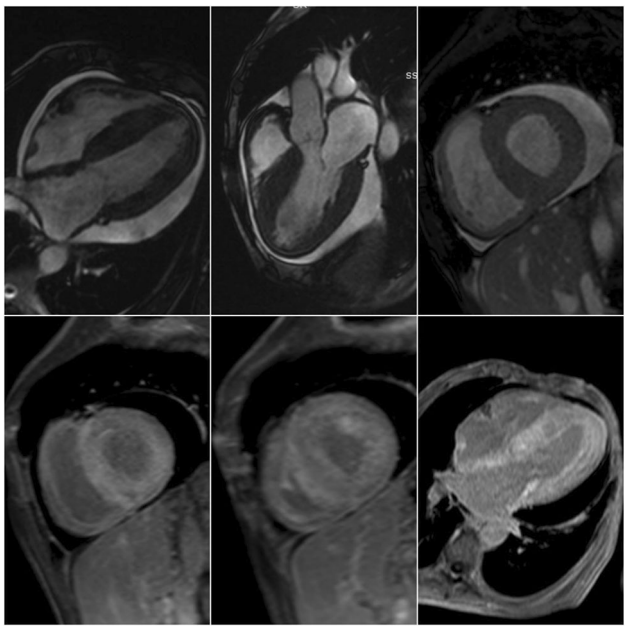

Cardiac amyloidosis in a 48-year-old man. At MRI we could see the pronounced concentric hypertrophy of a myocardium of LV and RV. The selection of the inversion time (TI) was complicated. On LGE we

see diffuse mainly subendocardial and less intromyocardial contrast enhancement in all chambers of the heart. Amosov NICVS/Kyiv, Ukraine.

**Pressure-loaded hypertrophy (arterial hypertension and aortic stenosis)**

Probably the most common variants of LV hypertrophy. Aortic stenosis is the most common heart valve disease in western countries.

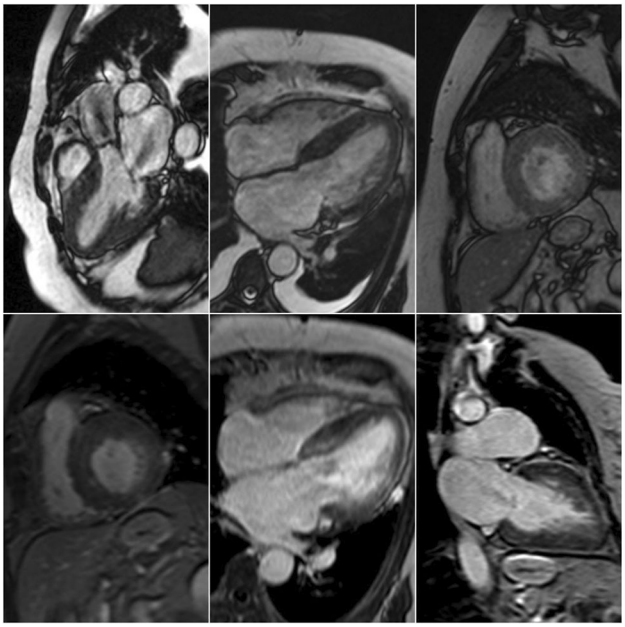

Secondary LV myocardial hypertrophy in 72-year-old women with critical aortic stenosis. There is a moderate concentric hypertrophy of the LV myocardium. LV function is slightly reduced (LV EF = 45%). There is a turbulent blood flow over the aortic valve and towards the LA. At LGE small focal areas of enhancement in IVS are noted. Amosov NICVS.

**Conclusion** Left ventricular hypertrophy is a very common indication for cardiac MRI. Identifying the cause of LV hypertrophy is a complex but very important issue. Cardiac MRI is a powerful additional tool that helps to study in detail the functional parameters of the heart and perfectly assess morphological changes in the myocardium.
Cardiac MRI in the examination of patients with LV hypertrophy provides very important information for diagnosis, management and prognosis.

## A-161

### Mitral annular disjunction in out-of-hospital cardiac arrest patients – a retrospective cardiac MRI study

**F. Troger[1], G. Klug[2], P. Poskaite[1], C. Tiller[2], P. Fink[2], I. Lechner[2], M. Reindl[2], M. Holzknecht[2], E. R. Gizewski[1], B. Metzler[2], S. Reinstadler[2], A. Mayr[1]**

[1]Medical University of innsbruck, Department of Radiology, Innsbruck, Austria, [2]Medical University of innsbruck, Department of Internal Medicine III, Cardiology and Angiology, Innsbruck, Austria.

**Purpose/Objectives** Mitral annular disjunction (MAD), defined as defective attachment of the mitral annulus to the ventricular myocardium, has recently been linked to malignant arrhythmias. However, its role and prognostic significance in patients requiring cardio-pulmonary resuscitation (CPR) remains unknown.
This retrospective analysis aimed to describe prevalence and significance of MAD by cardiac magnetic resonance (CMR) imaging, in out-of-hospital cardiac arrest (OHCA) patients.
**Methods & Materials** Eighty-six patients with OHCA and a CMR scan 5 days after CPR (interquartile range (IQR): 49 days before – 9 days after) were consecutively enrolled. MAD was defined as disjunction-extent $\geq$ 1 mm in CMR long-axis cine-images. Medical records were screened for laboratory parameters, comorbidities and prior arrhythmias.
**Results** In 34 patients (40%), no underlying cause for OHCA was found during hospitalization despite profound diagnostics. Unknown-cause OHCA-patients showed a higher prevalence of MAD compared to definite-cause patients (56% vs. 10%, $p < 0.001$) and had a MAD-extent of 6.3 mm (IQR: 4.4–10.3); moreover, these patients were significantly younger (43 years vs. 61 years, $p < 0.001$), more often female (74% vs. 21%, $p < 0.001$) and had fewer comorbidities (hypertension, hypercholesterolemia, coronary artery disease (CAD), all $p < 0.005$). By logistic regression analysis, presence of MAD remained significantly associated with OHCA of unknown cause (odds ratio: 8.49, 95% confidence interval: 2.37–30.41, $p = 0.001$) after adjustment for age, presence of hypertension and hypercholesterolemia.
**Conclusion** MAD is rather common in OHCA patients without definitive aetiology undergoing CMR. Presence of MAD remains independently associated to OHCA without identifiable trigger. Further research is needed to understand the exact role of MAD in OHCA patients.

## A-162

### Non-invasive evaluation of complex cardiovascular anomalies in newborns using CMR 4D-flow technique without anaesthesia and contrast medium: feasibility and preliminary result with feed-and-sleep technique

**M. L. Parisella[1], S. Nunno[2], S. Costa[2], A. Clemente[2], A. Monteleone[2], C. Marrone[2], N. Martini[3], F. Cademartiri[3], E. Neri[1], L. Ait-Ali[4], P. Festa.[2]**

[1]Pisa University, Translational Research, Academic Radiology, Pisa, Italy, [2]Tuscany Foundation G. Monasterio (FTGM), Massa, Italy, [3]Tuscany Foundation G. Monasterio (FTGM), Pisa, Italy, [4]Clinical Physiology Institute- CNR, Massa, Italy.

**Purpose/Objectives** Cardiac Magnetic Resonance (CMR) is increasingly used in the evolution of complex congenital heart disease (CCHD). The use of CMR in newborns is limited by risks associated with general anaesthesia [1]. 4D-flow CMR sequence is a validated technique for panoramic evaluation of vascular flow in CCHD [2]. In this study we sought to evaluate the feasibility of the 4D-flow for evaluation of the vessels anatomy and flows in newborns with CCHD using the feed-and-sleep technique (avoiding general anaesthesia), without medium contrast.
**Methods & Materials** Four neonates (aged 5–27 days, weighted 1.8–3 kg) with CCHD underwent a CMR examination. CMR was indicated to evaluate cardiac and great vessels anatomy, systemic and pulmonary venous return and quantify venous and arterial flow. The newborns were fed after a fasting of at least 4 h and the application of CMR electrodes; afterwards they were wrapped in a blanket and placed in a MR-compatible bed [3]. After localizer acquisition, a 4D-

flow sequence in axial or sagittal plan was performed with a temporal resolution < 40 ms and reconstructed isotropic spatial resolution of 1–1.3 mm. A Phase Contrast Magnetic Resonance Angiography (PCMRA) was subsequently reconstructed to evaluate venous and arterial vessels systemic and pulmonary flows were calculated in post processing using a dedicated software (Arterys 4D-flow AI suite).
**Results** CMR was successful in all patients, in one patient 4D flow was not completed. Time acquisition of 4D flow was < 3 min. In one patient the diagnosis was heterotaxic syndrome: partial anomalous left pulmonary venous return in left anonymous vein (Fig. 1a), malposition of the great arteries, pulmonary stenosis and right aortic arch (Fig. 1b). QP/QS 0.9 was calculated from the 4D-flow, as mild shunt. Anatomic findings were confirmed by the surgical report. Two others patients had the diagnosis of tortuosity syndrome, in particular: tortuous ascending aorta, right aortic arch with tortuous course and left descending aorta without aortic coarctation (Fig. 2a, b). Pulmonary arteries presented an abnormal proximal and distal course with a small distal narrowing, no ductus arteriosus was visualized and no-shunt was quantified (QP/QS 1).

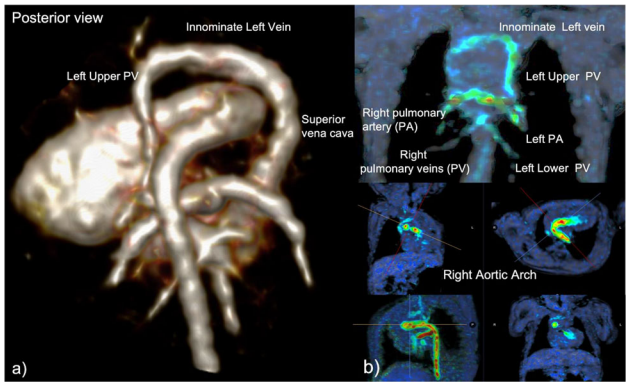


**Fig. 1** **a** Volume Rendering (VR) of PCMRA showing vertical vein draining in innominate left vein. **b**Flow derived MPR reconstruction of great vessels

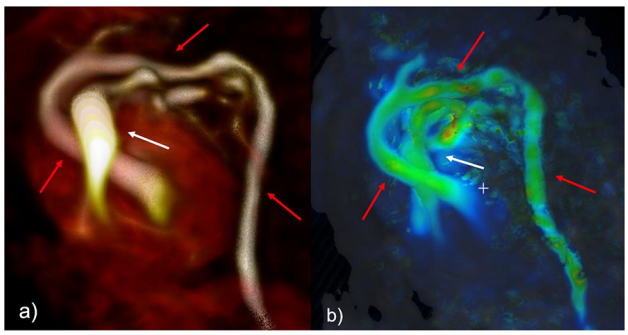


**Fig. 2** **a** VR of PCMRA and **b** Flow derived reconstruction of great vessels showing main pulmonary artery (white arrow) and the course of Aorta (red arrows): ascending aorta, aortic arch and descending aorta.

**Conclusion** From our preliminary results the feed-and-sleep scan method associated with acquisition of 4D-flow and PCMRA allows a non-invasive, non-ionizing, without sedation and contrast medium evaluation of complex intra and extracardiac anatomy and flows in newborns and infants. Further larger studies are needed to validate the technique in a larger population of congenital heart disease.

**Literature**

1. Gianpaolo Serafini et Al., (2008), Anaesthesia for MRI in the paediatric patient, Current Opinion in Anesthesiology, 499 – 503, 21.
2. Claire M Lawley et Al., (2017), 4D flow magnetic resonance imaging: role in pediatric congenital heart disease, SAGE-journal-Asian Cardiovascular & Thoracic Annals, 1–10.
3. Masoud Shariat et Al., (2014), Utility of Feed-and-Sleep Cardiovascular Magnetic Resonance in Young Infants with Complex Cardiovascular Disease, Pediatr Cardiol, 809–812, 36.

## A-164

### Short-term outcome of acute myocarditis and pericarditis after COVID-19 vaccines: a multicentric cardiac magnetic resonance study

**G. Cundari[1], C. Liguori[2], C. Mantini[3], L. Saba[4], G. D. Aquaro[5], A. Barison[5], F. Secchi[6], R. Faletti[7], S. Pradella[8], P. Di Renzi[9], E. Di Cesare[10], L. Lovato[11], A. Esposito[12], C. Catalano[1], M. Francone[13], N. Galea.[1]**

[1]Sapienza Università di Roma, Dipartimento di scienze radiologiche, oncologiche e anatomopatologiche, Roma, Italy, [2]Ospedale del Mare, Napoli, Italy, [3]Ospedale di Chieti, Chieti, Italy, [4]Ospedale di Cagliari, Cagliari, Italy, [5]Ospedale San Cataldo, Pisa, Italy, [6]Policlinico San Donato, Milano, Italy, [7]Ospedale Le Molinette, Torino, Italy, [8]Ospedale Careggi, Firenze, Italy, [9]Ospedale Fatebenefratelli, Roma, Italy, [10]Ospedale San Salvatore, L'Aquila, Italy, [11]Policlinico Sant'Orsola, Bologna, Italy, [12]Ospedale San Raffaele, Milano, Italy, [13]Humanitas, Milano, Italy.

**Purpose/Objectives** To evaluate clinical and CMR short-term follow-up (FU) in patients with acute myocarditis or pericarditis following COVID-19 vaccination.
**Methods & Materials** We retrospectively enrolled 39 patients (F, 2/39 [5.1%], with a mean age of 32.9 ± 15.5 years) who received CMR diagnosis of myocarditis or pericarditis following COVID-19 vaccination, from 13 large tertiary national centers. Inclusion criteria were troponin increase, interval between the last vaccination dose and onset of symptoms shorter than 25 days and symptoms-to-CMR shorter than 20 days. 27/39 patients underwent a short-term FU-CMR with a median of 3.3 months. Clinical baseline and FU data were acquired with electronic medical records, medical visits or phone interviews. Ventricular volumes and CMR features of tissue damage were collected in all exams. Acute myocarditis was defined in the presence of T1 and T2 criteria, as suggested by the revised Lake Louise criteria; acute pericarditis was considered in case of thickening and enhancement of the pericardial layers.
**Results** Mean time between the last vaccination dose and the onset of symptoms was 6.5 ± 5.5 days. 26/39 (66.7%) patients received a vaccination with BNT126b2, 11/39 (28.2%) with mRNA-1273, 1/39 (2.6%) with ChAdOx1-S and 1/39 (2.6%) with Ad.COV2.S. 18 patients presented with cardiac involvement after the first dose of vaccine, 15 after the second dose and 6 after the "booster" dose. Chest pain was the most frequent symptom (evidenced in 36/39). Other symptoms included fever (24/39), myalgia (13/39), palpitations (9/39) and dyspnea (9/39). ECG anomalies were found in 30/39. At baseline, left ventricular ejection fraction (LV-EF) was moderately reduced in 2 patients (5.1%) and mildly in 5 (12.8%); wall motion abnormalities have been detected in 10. Edema was found in 31/39 (79.5%) and LGE in 35/39 (89.7%) patients, both with a predominant

subepicardial or mesocardial distribution pattern (83.9% and 97.1%, respectively). Clinical FU revealed chest pain, palpitations and dyspnea still present in 5/39 (12.8%), 2/39 (5.1%) and 3/39 (7.7%), respectively. ECG anomalies were found in 5/39 (12.8%). At FU-CMR, LV-EF was reduced only in 2 patients (mildly); signs of active myocardial inflammation were still reported in 8/27 (29.6%) patients. LGE was found in 24/27 (88.9%) patients, with a subepicardial or mesocardial distribution in 100% of them. Residual signs of pericarditis were found in just one patient and pericardial effusion in 4/27 (14.8%).

**Conclusion** CMR plays an important role in the identification of acute myocarditis and pericarditis after COVID-19 vaccination, which appeared to have a mild clinical course at short-term follow-up.

## A-165

### Extracellular volume and fibrosis volume of left ventricular myocardium in vaccinated and unvaccinated patients with a history of SARS-CoV-2 infection

P. Gać[1,2], M. Poręba[3], R. Poręba[1]
[1]Wroclaw Medical University, Wroclaw, Poland, [2]4th Military Hospital, Wroclaw, Poland, [3]Wroclaw University of Health and Sport Sciences, Wroclaw, Poland.

**Purpose/Objectives** The aim of the study was to assess the extracellular volume (ECV) and the fibrosis volume (FV) of left ventricular myocardium in the T1 mapping sequence in patients with a history of SARS-CoV-2 infection, considering the vaccination status against COVID-19.

**Methods & Materials** The study group consisted of 97 patients without focal myocardial injury in late gadolinium enhancement (LGE) sequence in cardiac magnetic resonance (CMR), (mean age 52.54 ± 8.31 years). Based on the criteria of past SARS-CoV-2 infection and the vaccination status against COVID-19, 3 subgroups were distinguished: patients with a history of symptomatic SARS-CoV-2 infection, unvaccinated against COVID-19 (A, n = 39), patients with a history of symptomatic SARS-CoV-2 infection, with a full vaccination schedule against COVID-19 (B, n = 22) and persons without a history of SARS-CoV-2 infection constituting the control subgroup (C, n = 36). All patients underwent 1.5 T CMR, including CINE sequences, LGE sequence and T1-mapping sequences before (native) and 20-min after paramagnetic agent administration (post-contrast). ECV was calculated from native myocardial T1 time and post-contrast myocardial T1 time, native blood pool T1 time and post-contrast blood pool T1 time, and hematocrit values using a standard mathematical formula. The FV was calculated by multiplying the ECV by the ratio of the left ventricular mass and the myocardial density (constant: 1.05 g/ml). The mean ECV and mean FV of the whole myocardium (ECV and FV whole myocardium) were assessed. Moreover, the mean ECV was assessed in the 16-segment myocardial AHA model (ECV segment 1–16).

**Results** In the CINE sequence, no significant differences were found in the mean values of the heart cavities dimensions, thickness and mass of the left ventricular myocardium, as well as the functional parameters of the left and right ventricles between subgroups A, B and C. In subgroup A compared to subgroups B and C, both the ECV whole myocardium and ECV segments 2, 5–6, 8 and 10–11, were statistically significantly higher. In addition, the ECV segment 16 was statistically significantly higher in subgroup A than in subgroup C. Moreover, in subgroup A compared to subgroups B and C, the FV whole myocardium was statistically significantly higher. There were no statistically significant differences in ECV and FV between subgroups B and C.

**Conclusion** Unvaccinated against COVID-19 patients with a history of symptomatic SARS-CoV-2 infection have higher myocardial ECV and FV values in the T1 mapping sequence, compared to those without COVID-19 and those suffering from COVID-19, previously vaccinated with the full vaccination schedule.

## A-166

### TRoponin of unknown origin in STroke evaluated by multi-component cardiac Magnetic resonance imaging – the TRUST-MI study

S. Greulich[1], A. Mengel[2], J. Kübler[3], U. Ernemann[4], U. Ziemann[2], M. Gawaz[1], K. Nikolaou[3], P. Krumm[3]
[1]University of Tübingen, Cardiology and Angiology, Tübingen, Germany, [2]University of Tübingen, Neurology, Tübingen, Germany, [3]University of Tübingen, Radiology, Tübingen, Germany, [4]University of Tübingen, Neuroradiology, Tübingen, Germany.

**Purpose/Objectives** Increased high-sensitive cardiac troponin I (hs-cTnI) levels are common in patients with acute ischemic stroke. However, only a minority demonstrates culprit lesions on coronary angiography, suggesting other mechanisms, e.g. inflammation, as underlying cause of myocardial damage. Late Gadolinium Enhancement (LGE)-cardiac magnetic resonance (CMR) with mapping techniques (T1, T2, extracellular volume (ECV)) allows the detection of both focal and diffuse myocardial abnormalities. We investigated the prevalence of culprit lesions by coronary angiography and myocardial tissue abnormalities by a comprehensive CMR protocol in troponin-positive stroke patients.

**Methods & Materials** Patients with troponin-positive acute ischemic stroke (mirrored by CT and/or MR) and no history of coronary artery disease were prospectively enrolled. Coronary angiography and CMR (LGE, T1 + T2 mapping, ECV) were performed within the first days of the acute stroke.

**Results** Twenty-five troponin-positive patients (mean age 62 years, 44% females) were included. CMR was performed mean 4.4 ± 2.4 days after the acute ischemic stroke. 2 patients (8%) had culprit lesions on coronary angiography and underwent percutaneous coronary intervention. 13 patients (52%) demonstrated LGE: (i) n = 4 ischemic, (ii) n = 4 non-ischemic, (iii) n = 5 ischemic AND non-ischemic. In the 12 LGE-negative patients, mapping revealed diffuse myocardial damage in additional 9 (75%) patients, with a high prevalence of increased T2 values.

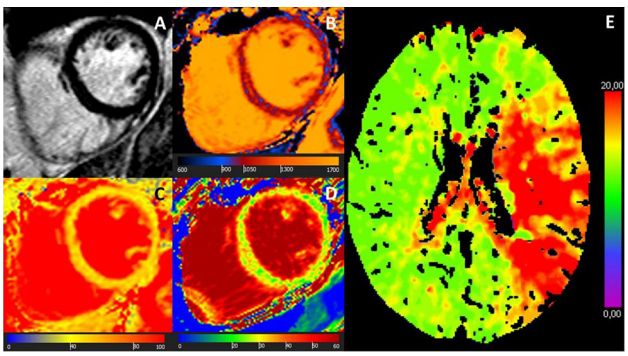


68-year-old female with troponin-positive ischemic stroke and unobstructed coronary arteries.(A) LGE-negative, (B) increased T1 (1074 ms), (C) increased T2 (52 ms), (D) increased ECV (30%) in an identical midventricular short-axis slice. (E) Cerebral volume

perfusion CT at admission showed prolonged time-to-peak perfusion in the territ.

**Conclusion** Our data show a low prevalence of culprit lesions in troponin-positive stroke patients. However, > 50% of the patients demonstrated myocardial scars (ischemic + non-ischemic) by LGE-CMR. Mapping revealed additional myocardial abnormalities (mostly inflammatory) in the majority of LGE-negative patients. Therefore, a comprehensive CMR protocol gives important insights in the etiology of troponin which might have implications for the further work-up of troponin-positive stroke patients.

## A-168

### CT imaging of combat-related injury of heart and great vessels

**Y. Vitkovskyi, M. Tregubova, M. Ishchenko**

Amosov National Institute of Cardiovascular Surgery, Radiology, Kyiv, Ukraine.

**Purpose/Objectives** This study aims to show the possibilities of computed tomography (CT) in the diagnosis and assessment of combat damage to the heart and great vessels caused by gunshots, knives, and explosive injuries.

**Methods & Materials** MDCT of the combat-related injuries of the chest is performed only in hemodynamically stable patients. As a rule, for combat injuries of a thorax in our clinic performance of 4 consecutive stages of scanning is practiced. The first non-enhancement CT is used to quickly and generally assess chest injury (trajectory of injuries, bone and organ damage, the presence and location of bullets or explosive fragments), and the second phase is CT images of cardiac gating with contrast enhancement (to exclude penetrating heart injury, rupture or dissections of ascending aorta, and coronary artery injuries); followed by arterial and venous phases, respectively, to exclude damage to large vessels of the heart.

**Results**

#### Classification of combat trauma to the heart

According to the nature of the striking element, combat injuries to the heart are divided into the bullet and mine explosions; according to clinical-anatomical features separated open (non-penetrating into the heart cavity, penetrating the heart cavity, and combined), and closed wounds (concussion, heart contusion, and rupture).

#### Vascular injuries

As for vascular injury in penetrating mediastinal injuries, it is most common in the ascending aorta and aortic arch, and in blunt chest trauma, the descending aorta in the area of the ligamentum arteriosum is usually affected.

Most often penetrating injuries of a thoracic aorta are carried out by gunshot or knives.

As usual, patients with penetrating mediastinal injuries are hemodynamically unstable and require emergency surgery.

On CT images after hemodynamic stabilization of patient often detect pseudoaneurysms, vascular occlusions, active contrast extravasation, dissections, and arteriovenous fistulas.

#### Cardiac injuries

Penetrating heart injuries are often lethal. It is reported that the mortality rate is about 85%.

The anterior chambers of the heart are most commonly affected.

MDCT has high sensitivity and specificity in penetrating heart injuries and the most common findings include hemopericardium, pneumopericardium; intracardiac foreign bodies (bullets or mine fragments) (Fig. 2); pseudoaneurysms, contrast material extravasation from cardiac chambers (Fig. 3); coronary arteries and cardiac veins injuries (Fig. 1).

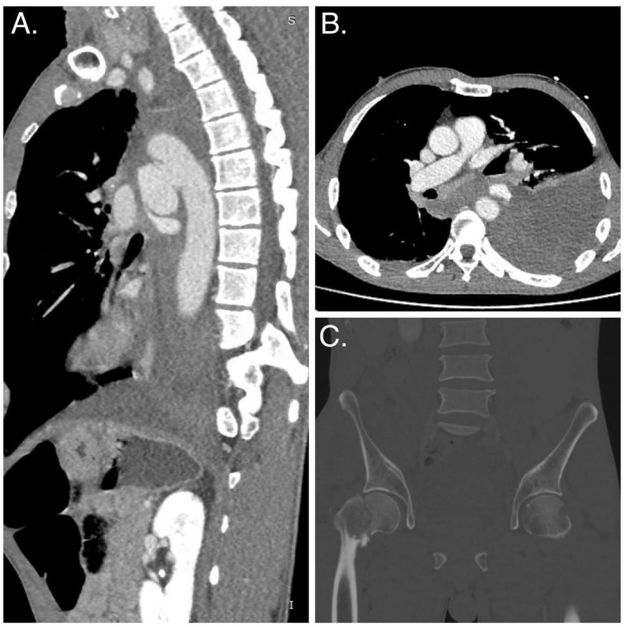


**Fig. 4** The casualty is 27 years old after a car accident. (A- sagittal, B-axial) MDCT shows pseudoaneurysm of the proximal segment of the descending thoracic aorta, with signs of active extravasation of the contrast agent, hemomediastinum, large left hemothorax, and fractures of the neck of the right femur (C)

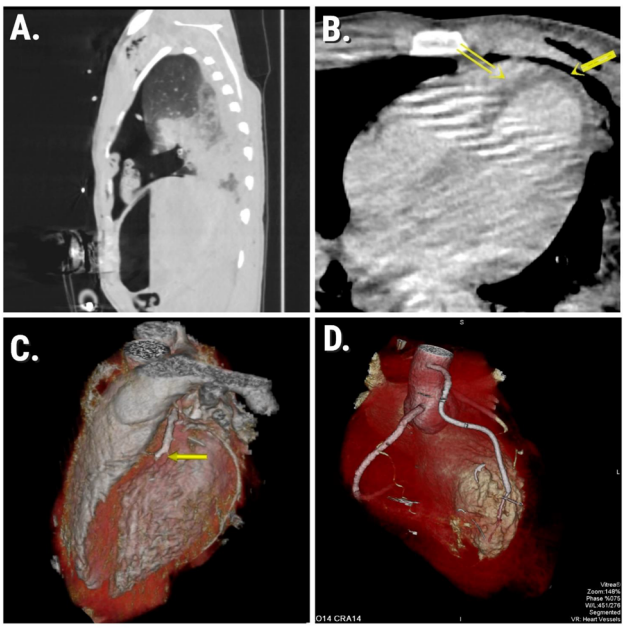


**Fig. 1** The postoperative patient was 25 years old, after a gunshot wound to the left axillary region. (A)Sagittal MDCT a large laceration of the left lung and pneumothorax are noted. Occlusion of the middle segment of the LAD (see VR (C) and areas of infarction (B) was observed in the MDCT as a result of penetrating injury in this region

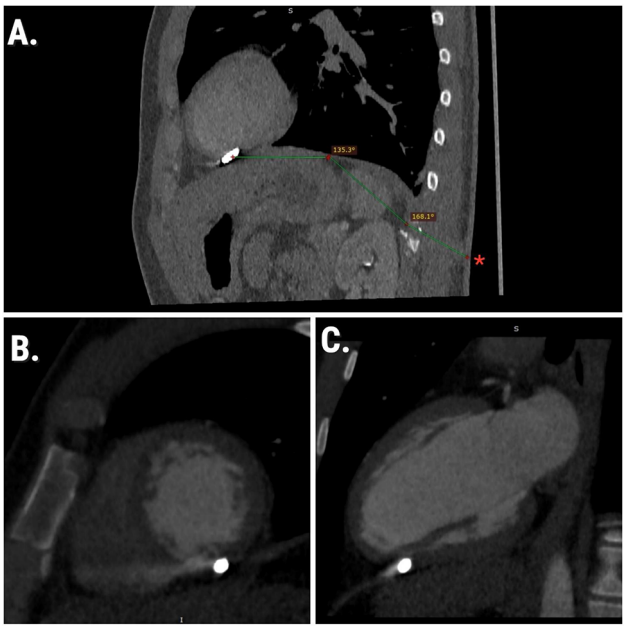


**Fig. 2** A gunshot wound to the left upper lumbar region in a 45-year-old man. (A) Sagittal MDCT shows the bullet's trajectory and demonstrates the entrance to the skin (arrowhead), rib fracture, laceration of the spleen, and penetrating of the diaphragm. (B,C) MDCT images show the bullet within the inferior wall left ventricle on the apical level

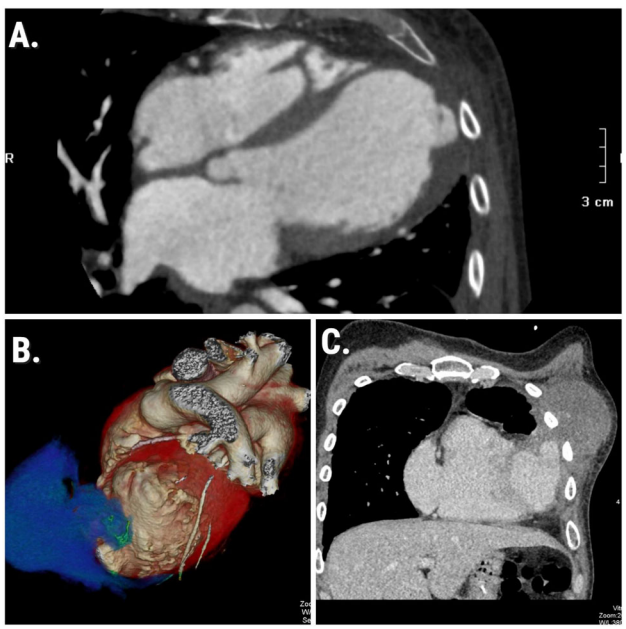


**Fig.3** A 44-year-old man with a stab wound to the left chest. (A) Axial CT show pseudoaneurysm of the anterior wall of the left ventricle with signs of active extravasation of the contrast agent and occlusion of the LAD (see VR (B). (C) Coronal CT shows a large hematoma of the left anterior chest wall, which is associated with pseudoaneurysm

**Conclusion** Multidetector computed tomography is a very valuable method for hemodynamically stable patients with combat injuries of the heart and large vessels, as it can help detect a wide range of lesions in a relatively short time, and recognizing these lesions is vital for further management and treatment of such patients.

## A-172

### CTA abnormalities are related to aortic remodeling in hybrid frozen elephant trunk prostheses for acute and chronic aortic syndrome

**H. Cuellar-Calabria[1], G. Burcet[1], J. Reyes-Juarez[1], A. Aubanell[1], R. Rios[2], R. Rodriguez-Lecoq[2], N. Zebdi[3], A. Roque[1]**

[1]IDI—Vall d'Hebron Barcelona Hospital Campus, Department of Diagnostic Imaging, Barcelona, Spain, [2]Vall d'Hebron Barcelona Hospital Campus, Department of Cardiac Surgery, Barcelona, Spain, [3]Vall d'Hebron Barcelona Hospital Campus, Department of Anesthesiology, Barcelona, Spain.

**Purpose/Objectives** Hybrid frozen elephant trunk prostheses (FET) in complex aortic arch surgery reduce operative times and facilitate positive remodeling in downstream aortic segments.
Our aim is to describe early abnormalities detected by CTA in FET for aortic dissection and intramural hematoma and their relation to remodeling and clinical complications.
**Methods & Materials** Thirty-two patients with acute (9) or chronic (23) aortic syndrome (29 aortic dissections and 3 intramural hematomas) were treated with FET and underwent an ECG-gated aortic CTA before discharge.
Key clinical and surgical parameters were genetic aortic disease, emergent or elective surgical timing, site of distal anastomosis, additional procedures and early and first-year clinical complications. We recorded and classified abnormal postsurgical CTA findings and quantified the remodeling of the descending thoracic aorta according to a scale: no false lumen thrombosis (FLT) (0), FLT < 50% (1), 50–100% (2), or exceeding the trunk length (3), and complete FLT or no residual dissection (4).
**Results** Fifty-six percent of patients presented early clinical complications (18/32), resulting in death before discharge in two cases (11% [2/18]). Along with these, late graft infection (2) and stroke (2) accounted for a first-year death rate of 19% (6/32).
Thirty-four percent of CTAs showed FET abnormal findings (11/32) and in eight these were trunk-related (73% [8/11]): type Ib leaks (3), floating thrombi (3), stent underexpansion (2) and a stent-induced new entry (1) (total = 9).

Complete remodeling of the descending thoracic aorta was achieved in 41% of patients (13/32) owing to replacement of the diseased ascending aorta and arch by the surgical tube of the FET without residual distal involvement (10), one-step thoracoabdominal aortic replacement procedure (2) or complete FLT of the residual dissection of the descending aorta (1). On the other hand, 13% of patients (4/32) had a completely patent false lumen which required early unscheduled additional procedures.

Acute surgical timing was related to death during the first year ($p < 0.05$). CTA abnormalities, and more specifically trunk abnormalities, were related to false lumen remodeling ($p = 0.02$ and $p < 0.01$, respectively) but not to early clinical complications (both $p = 1$) or death ($p = 0.15$ and $p = 0.63$, respectively).

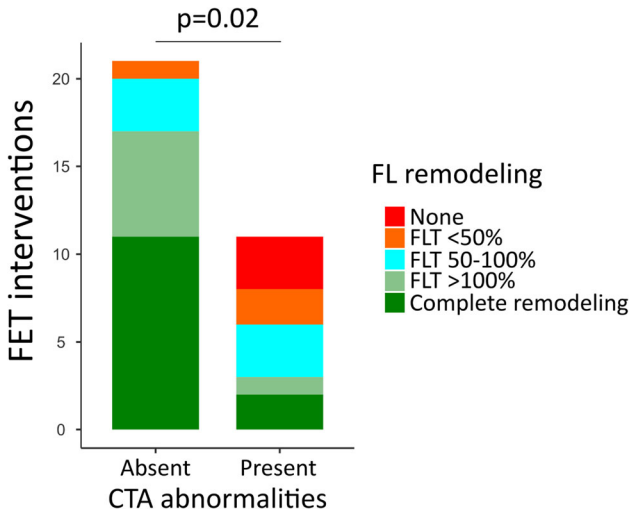


Abnormal findings related to the frozen elephant trunk procedure (FET) in a CTA before discharge were related to false lumen remodeling (p = 0.02). FLT: extent of false lumen thrombosis in relation to length of FET.

Volume rendered image of a CTA after FET for chronic type B aortic dissection shows an ascending type Ib leak (yellow arrows) from the non-sealing trunk anchor with false lumen patency (red arrows).

**Conclusion** CTA before discharge in FET for acute or chronic aortic syndrome detects prosthetic abnormalities related to clinically silent failed aortic remodeling and is key to planning of additional procedures.

## A-178

### Impact of retraining a deep learning algorithm to perform guideline-compliant diameter measurements on non-gated chest CT

**F. Lo Piccolo[1,2], J. Sperl[3], J. Cyriac[2], S. Yang[2], S. Rapaka[4], J. Bremerich[2], A. W. Sauter[2], M. Pradella[2]**

[1]Università Cattolica del Sacro Cuore, Agostino Gemelli University Policlinic, Radiology, Rome, Italy, [2]University Hospital Basel, Department of Radiology, Basel, Switzerland, [3]Siemens Healthineers, Forchheim, Germany, [4]Siemens Healthineers, Princeton, NJ, United States of America.

**Purpose/Objectives** Detection of thoracic aortic dilatation (TAD) is mandatory in clinical routine. Deep learning (DL) was successfully utilized to perform diameter measurements according to current guidelines on ECG-gated CT angiography (1,2), but limited reports are available regarding non ECG-gated CT (contrast-enhanced (CE) and non-CE). Moreover, result quality was location dependent with worse results found at the aortic root. Aim of this study was to investigate the impact of re-training the previously evaluated DL tool for aortic measurements in a cohort of non-ECG gated exams.

**Methods & Materials** A cohort of 995 patients (age 68 ± 12, 14% female) with CE (n = 392) and non-CE (n = 603) chest CT exams was selected, all had at least one false measurement reported by the initial DL version. The cohort consisted of cases with normal aortic diameter (30%) and TAD (70%), the latter defined as diameter ≥ 45 mm for aortic sinus (SA), sinotubular junction (STJ), ascending aorta (AA), and proximal arch (PA) or ≥ 40 mm for the other locations (4). All cases were processed by the DL tool (AI-Rad Companion Research, Siemens) which measured diameters of the thoracic aorta according to the current AHA guidelines (3). The cohort was processed, first by the initial version, trained on 1000 cases, and afterwards by the re-trained version (re-trained on an additional 250 pathologic cases (CE & non-CE)) (1,2). Furthermore, robustness of centerline fitting and cross-sectional plane placement were improved. DL results were evaluated by two radiologists regarding plane placement and diameter measurements. Coherent measurements were correctly measured diameters in both versions. Improved measurements were defined as correct diameter assessment by re-trained version only. False measurements were consisted of over/under-segmentation of diameters (± tilted plane).

**Results** We evaluated 8948 measurements. Coherent measurements were found in 3765 (42.1%) of cases (best: distal arch 655 (66%), worst: AS 221 (22%)). Furthermore, we found improved diameters in 4456 (49.8%) measurements, mainly at the aortic root (AS: 564 (57%), STJ: 697 (70%)) (Table 1, Fig. 1). In addition, the re-trained version performed 318 (3.6%) measurements which were not previously available. A total of 228 (2.5%) cases showed had false measurements because of tilted planes and 181 (2.0%) over-/under-segmentation with a focus at AS (n = 137 (14%) and n = 73 (7%), respectively) (Table 1; Fig. 2). In total, the re-trained version correctly measured 8539/8948 (95.5%) of diameters.

**Conclusion** Re-training of the DL tool improved diameter assessment, resulting in a total of 95.5% correct measurements. Our data suggests that the re-trained DL tool can be applied to chest CT exams, independent of contrast phase

(1) Pradella et al. "Fully automated guideline-compliant diameter measurements of the thoracic aorta on ECG-gated CT angiography using deep learning." Quantitative Imaging in Medicine and Surgery 11.10 (2021): 4245

(2) Rueckel J, Reidler P, Fink N et al. Artificial intelligence assistance improves reporting efficiency of thoracic aortic aneurysm CT follow-up. Eur J Radiol 2021;134:109,424

(3) American College of Cardiology Foundation, et al. "2010 ACCF/AHA/AATS/ACR/ASA/SCA/SCAI/SIR/STS/SVM guidelines for the diagnosis and management of patients with thoracic aortic disease." Journal of the American College of Cardiology 55.14 (2010): e27-e129

(4) Mansour AM, Peterss S, Zafar MA et al. Prevention of Aortic Dissection Suggests a Diameter Shift to a Lower Aortic Size Threshold for Intervention. Cardiology 2018;139:139–146

**Table 1** Measurements at a total of 8948 locations according to the current AHA guidelines in 995 cases: AS: Aortic sinus; STJ: Sinotubular junction; AA: Ascending Aorta; PA: Proximal Arch; MA: Mid Arch; DA: Distal Arch; MDA: Mid Descending Aorta; DDA: Distal Descending Aorta; ABA: Abdominal Aorta

| Re-trained version | | AS | STJ | AA | PA | MA | DA | MDA | DDA | ABA | Total |
|---|---|---|---|---|---|---|---|---|---|---|---|
| Coherent measurements | | 221 (22%) | 263 (26%) | 448 (45%) | 487 (49%) | 361 (36%) | 655 (66%) | 508 (51%) | 435 (44%) | 387 (39%) | 3765 (42.1%) |
| Improved measurements | | 564 (57%) | 697 (70%) | 421 (42%) | 481 (48%) | 615 (62%) | 256 (26%) | 400 (40%) | 487 (49%) | 535 (54%) | 4456 (49.8%) |
| Correct measurements, previously missing | | 0 | 0 | 13 (1%) | 14 (1%) | 14 (1%) | 69 (7%) | 64 (6%) | 72 (7%) | 71 (7%) | 318 (3.6%) |
| False measurements | Tilted Plane | 137 (14%) | 16 (2%) | 39 (4%) | 6 (1%) | 3 (0.3%) | 8 (1%) | 17 (2%) | 0 | 2 (0.2%) | 228 (2.5%) |
| | Over / under segmentation | 73 (7%) | 18 (2%) | 71 (7%) | 5 (1%) | 2 (0.2%) | 6 (1%) | 5 (1%) | 1 (0.1%) | 0 | 181 (2%) |

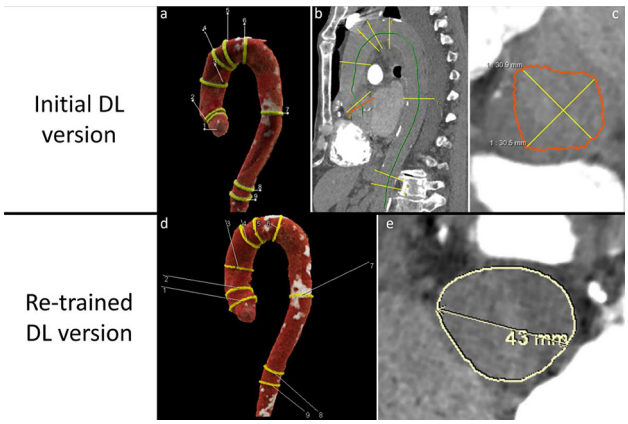


**Fig. 1** Initial (a-c) and re-trained DL (d,e) assessments in one non-CE chest CT case. Top row shows VRT (a), MPR (b) and axial through-plane at AS (c) using the initial DL version. The plane was tilted, leading to a false measurement. Bottom row (re-trained DL) shows improved plane placement on VRT(d) and improved aortic segmentation at AS

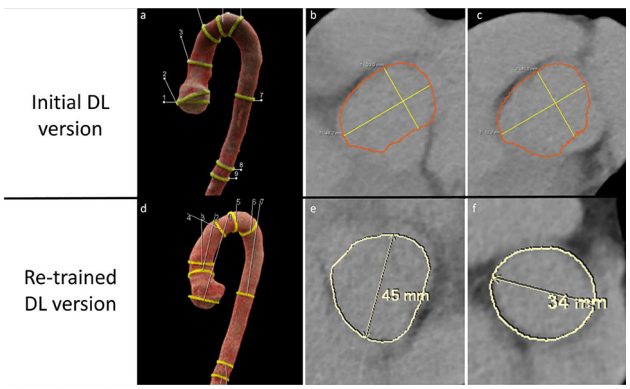


**Fig. 2** Case of diameter assessment in a non-CE chest CT performed by the initial (a-c) and re-trained DL tool (d-f). VRT (a) and through-plane view at AS (b) and STJ (c) showed tilted planes at AS (b) and STJ (c) landmarks. In the re-trained version, segmentation at STJ was correct (= improved) (f); AS (e) was still tilted and therefore false

## A-179

### Validation of a novel multi-task deep learning algorithm for automated coronary artery disease classification using an heterogenous multivendor coronary CT angiography dataset – impact of image quality

**R. Fari[1,2], C. N. De Cecco[1], M. Van Assen[1], P. Von Knebel Doeberitz[1], B. Boettcher[1], M. Schoebinger[3], G. S. Fung[3]**

[1]Emory University Hospital, Cardiothoracic Imaging, Atlanta, United States of America, [2]Università di Modena e Reggio Emilia, Radiologia, Modena, Italy, [3]Siemens Healthineers, Forchheim, Germany.

**Purpose/Objectives** This study aims to validate a fully automated deep learning (DL) algorithm for coronary artery disease (CAD) detection and classification in a heterogeneous multivendor coronary CT angiography (CCTA) dataset. In addition, the impact of image quality and artefacts is evaluated.

**Methods & Materials** One hundred twenty-three patients who underwent CCTA were included in this single-center retrospective study. Patients were scanned with multiple CT systems of four vendors (Siemens Healthineers, Philips, General Electrics, Canon). CAD Reporting and Data System (CAD-RADS) measured by an expert reader with more than two years of experience in CCTA was used as reference standard. A novel fully automated multi-task deep learning (DL) algorithm provides simultaneous detection and classification of coronary lesions and regions with imaging or reconstruction artifacts, as well as quantifications based on segmentations of the coronary lumen (Automatic Coronary Analysis prototype 2.0, Siemens Healthineers, Forchheim, Germany).

Statistical analysis was performed on a per-segment and per-patient basis, subdividing the patients based on risk of obstructive coronary artery disease (CAD) defined as moderate-high (CAD-RADS $\geq$ 3) or low (CAD-RADS $\leq$ 2). All CCTA images were scored for image quality as excellent (images with little or no noise), good (images adequate for diagnostic interpretation with few artifacts) or poor (images with limited clinical interpretation due to high noise or artifacts).

**Results**

The inter-reader agreement between the DL algorithm and R1 was good (Cohen's kappa coefficient = 0.73, $p < 0.001$). For the detection of obstructive vs non-obstructive CAD, the DL algorithm showed a sensitivity, specificity and accuracy of 86.7%, 90.3% and 89.4%, respectively. The performances of the software were similar throughout all three image quality groups, the accuracy was 85.7%, 94.3% and 90.6%, respectively in the excellent, good and poor-quality groups.

**Conclusion**

The fully automated DL algorithm showed a good agreement with expert readers and an excellent performance for the detection of obstructive CAD. The explicit detection and handling of image artefacts within the multi-task deep learning algorithm seems to effectively avoid impaired evaluation results in those regions.

## A-184

### Computed tomography-derived miocardial extracellular volume assessment in patients with gastrointestinal oncologic pathology subject to chemotherapy: an early marker of cardiotoxicity

**F. Sgalambro[1], A. Arceri[1], A. Di Carlo[1], M. Ranalli[1], A. Bracci[1], P. Palumbo[1], G. Bruera[2], E. Ricevuto[2], C. Masciocchi[1], E. Di Cesare[1]**

[1]University of L'Aquila, Department of Biotechnological and Applied Clinical Sciences, L'Aquila, Italy, [2]University of L'Aquila, Department of Oncology, L'Aquila, Italy.

**Purpose/Objectives** Our objective is to assess myocardial extracellular volume (mECV) by means of thoracic computed tomography without and with contrast performed for staging and follow-up in patients with gastric, pancreatic and colorectal (GI) carcinoma treated with chemotherapy.
**Methods & Materials** Thirty-four patients with GI tumours from July 2021 (including 18 males and 16 females, mean age 64.9 ± 13 years) who had undergone staging CT scans at the start of treatment and oncological re-evaluation CT scans after anti-HER drug therapy antiVEGF/VEGFR and fluoropyrimidines. The study was performed with 320-detector CT. The haematocrit performed no more than 5 days before the examination was used. mECV was calculated on baseline scans and after 3 min after contrast medium injection (volume 100 ml concentration, 400 mg iodine) using the formula according to Miler et al.: mECV = (1-hematocrit)*[(HU myocardium post-HU myocardium pre)/(HU blood post-HU blood pre)].
**Results** Pre-treatment haematocrit was 38% ± 4%. The pre-treatment chemotherapy mECV was 28.5% ± 3.9% at 3 min, similar to values reported in the literature for normal subjects. The post-treatment mECV was 36.8% ± 8.7% significantly higher than the pre-treatment value ($P < 0.005$) and indicative of enlargement of the interstitial space. The case series, although still limited, shows a clear increase in mECV value indicative of myocardial damage 28 months ± 29 after chemotherapy with anti-HER, anti-VEGF/VEGFR and fluoropyrimidine drugs.
**Conclusion** CT-derived mECV could be an imaging biomarker to monitor chemotherapy-related cardiotoxicity by contributing to the prevention of secondary cardiac damage through the use of data from examinations as part of the follow-up of tumour disease.

## A-187

### Right-to-Left Ventricular Blood Pool T2 Ratio Correlates with Exercise Capacity of Heart Failure Patients

**M. C. Halfmann[1], T. Schoeler[1], K.-F. Kreitner[1], C. Düber[1], A. Varga-Szemes[2], T. Emrich[1,2]**

[1]University Medical Center Mainz, Department of Diagnostic and Interventional Radiology, Mainz, Germany, [2]Medical University of South Carolina, Department of Radiology and Radiological Science, Charleston, SC, United States of America.

**Purpose/Objectives** T2 mapping has been proven to be sensitive to the level of blood oxygenation. We hypothesized that due to higher levels of peripheral blood desaturation, heart failure patients with impaired exercise capacity will have a greater difference of right (RV) to left ventricular (LV) blood pool T2 relaxation times compared to patients with preserved exercise capacity and healthy controls.
**Methods & Materials** A total of 70 heart failure patients who underwent both cardiac magnetic resonance imaging (CMR) and 6-min walk tests (6MWT) (mean time difference 69 ± 49 days) were retrospectively identified. 35 propensity score-matched healthy individuals served as a control group. CMR included cine acquisitions and T2 mapping using a commercially available sequence to obtain blood pool T2 relaxation times of the RV and LV. Age- and gender-adjusted nominal distances and respective percentiles were calculated for the 6MWT. Calculation of the RV/LV-ratio of T2 blood pool relaxation times, correlation with results from 6MWT, and regression analyses were performed using commercially available statistics software.
**Results** The RV/LV T2 ratio correlated strongly with the percentiles of nominal distances in the 6MWT (r = 0.66), while ejection fraction, end-diastolic and end-systolic volumes did not (r = 0.09, 0.07 and -0.01, respectively). In addition, there were significant differences in the RV/LV T2 ratio between patients with and without significant post-exercise dyspnea (p = 0.001), and logistic regression analysis showed that RV/LV T2 ratio was an independent predictor of the walking distance and the presence of post-exercise dyspnea.
**Conclusion** The proposed RV/LV T2 ratio (obtained by two simple atrial measurements on a routinely acquired four-chamber T2 map) strongly correlated with results from the 6-min walk test and independently predicted exercise capacity and the presence of post-exercise dyspnea in heart failure patients. Further studies will have to investigate its relationship to prognosis and its potential to aid in selecting patients who need a closer follow-up.

## A-189

### Multicenter consistency assessment of rapid CMR strain quantification

**M. C. Halfmann[1], K.-F. Kreitner[1], L. Hopman[2], H. Koerperich[3], E. Blaszczyk[4], J. Gröschel[4], J. Salatzki[5], F. André[5], T. Emrich[1,6]**

[1]University Medical Center Mainz, Department of Diagnostic and Interventional Radiology, Mainz, Germany, [2]Amsterdam UMC, Department of Cardiology, Amsterdam, The Netherlands, [3]Herz- und Diabeteszentrum NRW, Ruhr-Universität Bochum, Institute for Radiology, Bad Oeynhausen, Germany, [4]Charité-Universitätsmedizin Berlin, Working Group on Cardiovascular Magnetic Resonance, Experimental and Clinical Research Center, Berlin, Germany, [5]University Hospital Heidelberg, Department of Cardiology, Angiology, Pneumology, Heidelberg, Germany, [6]Medical University of South Carolina, Department of Radiology and Radiological Science, Charleston, SC, United States of America.

**Purpose/Objectives** Strain parameters have been under scrutiny for their reproducibility and generalizability, partly due to the black-box model used for the calculation. This multicenter study evaluated the interobserver agreement of a simplified rapid-strain algorithm depending solely on longitudinal ventricular shortening in a real-world setting.
**Methods & Materials** A total of 4 sites each retrospectively identified 20 patients with various cardiomyopathies and 20 healthy controls who had undergone cardiac MRI at their respective centers using locally available scanners from 2 manufacturers with both 1.5 and 3 T field strengths and local imaging protocols. First, conventional and rapid longitudinal strains were evaluated at each site and then independently re-evaluated by a core lab. The core lab did not contribute data in order to reduce potential bias towards their own data. Intraclass correlation coefficients (ICC) and Bland-Altmann plots were used to assess interobserver agreement. Pearson's correlation was used to evaluate agreement with conventional strain.
**Results** ICCs demonstrated excellent agreement between sites for left ventricular rapid strains (ICC ≥ 0.95 for all sites). Bland-Altmann plots showed no significant bias between site and core lab readings and limits of agreement (LoA) were well within clinically acceptable margins (Mean difference: -0.06%, 95% CI: -3.8 to 3.7%). In addition, there was a strong-to-excellent correlation between conventional and rapid ventricular longitudinal strain measurements (r = 0.89). Regression analyses showed that neither field strengths nor scanner vendors were significant confounders for the simplified ventricular strain algorithm.
**Conclusion** Advanced post-processing imaging biomarkers such as strain need careful reproducibility assessment in real-world scenarios

using different scanners, field strengths, and local imaging protocols. Independently of these, the simplified rapid ventricular strain algorithm could reliably assess left ventricular strain longitudinal strain.

## A-191

### Anomalous origin of coronary artery from the pulmonary artery in adults detected by coronary computed tomography angiography

**A. Michalowska[1,2], P. Tyczyński[3], I. Michalowska[4], I. Kowalik[5], P. Hoffman[6], M. Demkow[7], C. Kępka[7], M. Kruk[7], A. Witkowski[3], M. Kuśmierczyk[8], J. Pręgowski[3]**

[1]National Institute of Cardiology, Warsaw, Poland, [2]Central Clinical Hospital of the Ministry of Interior and Administration, Department of Diagnostic Radiology, Warsaw, Poland, [3]National Institute of Cardiology, Department of Interventional Cardiology and Angiology, Warsaw, Poland, [4]National Institute of Cardiology, Department of Radiology, Warsaw, Poland, [5]National Institute of Cardiology, Department of Coronary Artery Disease and Cardiac Rehabilitation, Warsaw, Poland, [6]National Institute of Cardiology, Department of Congenital Heart Disease, Warsaw, Poland, [7]National Institute of Cardiology, Department of Coronary and Structural Heart Diseases, Warsaw, Poland, [8]Medical University of Warsaw, Department of Cardiac Surgery, Warsaw, Poland.

**Purpose/Objectives** Anomalous origin of coronary artery from the pulmonary artery (ACAPA) is a rare congenital coronary artery abnormality. Although, most of the patients die during the first year of life if not treated, some types of ACAPA might be clinically silent and being diagnosed in adulthood. Three main types of ACAPA might be distinguished: 1) anomalous left, 2) right, and 3) single coronary artery from the pulmonary trunk (ALCAPA, ARCAPA and ASCAPA, respectively). The aim of the study was to assess the prevalence and anatomic characteristics of ACAPA in patients who underwent coronary computed tomography angiography (CTA).

**Methods & Materials** From 2008 to 2020, in 39,066 patients 45,817 coronary CTA examinations were performed in a single high-volume hospital. With the application of specific keywords, the electronic database was manually screened to select subjects with ACAPA. Inclusion criteria were as follows: 1) age $\geq$ 18 years, 2) coronary CTA performed before eventual invasive treatment. In coronary CTA examinations of the patients with ACAPA following features were assessed: 1) coronary artery originating from the pulmonary artery (PA), 2) site of origin of coronary artery from PA, 3) presence of collateral circulation: collaterals between the right and left coronary arteries (RCA, LCA, respectively) (Fig. 1), dilated septal vessels, dilated bronchial arteries, and 4) presence of coronary steal phenomenon.

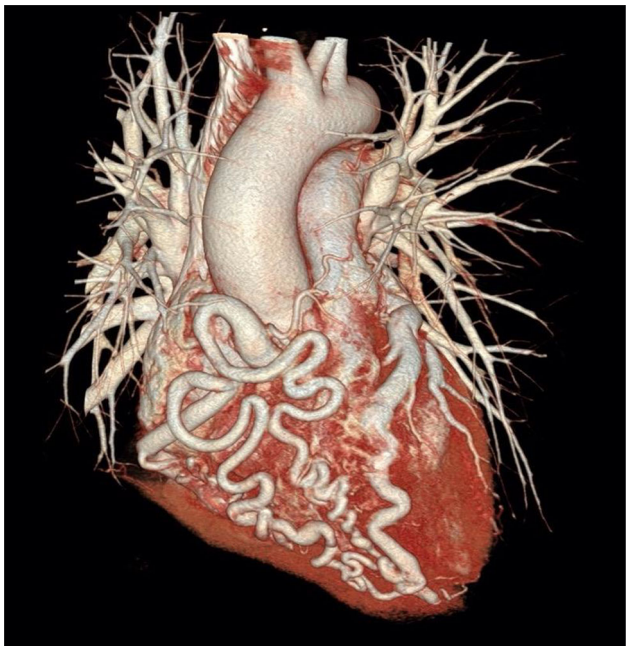

Anomalous left coronary artery from the pulmonary artery (ALCAPA), coronary computed tomography angiography, volume rendering, collaterals between the right and left coronary arteries.

**Results** Out of 39,066 patients, ACAPA was diagnosed in 6, with the prevalence of 0.015%. The prevalence of specific types of ACAPA was as follows: ALCAPA = 0.0077% (3/39,066), ARCAPA = 0.0051% (2/39,066), and ASCAPA = 0.0026% (1/39,066). The mean age of the patients at which the CT examination was performed was 33.2 $\pm$ 16.5 years. ACAPA was often diagnosed in females (5/6 patients). Of 6 subjects, 4 (66.7%) required invasive treatment. Two of 5 female patients gave birth twice. In 3 patients numerous septal collaterals in ventricular septum were seen. The presence of numerous collaterals between RCA and LCA was observed in 2 patients as well as dilated bronchial arteries. In 4 subjects the coronary steal phenomenon was detected.

**Conclusion** ACAPA is an extremely rare congenital coronary artery abnormality in adults, with ALCAPA as the most common type. The anomaly is characterized by a usually severe clinical course and necessitates invasive treatment. However, an uncomplicated pregnancy is feasible even in female patients with uncorrected ALCAPA.

## A-192

### Prevalence of Bicuspid Aortic Valve and Associated Aortopathy in patients who undergo CT Coronary Angiography in a 7-year retrospective dataset

**M. Theodorou, A. Rigkas, F. Sarafis, C. Kyriakou, S. Stratilati**

Papageorgiou General Hospital, Radiology, Thessaloniki, Greece.

**Purpose/Objectives** Bicuspid aortic valve (BAV) is the most common congenital heart disease in the developed world. BAV refers to the morphology of the aortic valve, which may have two cusps or three cusps with malformation of a commissure between the coronary sinuses. It is generally believed that 0.5–2% of the population is affected by BAV.

BAV is typically asymptomatic at younger ages and the diagnosis is made incidentally during routine examinations. However, in adulthood, the diagnosis is usually made because of complications (aortic aneurysm, valvular dysfunction, or aortic dissection). In referral centers, BAV-associated aortopathy has a prevalence of 40%.

In an observational case series with a retrospective chart review of 2038 patients who came to our department for examination with Computed Tomography Coronary Angiography (CTCA) in a 7-year period (January 2015-February 2022), 55 cases (2.7%) of BAV were found. We investigated the prevalence of bicuspid aortic valve types in adults examined with Computed Tomography Coronary Angiography (CTCA) with associated aortopathy.

**Methods & Materials** This is a single-center retrospective study. Each examination was performed with a 256 Multislice CT. The original CT scans were then transferred to an independent workstation for image processing. For each examination, we produced systolic and end-diastolic MPR images. We identified patients with BAV who underwent Computed Tomography Coronary Angiography (CTCA), between January 2015 and February 2022.

In each patient, we recorded age, gender, valve morphology, and function, as well as the diameter of the ascending aorta and associated pathologies.

According to Sievers and Schmidtke, BAV morphology was classified into three types: type 0, 1, or 2, based on the number of raphes.

**Results** In total, 2038 patients underwent CTCA in our department in a 7-year period. BAV was identified in 55 patients, corresponding to a prevalence of 2.7%. The male–female ratio of BAV was approximately 2.7:1.

The most frequent subtype was Type 1 ($\sim$ 87%), with the raphe positioned between the left and right coronary sinuses being the most common ($\sim$ 91.7% of type 1).

The least frequent subtype of all diagnoses BAVs was Type 2—2 raphes- ($\sim$ 3.6%).

Aortic dilatation ($>$ 4 cm) was seen in 26 patients with BAV (47,3%).

**Conclusion** CT imaging plays a vital role in the evaluation of various aspects of Cardiovascular imaging. It is particularly important for the evaluation of the coronary arteries. Furthermore, it is useful in detecting BAV and its complications.

## A-196

### AI denoising improves image quality and radiological workflows in cardiac computed tomography scans

**D. Wessling, S. Afat, A. Brendlin**

University hospital of Tuebingen, Diagnostic and Interventional Radiology, Tuebingen, Germany.

**Purpose/Objectives** To evaluate the impact of an AI denoising algorithm on image quality, diagnostic confidence, and radiological workflows in the context of cardiac Computed Tomography (CT).

**Methods & Materials** 42 consecutive patients with cardiac CT were included and reconstructed using iterative reconstruction (ADMIRE 2), and AI denoising (ClariCT). Place-consistent noise measurements were used to compare objective image quality. Two blinded readers independently performed assessment of subjective image quality, diagnostic confidence, sharpness, and contrast in a forced-choice setup. The results of these assessments were summarized for a semiquantitative overall quality score.

Agatston-score and cardiac age were analyzed semiautomatically for both datasets using proprietary software before, and after manual correction of the initial software output. The time required for manual corrections was measured for each reader to compare possible workflow benefits. Properly corrected mixed-effects analysis with posthoc subgroup tests were used. Spearman's correlation coefficient measured inter-reader agreement for the image quality analysis.

## Results

Noise in ADMIRE 2 reconstructions was significantly higher than for ClariCT (26.00 $\pm$ 4.32 vs. 13.33 $\pm$ 2.87 HU; $p < 0.001$). ClariCT reconstructions had a significantly higher mean overall quality score than ADMIRE 2 (3.5 $\pm$ 1.0 vs. 0.48 $\pm$ 1.0, $p < 0.001$) with good inter-rater agreement ($r \geq 0.790$; $p \leq 0.001$). There were no significant differences between standard and denoised cardiac age results (mean overall: 48.8 $\pm$ 0.5 years, F (1; 41) = 0.8169; p = 0.3714), as well as between standard and denoised Agatston score values (mean overall: 161.31 $\pm$ 27.08 points, F (1; 41) = 0.7732; p = 0,3843). However, the time required for manual corrections was significantly shorter for ClariCT than for ADMIRE 2 (34.68 $\pm$ 29.25 vs. 21.98 $\pm$ 17.52 s, $p < 0.001$).

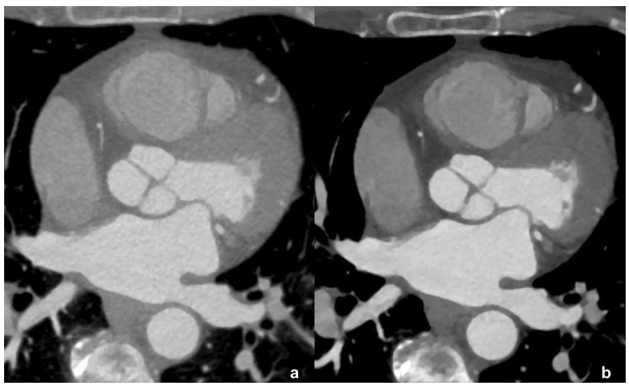


Coronary CT images of a 51-year-old woman with abnormalities in an exercise electrocardiography. AI based ClariCT reconstruction (b) shows a better noise, image quality, sharpness and contrast of the coronary vessels and therefore, a better diagnostic confidence than the images than the images that were processed with iterative reconstruction (a).

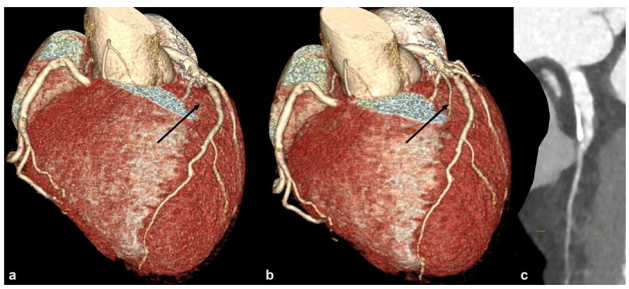


Volume rendering technique (VRT) reconstruction images of a 51-year-old male patient with history of familial coronary heart disease and atypical angina pectoris. The VRT reconstruction based on

ClariCT (b) allows the identification and evaluation of a coronary branch (arrows; c) that could not be identified with iterative reconstruction (b).

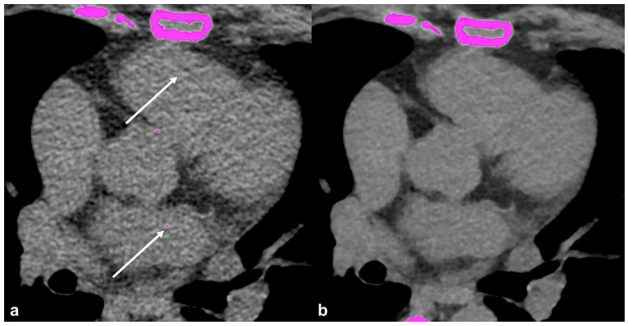


Calcium scoring of a 63-year-old woman with atypical angina pectoris. The images that were reconstructed with ADMIRE 2 (a) show supposed calcifications (arrows) that cannot be confirmed as such. The images that were reconstructed with ClariCT (b) show no false positive findings and thus facilitate the reading process.

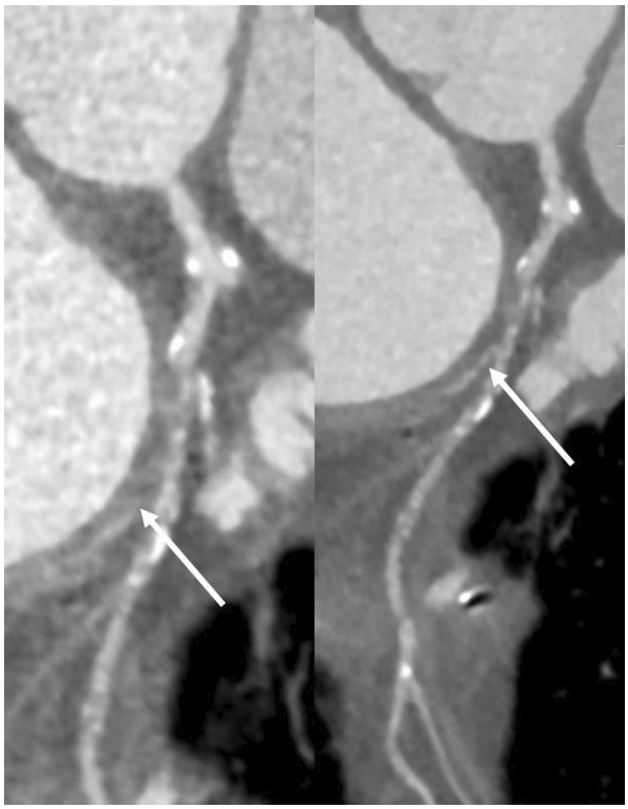

Images of a 63-year-old patient after emergency bypass surgery. The images that were reconstructed with ClariCT (b) allow a better assessment of even smaller coronary vessels of the circumflex coronary artery than the images that were reconstructed with interative reconstruction ADMIRE 2 (a).

**Conclusion** AI denoising significantly improves image quality in cardiac CT and reduces the time required for manual corrections in cardiac age assessment substantially.

## A-197

### Evaluation of liver transplantation candidates with coronary CT angiography

**G. Burcet[1], J.-L. Reyes-Juarez[1], A. Roque[1], A. Aubanell[1], I. Campos[2], L. Castells[2], H. Cuellar-Calabria[1]**

[1]Hospital Universitari Vall d'Hebron, Radiology, Barcelona, Spain, [2]Hospital Universitari Vall d'Hebron, Internal Medicine, Barcelona, Spain.

**Purpose/Objectives** Liver transplantation is the treatment of choice in patients with end-stage liver disease. Over the years there has been a shift in the baseline characteristics of the Liver Transplantation (LT) candidates, with patients having more comorbidities.
Our aim is to describe the results of a Coronary Computed Tomography Angiography (CCTA) performed for the workup of LT candidates and their relation with clinical events before LT.
**Methods & Materials** This is a preliminary retrospective analysis of the first 40 patients who underwent CCTA for inclusion in the LT program from March 2019 to August 2020. We searched the hospital information system for patient demographics, aetiology of the end-stage liver disease and clinical events after CCTA (LT, death before LT, LT not performed). We recorded the CCTA quality (good, fair or suboptimal), the Agatston and the CAD-RADs scores and the number of vessels with plaque. CAD-RADS N was considered as positive for the analysis.
**Results** Aetiologies of end-stage liver disease in the 40 patients were alcoholic liver disease (16), viral liver disease (8), combined alcoholic and viral liver disease (3), genetic disease (6), nonalcoholic steatohepatitis (3), cryptogenic cirrhosis (3) and IgG4 related disease (1). Main cause for LT was hepatocellular carcinoma (24).
Fifty-five percent (22/40) of the group underwent LT 143 $\pm$ 106 days after CCTA and 30% (12/40) died before LT (mean time 154 $\pm$ 103 days). Six patients (15%) were excluded[HC1] from the waiting list owing to tumoral relapse (3), partial functional hepatic recovery (2), and persistent alcoholic intake (1). No cardiac events were recorded after the CCTA.

The quality of the CCTA was good, fair and suboptimal in 35% (14/40), 50% (20/40) and 15% (6/40) of patients, respectively.

Seventeen patients (43%) had an Agatston score $\geq$ 400 units (mean 752 units and range: 0 – 3564 units). Thirty-eight percent (15/40) were considered positive for coronary artery disease (13 CAD-RADS $\geq$ 3, 2 non-diagnostic).

Suboptimal CCTA quality was related to death before LT ($p = 0.034$). CCTA quality in patients with alcoholic liver cirrhosis (ALC) was worse (fair or suboptimal) ($p = 0.025$).

The Agatston and the CAD-RADS scores were not related to death before LT ($p = 0.94$ and $p = 0.29$, respectively). The Agatston Score was related to CAD-RADS $\geq$ 3 ($p < 0.001$).

Patients with ALC and/or viral cirrhosis had a trend towards larger plaque load ($p = 0.054$) and CAD-RADS scores $\geq$ 3 ($p = 0.06$).
**Conclusion** The prevalence of coronary artery disease in our group of LT candidates was 38%, with no cardiac events after CCTA. Worse CCTA quality was related to non-cardiac death before LT and to alcoholic liver cirrhosis.

## A-200

### Image quality assessment of spectral virtual monoenergetic imaging in coronary computed tomography angiography

**L. R. M. Lanzafame, A. Micari, G. Ascenti, A. Blandino, S. Mazziotti, T. D'Angelo**

Azienda Ospedaliera Universitaria Policlinico "G. Martino", Department of Biomedical Sciences and Morphological and Functional Imaging, University Hospital Messina, Italy, Messina, Italy.

**Purpose/Objectives** To define quantitative and qualitative image quality of virtual monoenergetic imaging (VMI) reconstructions and the assessment of coronary stenosis in Spectral Coronary Computed Tomography Angiography (S-CCTA).
**Methods & Materials** 28 patients with suspected coronary artery disease (CAD) underwent a S-CCTA with Dual-Layer Spectral Detector CT scanner (IQon Spectral CT, Philips). Firstly, conventional images and VMI from 40 to 100 keV, in 10-keV intervals, datasets were reconstructed. Objective image quality was evaluated with signal-to-noise ratio (SNR) and contrast-to-noise ratio (CNR) measurements of coronary vessels. Secondly, two radiologists subjectively rated vascular contrast, image sharpness, noise and overall impression for conventional images, 70 keV-VMI (equivalent to conventional CT at 120 kVp) and the VMI dataset with highest CNR, using 5-point Likert scales. Thirdly, detection and grading of coronary stenosis was performed per-vessel either on conventional images, 70-keV VMI and 40-keV VMI with a semi-automated dedicated software, and a correlation analysis was performed.
**Results** VMI-40 keV obtained the highest CNR and SNR values (SNR: 159,9—CNR: 141,6), significantly superior compared to every other dataset (all $p < 0.001$), and the best scores for sharpness, vascular contrast, and for the overall impression (all $p < 0.001$) – (Fig. 1).


Curved-MPR of right coronary artery (RCA) showing a non calcified plaque. 40-keV VMI reconstruction improves image quality compared to conventional (A) and 70-keV VMI (B).

VMI-40 keV also showed excellent correlation (ICC: 0,99) and agreement with conventional images for coronary stenosis grading (Fig. 2).

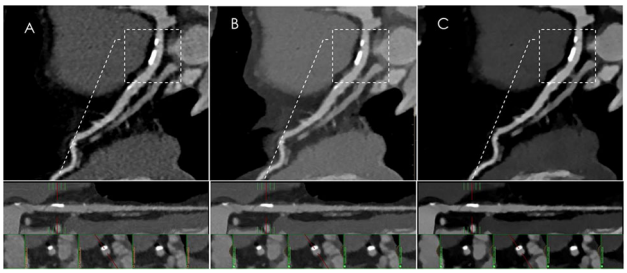


Curved-MPR, stretched MPR and trans-axial reconstructions of left descending coronary artery (LAD) showing calcified plaques on the proximal segment. Trans-axial images demonstrate the excellent correlation of stenosis perception in conventional (A), 70-keV VMI (B) and 40-keV VMI datasets.

**Conclusion** VMI-40 keV allows for significant improvement of both objective and subjective image quality, maintaining an excellent correlation and agreement in coronary stenosis evaluation with conventional images.

## A-201

### Diffuse systemic right ventricular myocardial fibrosis in atrial switch patients in comparison to congenitally corrected transposition of great arteries

**S. Khalil**

Ain Shams University, Cairo, Egypt.

**Purpose/Objectives** The atrial switch operation is performed due to late diagnosis. Systemic right ventricle will support the high-pressure systemic circulation which makes the right ventricle vulnerable for failure. However, the exact cause of the systemic right ventricular failure remains unclear. The effect of pre-operative hypoxia and presence of interstitial myocardial fibrosis on systemic right ventricular function has not been yet evaluated. Recently, T1 myocardial maps has been introduced to measure of the extracellular volume (ECV) representing the interstitial myocardial fibrosis.
**Methods & Materials** We performed a comparative study including 16 patients after atrial switch in comparison to 12 patients with congenitally corrected transposition of great arteries (cc-TGA), with an oxygen saturation above 90%.
**Results** Assessment of myocardial fibrosis (native T1 and ECV) in systemic right ventricular using the 9-segment model and in the left ventricle using 17-segment model was done and correlated to NT-brain natriuretic peptide (NT-proBNP).
Interstitial fibrosis parameters (ECV and native T1) were not correlated with the decreased oxygen saturation before surgery or at time of surgery in TGA patients. They were not correlated the systolic ventricular dysfunction or the dilated systemic right ventricle. This raises the possibility that interstitial fibrosis is an independent marker for the mechanical stress of the systemic right ventricle that appears earlier before deterioration of the ventricular function.

Interstitial fibrosis increases in both ventricles which confirms that it is a problem for the left ventricle to be deprived from its high aortic pressure as the pressure load problem effect in the systemic right ventricle.

No systemic right ventricle territorial predilection in both interstitial fibrosis parameters in Mustard and cc TGA groups. This is

against the theory of increased systemic right ventricle dysfunction as a result of its limited blood supply in comparison to the left ventricle.
**Conclusion** Interstitial myocardial fibrosis is an independent parameter for assessment of systemic right ventricular which is not related to hypoxic stress. It is related to the hemodynamic stress of being under high pressure circulation.

## A-205

### CT-coronary-angiography in high-pitch-TAVI-planning-CT: Why it rarely works

**P. Seitz, R. Gohmann, C. Luecke, M. Gutberlet**

Heart Center Leipzig at University of Leipzig, Department of Diagnostic and Interventional Radiology, Leipzig, Germany.

**Purpose/Objectives** Depiction of the access route and annular dimensions are now mandatory before TAVI. Seemingly coincidently, the coronary arteries are sometimes diagnostically depicted during high-pitch-TAVI-planning-CT. In this retrospective analysis we investigated the factors influencing the diagnostic depiction of coronaries in high-pitch-TAVI-planning-CT.
**Methods & Materials** 100 patients (46 female, mean age 79 ± 5.9 years) underwent Dual-Source-CT-Scan (Siemens, Definition FLASH) in prospectively-ECG-triggered-High-Pitch-Mode after injecting 70 ml contrast medium (Iomeprol 400mgI/ml; 3.5 ml/s) for evaluation of the access route and annulus dimensions.
Number of diagnostic coronary-segments (DSpP) per patient were analyzed and set in relation to heartrate, BMI, coverage along the z-axis (CaZA) and heart-rhythm.
**Results** Overall, 30.3% of coronary segments were diagnostically depicted. Mean heartrate was 75 ± 19 bpm and correlated inversely with DSsP (r = -0.35; $p < 0.001$). CaZA (% of RR-interval) correlated inversely with DSpD (r = -0.33; $p < 0.001$). CaZA correlated strongly with heartrate (r = 0.71; $p < 0.0001$). BMI correlated negatively with DSpP (r = -0.26; $p < 0.01$).
Subgroup-analysis of patients with atrial fibrillation and sinus rhythm showed no significant difference in DSpP between the groups ($p = 0.11$). Mean heartrate variability was 15 ± 23 bpm and showed no correlation to DSpP (r = 0.256; $p = 0.11$).
**Conclusion** The most significant factors influencing DSsP are CaZA, HR and BMI. As most of these parameters are either intrinsic to the patient or are difficult to influence in this patient group, fully diagnostic exams are rare and only occur under very special circumstances (low heartrate and narrow CaZA) with this technique.
Thus, limiting the ECG-synchronized scan range to optimize CaZA could potentially improve the frequency of fully diagnostic studies and should be investigated further.

## A-207

### Between a clot and a hard place: Watchman device superior to warfarin but inferior to DOACs for ischemic stroke prevention in patients with atrial fibrillation

**B. Miles**

University of Texas Medical Branch at Galveston, Galveston, United States of America.

**Table 1** Comparison of outcomes at 1 and 5 years

| | | |
|---|---|---|
| Watchman vs Warfarin 1 yr: RR 0.85 | 95% CI (0.78,0.94) | P value 0.001 |
| Watchman vs Warfarin 5 yr: RR 0.94 | 95% CI (0.86,1.02) | P value 0.1156 |
| Watchman vs DOAC 1 yr: RR 1.26 | 95% CI (1.13,1.40) | P value < 0.0001 |
| Watchman vs DOAC 5 yr: RR 1.30 | 95% CI (1.19,1.43) | P value < 0.0001 |

**Purpose/Objectives** The Watchman device is approved in the United States for use in patients with atrial fibrillation for closure of the atrial appendage and reduction of embolic stroke risk. The PREVAIL and PROTECT AF trials have shown the Watchman to be noninferior to Warfarin, but not much is known about the Watchman's ischemic stroke reduction compared to the newer direct oral anticoagulants (DOACs). The purpose of this study is to determine any difference in ischemic stroke reduction between the Watchman device as compared to warfarin and DOAC medication.
**Methods & Materials** The federated global TriNetX research network was used to compare the Watchman device against warfarin and the newer direct oral anticoagulants for risk of subsequent ischemic stroke at 1 and 5 years. Three patient cohorts were created, all with atrial fibrillation determined by International Classification of Disease-10 (ICD-10) code I84. One cohort was on treatment with warfarin, one was on treatment with direct oral anticoagulants, and one received the watchman device. After balancing the cohorts for age, race, gender, and ethnicity, each cohort contained 6,463 patients. The primary endpoint was the risk of ischemic stroke via ICD-10 code I63 at 1 and 5 years.
**Results** At 1 year, the relative risk of ischemic stroke for the Watchman device was 0.85 against warfarin but 1.26 against the newer direct oral anticoagulants, and the results were statistically significant. By year 5, the Watchman and warfarin cohorts showed comparable ischemic stroke risk and loss of statistical significance. The relative risk of ischemic stroke for the Watchman against DOACs was higher and statistically significant at both 1 and 5 years (1.26 and 1.3, respectively). See Table 1.
**Conclusion** This data is consistent with the results of the PREVAIL and PROTECT AF trials, showing noninferiority between the Watchman and warfarin for ischemic stroke risk reduction. The watchman device was superior to warfarin at 1 year, but equivalent by year 5. However, this data also shows that patients with atrial fibrillation will have the greatest risk reduction for ischemic stroke when treated by direct oral anticoagulants, with the outcome statistically significant at both 1 and 5 years. The Watchman is an option for patients who cannot tolerate oral anticoagulation, but patients who can might best be served by treatment with DOAC medication.

## A-208

### Multiparametric CT-characterisation of myocardial tissue remodelling in patients with severe aortic stenosis candidate to transcatheter aortic valve implantation

**C. Gnasso[1], A. Palmisano[2], D. Vignale[2], D. Margonato[2], E. Agricola[2], A. Esposito.[1]**

[1]IRCCS Ospedale San Raffaele, Radiology, Milan, Italy, [2]IRCCS Ospedale San Raffaele, Milan, Italy.

**Purpose/Objectives** Case–control study aimed to investigate structural adaptations of the myocardium on CT examination in Low Flow Low Gradient (LFLG) and High Gradient (HG) aortic stenosis (AS) patients candidate for transcatheter aortic valve implantation (TAVI).
**Methods & Materials** Eighty-eight consecutive patients candidate to TAVI, 19 (22%) LFLG e 69 (78%) HG according to echocardiographic data, were enrolled.
A multiparametric TAVI-planning CT protocol was implemented including a time-resolved volumetric reconstruction of aortic valve (AV) and cardiac chambers and 5-min late contrast enhancement scan with left ventricle (LV) extracellular volume (ECV) map reconstruction. Quantitative CT-derived variables were: AV area, AV calcium score (AVCS), AV regurgitant volume (AVRV), LV myocardial mass and ECV, ventricles volumes (end systole, ESV; and end diastole, EDV) and ejection fraction (EF). Measurements were generated by semi-automatic post-processing on dedicated softwares.
**Results** Mean gradient in LFLG group was 30 mmHg [IQR, 22.5 – 35.5] vs 46 mmHg [IQR, 41 – 53] in HG group ($p < 0.0001$). At CT-scan, mean ESV on overall population was 70.8 ml (± 54,9), EDV 161 ml (± 55), mean AVRV was 16.5 ml (± 20,9), mean LV mass 162.5 g (± 48,5) and AVCS was 2738 (± 1994). There was a significant difference in ECV (35% vs 28%, $p = 0.001$), LV-EF (45% vs 63%, $p = 0.037$), AVA (1 cm2 vs 0.90 cm2; $p = 0.036$) and global longitudinal strain (-12% vs -16%, $p < 0.05$) between LFLG and HG groups. ECV had a significant negative correlation with LV-EF ($R = -0,253$ $p = 0.017$), mean transvalvular gradient ($R = -0,415$; $p < 0.001$) and AV calcium score ($R = -0.226$; $p = 0.035$).
**Conclusion** Improved CT-scan protocol may provide additional information about myocardial remodelling and tissue characterisation in patients with different AS functional stages.
Further studies are needed to assess the prognostic value of this approach.

This study was approved by an ethics committee and consent was signed.

## A-209

### The utility of cardiac MR in the diagnosis of straight Back Syndrome – an underdiagnosed condition

**W. K. Lau[1], C. C. Ong[1], C. H. Sia[2], D. Singh[2], L. L. S. Teo[1]**

[1]National University Hospital, Department of Diagnostic Imaging, Singapore, Singapore, [2]National University Hospital, Department of Cardiology, Singapore, Singapore

**Purpose/Objectives** Straight Back Syndrome (SBS) has been described as a pseudo-heart syndrome, whereby a loss of the normal thoracic kyphosis results in mass effect on the underlying heart, producing clinical signs and symptoms that can mimic congenital heart diseases. For example, clinically, the presence of a systolic murmur suggests a ventricular septal defect, an atrial septal defect, pulmonary stenosis or aortic stenosis. Occasionally, SBS can be associated with other cardiac abnormalities such as mitral valve prolapse and a bicuspid aortic valve. The incidence of SBS in the general population is unknown. The standard evaluation of SBS involves a multimodality approach, requiring thoracic radiographs, electrocardiography and echocardiography. As a modality that can provide both structural and functional imaging of the heart and thoracic cage, cardiac MR is an increasingly favoured option in the evaluation of SBS, due to its ability to both establish the diagnosis, exclude other congenital cardiac abnormalities as a cause for symptoms, as well as assess for associated cardiac pathology. We aim to demonstrate the utility of cardiac MR in the diagnosis of SBS using clinical cases.
**Methods & Materials** As above.
**Results** As above.
**Conclusion** As above.

## A-210

### Coronary plaque features and stenosis assessment on coronary CT angiography acquisitions in patients with clinical suspicion of stable coronary artery disease

**R. M. Popa[1], R. E. Bîrlă-Coroiu[1], R. M. Manea[1,2]**

[1]Clinical Emergency County Hospital of Braşov, Romania, Department of Radiology and Medical Imaging, Braşov, Romania, [2]Faculty of Medicine, "Transilvania" University of Braşov, Romania, Radiology, Braşov, Romania

**Purpose/Objectives** Coronary artery disease (CAD) remains the leading cause of mortality worldwide. Thanks to its non-invasive features and its high diagnostic value of ruling out obstructive CAD, without the need of further invasive testing, such as coronary angiography, coronary CT angiography is recommended as the initial test for evaluating patients with clinical suspicion of stable CAD.
The purpose of this study is to fully illustrate the features of coronary plaques and the presence of coronary stenosis on CTA acquisitions.
**Methods & Materials** 68 patients who were admitted to the Cardiology Department of Clinical Emergency County Hospital Braşov for clinical suspicion of stable CAD between November 2018 to June 2019, who had performed a coronary CTA on admission, were included in this retrospective study. Inclusion criteria: age $\geq 30$, hemodynamically stable, typical/atypical angina/dyspnoea, heart rate $< 60$ bpm, no contraindications to iodinated contrast agents/beta-blockers/nitroglycerin, no pregnancy, no arrythmias.
**Results** Out of 68 patients aged between 34–75 years, 63.24% were females and 36.76% were males. Because coronary CTA allows simultaneous assessment of luminal dimensions/stenosis and the vessel wall and also detailed plaque characterization, it can identify the existence of an atherosclerotic process at an early stage. Two scanning protocols were used: calcium score (no contrast, low radiation dose) present in 42.65% patients and absent in 57.35% of patients (ruling out CAD). Extensive calcium score was present in 5 patients (excluded out of the study), who were referred to the catheterization lab. imediately for further invasive testing without performing contrast-enhanced CTA acquisitions—more data will be presented.
However, it is at the utmost importance to evaluate the type of atherosclerotic plaque, because the presence of non-calcified plaques cannot be excluded based on calcium score, therefore the second protocol included contrast-enhanced CTA acquisitions (intravenous contrast, higher radiation dose), which showed that stenosis were present in 51.47% patients. Detailed characterisation of plaque components showed 75.64% calcified, 19.23% non-calcified, 5.13% mixed plaque. The most frequent artery affected was the left anterior descending artery.
**Conclusion** CTA allows comprehensive assessment of plaque of the coronary artery wall before luminal narrowing develops (early stage), which plays a vital role in the evaluation and further accurate management of patients with CAD. Besides its high diagnostic value of ruling out obstructive CAD in patients with clinical suspicion of stable CAD, it has the advantage of quickly obtaining images. In patients with extensive calcium score referral to the catheterization lab is mandatory.

## A-211

### Imaging features of the anatomical variants of the superior Vena Cava and its affluences on contrast enhanced CT acquisitions—a pictorial review

R. M. Popa[1], R. E. Bîrlă-Coroiu[1], R. M. Manea[1,2]

[1]Clinical Emergency County Hospital of Braşov, Romania, Department of Radiology and Medical Imaging, Braşov, Romania, [2]Faculty of Medicine, "Transilvania" University of Braşov, Romania, Radiology, Braşov, Romania.

**Purpose/Objectives** Anatomical variants of the superior vena cava and its affluences are relatively common in the current medical imaging field, due to the complex embryology of the venous system. The aim of this pictorial review is to fully illustrate these anatomical variants in order to obtain a correct interpretation of cross-sectional images acquired from contrast enhanced CT scans, avoiding erroneous diagnosis. A comprehensive preoperative or pre-interventional assessment of the anatomy of the superior vena cava is also at the utmost importance, in order to avoid potential sources of complications, which might occur.
**Methods & Materials** Cases were selected from the database of the Clinical Emergency County Hospital of Braşov, Romania between 01.01.2018 – 20.05.2022, which fully illustrate anatomical variants of the superior vena cava and its affluences incidentally identified on contrast enhanced CT acquisitions. Cases were investigated with a GE Optima660 128-slice CT scanner, with different scanning protocols including unenhanced, arterial and venous phase, acquired for different suspicion diagnosis.
**Results** The imaging particularities of each anatomical variant and their pathophysiological impact (if present) were noted. The symptomatology varies from completely asymptomatic, incidentally discovered on contrast enhanced CT acquisitions, acquired for other suspicion diagnosis, to the presence of right-to-left shunt (rare) in case of left-sided SVC with drainage situs in the left atrium.
Detailed knowledge and accurate identification of these anatomical variants represent crucially important aspects in the current medical, interventional and surgical practice, in order to exclude a venous pathology, but also to identify the presence of frequently associated abnormalities and syndromes, and nevertheless for further management and treatment, which might be necessary in some cases. The treatment usually depends on the patient's symptomatology and the type of anatomical variant involved and it varies from medical treatment to imaging follow-up or surgical intervention.
**Conclusion** To sum up, comprehensive knowledge and accurate imaging identification of the anatomical variants of the superior vena cava and its affluences are key to a correct preoperative evaluation of the patient, in order to avoid potential complications during surgical interventions. A thorough evaluation of the anatomy of the superior vena cava and its affluences on contrast enhanced CT acquisitions should represent a fundamental search pattern in the current medical imaging field.

## A-215

### The role of coronary CT angiography in the diagnosis of myocardial bridging – a pictorial review

R. M. Popa[1], E. M. Aron[1], R. E. Bîrlă-Coroiu[1], R. M. Manea[1,2]

[1]Clinical Emergency County Hospital of Braşov, Romania, Department of Radiology and Medical Imaging, Braşov, Romania, [2]Faculty of Medicine, "Transilvania" University of Braşov, Romania, Radiology, Braşov, Romania.

**Purpose/Objectives** Myocardial bridging is a common congenital anomaly of the coronary arteries, where a coronary artery courses through the myocardium. It is found approximately in 20–30% of the adult population in autopsy studies. The incidence on coronary angiograms varies between 2–15% and they can also be easily identified on coronary CT angiography acquisitions. Myocardial bridging is most commonly a benign condition, but sometimes it can lead to severe complications, such as myocardial infarction, acute coronary syndromes, arrythmias, ventricular tachycardia, left ventricular dysfunction and even sudden cardiac death. Therefore, the aim of this pictorial review is to clearly highlight the most important imagistic features of myocardial bridging on coronary CT angiography aquisitions and richly illustrate the importance of properly diagnosed myocardial bridging of the coronary arteries and the severity of complications, that may occur, in case of misdiagnosis.
**Methods & Materials** The following pictorial review includes a series of cases, meaning a total number of 23 patients collected from the Database of the Clinical Emergency County Hospital of Braşov, Romania, between 01.01.2016—20.05.2022, who had performed coronary CTA on admission and myocardial bridging was present. Details regarding the patients' age, gender, symptoms on admission, associated cardiac diseases and a comprehensive imagistic interpretation of acquisitions acquired from coronary CTA are also included in this pictorial review.
**Results** The selected cases with myocardial bridging were classified based on the coronary artery involved, the most frequent location being the left anterior descending artery (LAD), also taking into account the coronary segment (using the 17 segment model based on the American Heart Association published in 1975 by Austen et al.) for an exact localization. The cases were also classified in superficial (incomplete) or deep (complete) myocardial bridging, fully noting the particularities of each case and the pathophysiological impact, if present. The symptomatology varies from completely asymptomatic, incidentally discovered on coronary CTA acquisitions, acquired for other suspicion diagnosis, to ischemia-related symptoms, such as angina (tyipical or atypical), dyspnoea, tachycardia, arrythmias etc.
**Conclusion** In conclusion, coronary CTA is an established and reliable imaging method to accurately identify and classify myocardial bridging. Thorough knowledge of myocardial bridging represent important aspects for radiologists in order to obtain a correct and comprehensive interpretation of coronary CTA acquired acquisitions, which are crucially important for further therapeutic management of the patients, in order to avoid major complications in case of misdiagnosis.

## A-218

### Perivascular fat attenuation measured with coronary CT angiography is a predictor of cardiac mortality in post cardiac transplant surveillance

P. Moser[1], R. Schernthaner[1,2], C. Loewe[1], V. Nizhnikava[3], A. Zuckermann[4], M.-E. Stelzmüller[4], D. Beitzke[1]

[1]Medical University of Vienna, Department of Biomedical Imaging and Image-guided Therapy, Vienna, Austria, [2]Klinik Landstraße, Radiologie, Vienna, Austria, [3]Medical University of Graz, General Radiology, Graz, Austria, [4]Medical University of Vienna, Cardiac Surgery, Vienna, Austria

**Purpose/Objectives** Cardiac allograft vasculopathy (CAV) is a leading cause of morbidity and mortality beyond the first year after cardiac transplantation. Intimal hyperplasia in early-stage CAV can be difficult to detect in coronary computed tomography angiography (CCTA). Recently, a novel imaging biomarker, perivascular adipose

tissue (PVAT) density measured with CCTA, was demonstrated to have diagnostic and value in inflammatory coronary artery disease in native hearts. Here, we evaluate longitudinal PVAT measurements with CCTA in a cardiac transplantation cohort.

**Methods & Materials** We included 39 cardiac transplant patients with two or more post-transplant CCTAs between 2010 and 2021. Tube voltages ranged from 70 to 140 kV, depending on patient size. The fat attenuation index (FAI) measured from the vessel wall radially at the length equal to the diameter of the vessel was analysed along the proximal left anterior descending (LAD), right coronary artery (RCA) and left circumflex artery (LCx) at a threshold of − 30 to − 190 Hounsfield Units (HU).

**Results** In total, FAI measurements in 113 CCTAs obtained on two different machine models from a single vendor were analysed. The FAI values of each coronary vessel in CCTAs measured at 120kv versus non-120kv were significantly different (RCA -77.9 ± 12.2 vs. -88.0 ± 9.2, $p < 0.0001$; LAD -77.5 ± 9.1 vs -86.2 ± 9.4, $p < 0.0001$; LCx -72.6 ± 10.2 vs -79.6 ± 7.3, $p < 0.0001$, respectively). Within CCTAs at one time point, the FAI between coronary vessels was strongly correlated (RCA and LAD R = 0.67 ($p < 0.0001$), RCA and LCx R = 0.58 ($p < 0.0001$), LAD and LCx R = 0.67 ($p < 0.0001$)). The FAIs of each coronary vessel between a patient's first and last CCTA completed at 120 kV were also highly correlated (RCA R = 0.73 ($p < 0.0001$), LAD R = 0.81 ($p < 0.0001$), LCx R = 0.55 ($p = 0.0069$). Finally, high mean FAI values in the perivascular fat of all three coronary vessels at baseline (mean ≥ -71 HU) were associated with cardiac mortality or re-transplantation, however, were not associated with all cause-mortality.

**Conclusion** High baseline FAI values may be useful in identifying a higher risk cardiac transplant population; thus, FAI measurements may support implementation of CCTA in routine post-transplant surveillance.

## A-219

### Cardiac magnetic resonance to detect subacute myocarditis

**J. M. Brendel[1], J. Kübler[1], K. Klingel[2], K. Müller[3], F. Hagen[1], M. Gawaz[3], K. Nikolaou[1], S. Greulich[3], P. Krumm[1]**

[1]Universitätsklinikum Tübingen, Diagnostic and Interventional Radiology, Tuebingen, Germany, [2]Universitätsklinikum Tübingen, Cardiopathology, Tuebingen, Germany, [3]Universitätsklinikum Tübingen, Cardiology, Tuebingen, Germany

**Purpose/Objectives**

(1) To non-invasively detect patients with subacute myocarditis and
(2) To compare acute vs. subacute myocarditis with CMR.

**Methods & Materials** 48 patients (age 37 [28–55] years; 52% female) with acute onset or subacute course of cardiac symptoms and clinically suspected myocarditis were consecutively included. Patients with onset of symptoms ≤ 2 weeks prior to CMR were grouped as *acute* (n = 25, 52%), onset of symptoms ≤ 2 months as *subacute* (n = 23, 48%). CMR protocol comprised current Lake Louise criteria (LLC) including late gadolinium enhancement imaging (LGE) and mapping (T1, ECV, T2) as well as additional detection of pericardial effusion and acquisition of morphology, volumetry, and 3D-strain.

**Results** (1) In the detection of subacute myocarditis and the distinction from healthy volunteers, LGE yielded the most accurate diagnostic performance with an area under the curve (AUC) of receiver-operating curve (0.96) followed by ECV (0.90), $T_2$ (0.79) and $T_1$ (0.76). (2) In comparison of acute from subacute myocarditis, the best differentiation was provided by LGE (0.76) followed by $T_2$ (0.66).

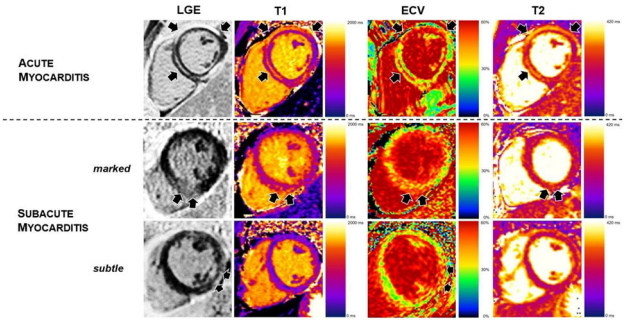


**Fig. 1** CMR findings. Appearance of acute and subacute myocarditis in CMR

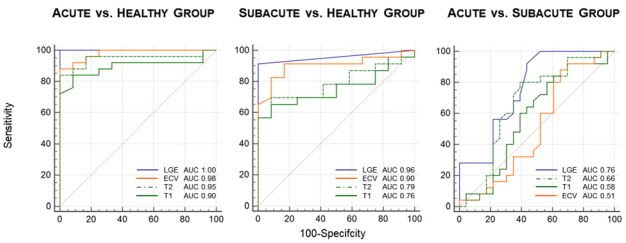


**Fig. 2** ROC curve for distinction of subacute myocarditis from healthy volunteers and comparison of acute vs. subacute myocarditis

**Conclusion** (1) Subacute myocarditis can be detected by elevated $T_1$, $T_2$ and ECV as well as high prevalence of LGE, hereby LGE and ECV with the best diagnostic performance. (2) The best differentiation to acute myocarditis was provided by LGE and $T_2$. However, differentiation of acute and subacute myocarditis can be difficult in CMR alone.

## A-222

### Preliminary data on fully automated left ventricular late gadolinium enhancement detection by a convolutional neuronal network in chronic myocardial infarction

**M. Pamminger[1], M. Schwab[1], C. Kremser[1], D. Obmann[2], M. Haltmeier[2], A. Mayr[1]**

[1]Medical University Innsbruck, University Hospital for Radiology, Innsbruck, Austria, [2]University of Innsbruck, Department of Mathematics, Innsbruck, Austria.

**Purpose/Objectives** To compare fully automated segmentation of left ventricular late gadolinium enhancement (LGE) as evaluated by a convolutional neuronal network (CNN) with manual segmentation in chronic myocardial infarction.

**Methods & Materials** Cardiac magnetic resonance imaging including two-dimensional LGE imaging was performed on a 1.5 T clinical scanner 12 months after ST-elevation myocardial infarction. LGE images were presented to a trained CNN for automated segmentation of left ventricular myocardium and consequently absolute LGE volume. Manual LGE segmentation according to the + 5-SD method

was used as reference standard. Image quality was assessed according to a 3-point Likert scale (2 = perfect image quality, 1 = some artifacts without impaired LGE delineation, 0 = strong artifacts with impaired LGE delineation). Regression and Bland–Altman analysis were performed.
**Results** In 207 included patients (177 male, mean age 57 years) LGE volume was 10.1 (interquartile range 3.8 to 17.0) ml according to manual segmentation and 8.9 (2.9 to 17.0) ml according to CNN segmentation. Bland–Altman analysis showed little average difference (0.6 ml, $p = 0.370$), however, limits of agreement ranged from -13.8 to 15.0 ml. Linear correlation was fair (0.75, $p < 0.001$). Subgroup analysis according to image quality showed comparable performance of CNN segmentation in all three groups.
**Conclusion** Our fully automated LGE segmentation approach based on a CNN in two-dimensional data sets provides measurements with little average difference compared to very time-consuming manual segmentations. However, dispersion is substantially and limits the current application of this approach on a per-patient basis. Image quality does not affect CNN performance.

## A-224

### Post-mortem cardiac magnetic resonance in explanted heart of patients with sudden death: a validation study

**G. D. Aquaro[1], C. De Gori[2], B. Guidi[3], A. Pucci[4], E. Chiti[5], P. Di Marco[3], E. Neri[2]**

[1]G. Monasterio CNR-Tuscany Foundation, Pisa, Italy, [2]University of Pisa, Academic Radiology, Department of Translational Research, Pisa, Italy, [3]University of Pisa, UO Medicina Legale, Pisa, Italy, [4]University of Pisa, Department of Histopathology, Pisa, Italy, [5]University of Pisa, Clinical and Translational Science Research Department, Pisa, Italy.

**Purpose/Objectives** Post-mortem Cardiac Magnetic Resonance (PMCMR) is an emerging ancillary tool for forensic medicine. We sought to evaluate the diagnostic accuracy of PMCMR to detect cardiac disease in consecutive patients with sudden death.
**Methods & Materials** PMCMR was performed in formalin-fixed explanted death of 115 cases of sudden death.
**Results** Forensic diagnosis of cardiac cause of death was ascertained in 72 (63%) patients; a negative cardiac analysis in 37 (32%). In 6 cases analysis was not performed because of inadequate body preservation. PMCMR interpretation matched with final forensic diagnosis in 93 out of 115 cases (81%) with sensitivity 88%(79–95%), specificity 65%(47–80%), PPV 84% (78–90%), NPV 73% (58–84%), accuracy 81% (72–88%), AUC 0.77 (0.68–0.84). However, a PMCMR-driven approach permitted to identify 9 of myocardial fat infiltration that were missed using only the guideline-driven histological sample. The overall sensitivity of PMCMR in diagnosing ischemic heart disease (IHD) as cause of death was 96% (84–99.9%), specificity 98% (92–99.9%), PPV 97% (85–99.6%), NPV 97% (89–99%), accuracy 97% (93–99%). The AUC for IHD diagnosis was 0.97 (0.93–0.99).
**Conclusion** PMCMR has high accuracy to identify the cardiac cause of sudden death and may be considered a valid auxilium for forensic diagnosis. Its diagnostic value is particularly high in case of ischemic heart disease and in conditions with focal myocardial damage.

## A-226

### Myocardial function and characterization in pediatric patients with covid-19 related multisystem inflammatory syndrome (MISC)

**D. Capra[1], C. B. Monti[1], L. Mauri[2], S. Mannarino[3], M. Garbin[3], I. Raso[3], F. Sardanelli[1,4], F. Secchi[1,4]**

[1]Università degli Studi di Milano, Department of Biomedical Sciences for Health, Milan, Italy, [2]Fondazione IRCCS Ca' Granda, Unità di Cardiologia, Milan, Italy, [3]Ospedale dei Bambini "Vittore Buzzi", Unità di Cardiologia Pediatrica, Milan, Italy, [4]IRCCS Policlinico San Donato, Unità di Radiologia, San Donato Milanese, Italy.

**Purpose/Objectives** To assess the myocardial status of pediatric patients who had COVID-19-related Multisystem Inflammatory Syndrome (MISC) at cardiac magnetic resonance (CMR).
**Methods & Materials** We retrospectively reviewed pediatric patients with MISC who underwent echocardiography at hospital admission and CMR at follow-up. A left ventricular (LV) ejection fraction (EF) < 50% at echocardiography was considered reduced. LV indexed end-diastolic (EDVi), end-systolic (ESVi) volumes, stroke volume (SV) and EF were calculated from CMR. Moreover, we measured LV native and post-contrast T1 times in a 4-chamber view, and we performed extracellular volume (ECV) analysis using synthetic haematocrit.
**Results** 36 patients were included, 8 (22%) of whom females, with a median age of 11 years (9–13 years). 17 (47%) patients had reduced EF at echocardiography. The median interval between echocardiography and CMR was 41 days (23–54 days). At CMR LV EDVi was 69 ml/m$^2$ (63–73 ml/m$^2$); LV ESVi 22 ml/m$^2$ (20–24 ml/m$^2$); LV SV 62 ml/m$^2$ (54–74 ml/m$^2$); LV EF 68 ml/m$^2$ (64–72 ml/m$^2$). No patients had reduced LV EF at CMR. Native T1 times were 1016.7 ms (974.0–1070.1 ms), whereas post-contrast T1 times were 511.5 ms (479.9–528.5 ms). Median ECV was 24.7% (22.3–26.8%). No significant differences were found by age, weight, and time interval between echocardiography and MRI between patients with preserved or reduced EF ($p > 0.057$). Patients with reduced EF had increased LV EDVi (72 ml/m$^2$ [68–75 ml/m$^2$] vs 66 ml/m$^2$ [61–70 ml/m$^2$], $p = 0.017$) and LV ESVi (23 ml/m$^2$ [21–28 ml/m$^2$] vs 21 ml/m$^2$ [20–22 ml/m$^2$], $p = 0.019$), and reduced ECV (23.3% [20.9–24.7%] vs 25.9% [24.6–27.6%], $p = 0.003$).

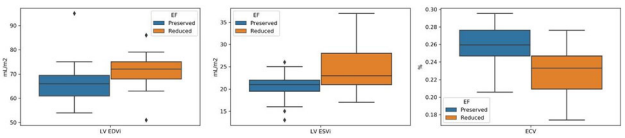


Boxplots of LV EDVi, LV ESVi, and ECV differences among patients with preserved or reduced ejection fraction at hospitalization.

**Conclusion** Over 35% of patients with MISC showed a transient reduced EF, that reverted to normal at follow-up. Increased LV EDVi, ESVi and reduced ECV at follow-up CMR in such patients may be early signs of myocardial remodeling. CMR in pediatric patients that suffered from COVID-19 related MISC could reveal early signs of myocardial remodeling and should hence be part of the follow-up of these patients.

## A-227

### Diagnostic role of native T1 mapping compared to conventional magnetic resonance techniques in cardiac disease: a real-life study

C. De Gori[1], M. Adami[1], G. Todiere[2], A. Barison[3], C. Grigoratos[3], M. L. Parisella[1], L. Faggioni[1], R. De Caterina[4], G. D. Aquaro[3], E. Neri.[1]

[1]University of Pisa, Academic Radiology, Department of Translational Research, Pisa, Italy, [2]G. Monasterio CNR-Tuscany Foundation, Pisa, Pisa, Italy, [3]G. Monasterio CNR-Tuscany Foundation, Pisa, Italy, [4]Pisa University Hospital, University of Pisa, Cardiovascular Division, Pisa, Italy.

**Purpose/Objectives** T1 mapping is a validated technique in cardiac magnetic resonance (CMR), however in real-life clinical practice its effectiveness to diagnose myocardial disease is still unclear. We sought to compare native T1 mapping to conventional Late gadolinium enhancement (LGE) and T2-STIR techniques for the evaluation of a cohort of consecutive patients undergoing CMR for the suspicion of myocardial disease.

**Methods & Materials** CMR was performed in 323 patients, 206 males (64%), mean age 54 ± 8 years and in 27 age- and sex- matched healthy controls. LGE, T2-STIR and pre and post-contrast T1 mapping were acquired as suggested by the SCMR position paper. The CMR findings of global and regional T1 mapping were compared to the respective results of LGE and T2-STIR techniques. The main baseline indications for CMR were: suspicion of ARVC in 20%; non-ischemic DCM in 19%; HCM in 16%; chest pain without obstructive coronary artery in 14% of patients (suspicion of MINOCA, Takotsubo or myocarditis); other indications (amyloidosis, scleroderma, previous myocardial infarction, pericarditis, LV non compaction) in the remaining of cases.

**Results** At T2-STIR images myocardial hyperintensity suggesting edema was found in 41 patients (27%). LGE images were positive in 206 patients (64%). Native T1 mapping was abnormal in 171 (49%). In 206 patients (64%) a matching between LGE and native T1 was found (both positive in 132 and negative in 74). T1 was also abnormal in 32 out of 41 (78%) with edema at T2-STIR. Overall, LGE and/or T2-STIR were abnormal in 209 patients, whereas native T1 in 154(52%). Conventional techniques and T1 mapping were concordant in 208 patients (64%). Conventional techniques were abnormal in 76 (24%) of patients with negative T1 mapping. Finally, in 39 patients T1 mapping was positive despite negative conventional techniques (12%). Among these latter 39 patients, only in 18 T2-STIR were acquired based on clinical decision. Then, the percentage of cases where T1 mapping could have an additive role would range between 6 and 12%.

T1 mapping was particularly able in conditions with diffuse myocardial damage as cardiac amyloidosis, scleroderma and fabry disease (additive role in 42%). On contrast, T1 mapping was less effective in cardiac disease with regional distribution of myocardial damage as myocardial infarction, HCM, myocarditis (additive role in 1%).

**Conclusion** T1 mapping may give additive information in 6–12% of patient but is less effective cardiac disease presenting with regional or segmental distribution of myocardial damage. Results of the present study suggest that Conventional LGE/T2-STIR and T1 mapping are complementary techniques and should be used together in every CMR examination.

## A-228

### Detection and estimation of breast arterial calcifications on mammograms with deep transfer learning

N. Mobini[1], M. Codari[2], F. Riva[3], M. G. Ienco[3], D. Capra[1], A. Cozzi[1], S. Carriero[4], D. Spinelli[4], R. M. Trimboli[5], G. Baselli[3], F. Sardanelli[1,5]

[1]Università degli Studi di Milano, Department of Biomedical Sciences for Health, Milan, Italy, [2]Stanford University School of Medicine, Department of Radiology, Stanford, CA, United States of America, [3]Politecnico di Milano, Department of Electronics, Information and Bioengineering, Milan, Italy, [4]Università degli Studi di Milano, Postgraduation School in Radiodiagnostics, Milan, Italy, [5]IRCCS Policlinico San Donato, Unit of Radiology, Milan, Italy.

**Purpose/Objectives** Breast arterial calcifications (BAC) are common incidental findings on routine mammograms which are correlated with coronary arteries calcium score and have been suggested as a sex-specific cardiovascular disease (CVD) biomarker that might improve female CVD risk stratification. In this study, we implemented and evaluated the performance of a transferred deep convolutional neural network (CNN) model for automatic detection and estimation of BAC burden.

**Methods & Materials** Four-view standard mammograms were included in this retrospective study and labelled as BAC positive (BAC +) or BAC negative (BAC-) by 4 expert readers. The study included 1493 women (194 BAC +) with a median age of 59 (interquartile range: 52–68) years. Using transfer learning principles, the 16-layer pre-trained Visual Geometry Group (VGG16) model was fine-tuned in the last convolutional layers and modified in the dense end to learn high-level features for detecting vascular calcifications, discriminating BAC + from BAC- images. To account for class imbalance during model training, we randomly undersampled the majority BAC- class in the training set to reach a 30% BAC + prevalence; the validation and test sets remained intact to reflect the BAC real prevalence. The training, validation, and test sets consisted of 410 (134 BAC +), 222 (28 BAC +), and 229 (32 BAC +) women. Algorithm-level approach was also applied to deal with the imbalanced dataset using a cost-sensitive re-weighting method. Accuracy, F1-score (harmonic mean of precision and recall), and area under the Receiver Operating Characteristic curve (AUC-ROC) were used to assess the diagnostic performance at image-level. Predictions of the calcified area were generated using the Generalized Gradient-weighted Class Activation Mapping (Grad-CAM + +) method, and their correlation with manual measurement of BAC length in a subset of 57 cases was assessed using Spearman's rho.

**Results** The resulting accuracy, F1-score, and AUC-ROC were 0.93, 0.85 and 0.98 for the training, 0.96, 0.78 and 0.95 for the validation, and 0.95, 0.76 and 0.94 for the test subset, respectively. The Grad-CAM + + predictions displayed a strong correlation with BAC measured length (rho = 0.90, $p < 0.001$).

**Conclusion** Our model showed promising performances in BAC detection, confirmed by an AUC of 0.94 in the test subset, and also a strong correlation between the estimation of BAC burden and manual length measurements. A reliable automatic tool for BAC detection could allow large-scale studies on women's CVD risk stratification leveraging the mammographic screening program.

| | Total Population | BAC Positive (Patient-level) | BAC Negative (Patient-level) |
|---|---|---|---|
| Frequency | 1493 | 194 | 1299 |
| Prevalence | 100% | 12.99% | 87.01% |
| Age [IQR] | 59 [16] | 70.5 [13] | 57 [13] |

Study poulation.

| | Accuracy | Precision | Recall | F1-Score | AUC-ROC |
|---|---|---|---|---|---|
| Training set | 0.93 | 0.94 | 0.78 | 0.85 | 0.96 |
| Validation set | 0.96 | 0.84 | 0.72 | 0.78 | 0.95 |
| Test set | 0.95 | 0.78 | 0.73 | 0.76 | 0.94 |

Diagnostic performance of the deep transferred learned model in BAC detection.

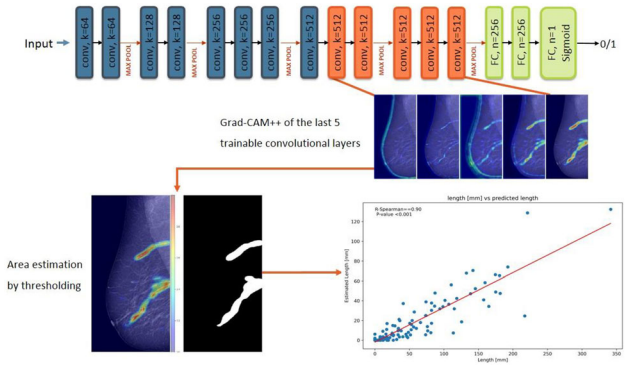


## A-230

### The role of adenosine-stress cardiac magnetic resonance in patients with CAD and preserved ejection fraction

**C. Acanfora, A. Bracci, L. Evangelista, A. Arceri, P. Palumbo, E. Di Cesare**

University Of L'Aquila, Radiology dep, L'Aquila, Italy.

**Purpose/Objectives** Ischemic heart disease is to be the most frequent cause of death, especially in industrialized countries. Historically, CAD has been defined on the base of the presence or absence of one or more atheromatous plaques on the coronary tree; however, currently, the intention is to define the presence or absence of myocardial ischemia, a process in which several factors are involved in addition to the atheromatous plaque itself. Nowdays, advanced cardiac imaging plays a fundamental role, but some aspects need to be clarified especially regarding to their use in the different phases of the natural history of CAD. In fact, the aim of this study is to identify the prognostic role of magnetic resonance imaging with adenosine-stress cardiac magnetic resonance in patients with non-obstructive CAD undergoing a medium-long term follow-up.
**Methods & Materials** We retrospectively selected patients with non-obstructive CAD who underwent to coronary CT and subsequently adenosine-stress cardiac magnetic resonance in deepening of known lesion. No one of these patients had a history of AMI episodes. The CT characteristics of the atheromatous lesion and any perfusion defect observed in MRI of the aforementioned patients were analyzed. The global strain was also analyzed (with specific analysis of the longitudinal, circumferential and radial strains). Risk factors and symptoms of the patients included in the study were considered. Patient follow-up was based on posthumous anamnestic collection based on the search for major cardiac events.
**Results** The final analysis included 35 patients, all of them with negative LE. Of these, 9 patients showed specific symptoms (angor and ischemic equivalents). 12 patients showed outcome, including 2 MACE. In 15 patients, the lesion detected in CT was considered to be at high risk. 12 patients showed a defect in perfusion on functional examination. The analysis of the strain values has shown that only the longitudinal is characterized by a statistically significant variability, both in patients with perfusion defects and in patients without. All strain values showed variability in the presence of CT lesions considered to be high risk. The best CI index was observed for the predictive model including the reduction of longitudinal strain and the presence of perfusion defect (92%).
**Conclusion** The results obtained demonstrate that adenosine-stress cardiac magnetic resonance is also useful in patients with non-obstructive CAD and seems to be a useful tool in the risk stratification of patients with non-obstructive CAD.

## A-232

### Incidental findingr of arteria Lusoria in patients with normal aortic arch and right sided aortic arch

**E. Musina[1], R. Mircea[1], R. Manea[1,2]**

[1]Clinical Emergency Hospital of Brasov, Radiology, Brasov, Romania, [2]University Transilvania Brasov, Faculty of Medecine, Brasov, Romania

**Purpose/Objectives** Introduction: Arteria Lusoria or the aberrant right subclavian artery is the most common anomaly of the aortic arch, occurring in 0.5 to 2.5% cases. Usually, three vessels arise from the aortic arch: the brachiocephalic trunk, the left common carotid artery and the left subclavian artery. When this anomaly is present, the brachiocephalic trunk is absent and four arteries arise from the aortic arch: the right common carotid artery, the left common carotid artery, the left subclavian artery and the aberrant right subclavian artery, which crosses posterior between the esophagus and spine. In 0,1% cases, an aberrant left subclavian artery can be associated with right sided aortic arch. In most of the cases, it is asymptomatic, but when it becomes symptomatic, usually in the association with Kommerell's diverticulum, it causes dysphagia, dyspnea, cough. The diagnosis of this aortic arch anomaly is based on findings at chest radiography in association with multi-slice computer tomography, angiography, nuclear magnetic resonance or swallowing transit.
**Purpose** The aim of this study is to assess the frequency of arteria Lusoria and other arch anomalies associated in patients admitted at our hospital, who were examined with multi-slice computed tomography for different reasons, over two years. Another purpose of the study is to review the anatomy and embryology of the aortic arch.
**Methods & Materials** We retrospectively reviewed a series of 6254 multi-slice computed tomography performed on patients admitted at our department during January 2020 to December 2021.
**Results** From a series of 6254 patients, aberrant right subclavian artery with left sided aortic arch was found incidentally in 16 patients and right sided aortic arch with left aberrant subclavian artery was found in 1 patient. Also 1 patient had a Kommerell's diverticulum associated with arteria Lusoria. There were 10 males and 7 females with mean age of 60 years old. Dysphagia was the most common symptom revealed by patients (in 11 cases).
**Conclusion** Arteria Lusoria is the most common aortic arch anomaly and it can be detected on multi-slice computed tomography, even in the absence of injection of contrast agent. Although it is considered an uncommon anomaly, performing a large number of CT examinations

in the Emergency Department has led to an increase in the diagnosis of this anomaly. The association with Kommerell's diverticulum although increased in literature, in our group of patients was low. The development of multi-slice CT and its availability has led to an easier diagnosis of arteria Lusoria or another associated arch anomallies. The 3D reconstructions had shown the anatomical relations of the mediastinum and the compression of the oesophagus or trachea.

## A-234

### Impact of deep learning image reconstruction algorithm on image quality and diagnostic accuracy of coronary computed tomography angiography

**T. Polidori, D. De Santis, G. Tremamunno, C. Rucci, G. Piccinni, M. Zerunian, L. Pugliese, G. Guido, A. Del Gaudio, L. Barbato, A. Laghi, D. Caruso**

Sant'Andrea University Hospital, Department of Medical Surgical Sciences and Translational Medicine, Rome, Italy.

**Purpose/Objectives** Deep learning image reconstruction (DLIR) algorithms have been recently released for clinical purposes and are currently under active investigation. The aim of this study was to perform a comprehensive intraindividual objective and subjective image quality evaluation of coronary CT angiography (CCTA) reconstructed with DLIR and to assess diagnostic accuracy compared to invasive coronary angiography (ICA).

**Methods & Materials** Fifty-one patients (29 males; mean age, 64 ± 15 years) who had undergone clinically indicated CCTA from April to December 2021 were included in this prospective study. A total of fourteen datasets were reconstructed for each patient: DLIR at three strength levels (DLIR_L, DLIR_M, and DLIR_H, respectively), hybrid iterative reconstructions (ASiR-V) from 10 to 100% in 10%-increments, and filtered back-projection (FBP). Signal-to-noise ratio (SNR) and contrast-to-noise ratio (CNR) were calculated to assess objective image quality. Objective image quality was assessed with a 4-point Likert scale. Diagnostic accuracy of DLIR_M and ASiR-V 50% was compared against ICA in a subgroup of six patients referred to invasive test after CCTA. ANOVA and Friedman test were used for statistical comparison. Post-hoc pairwise comparisons were adjusted for multiple comparisons by the Bonferroni correction.

**Results** DLIR algorithm did not impact vascular attenuation compared with ASiR-V and FBP [($P \geq 0.374$) Fig. 1].

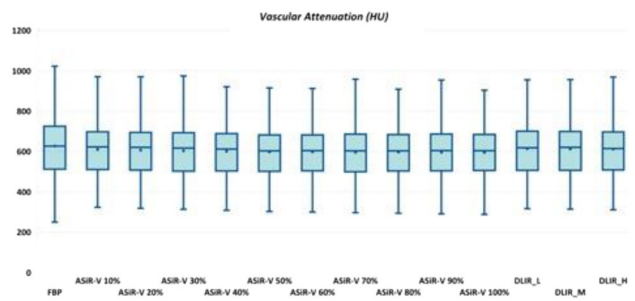


Box-and-whisker plots for vascular attenuation.

DLIR_H showed the lowest noise, comparable with ASiR-V 100% ($P = 1$) and significantly lower than other reconstructions [($P \leq 0.021$) Fig. 2].

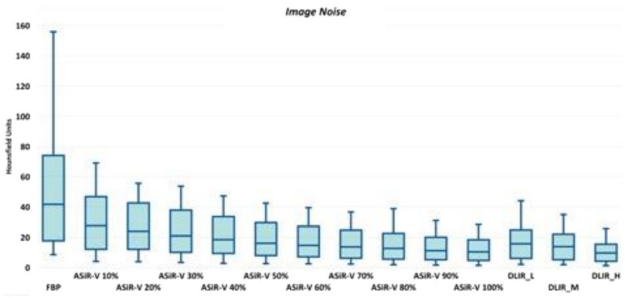


Box-and-whisker plots for image noise.

DLIR_H achieved the highest objective image quality (Fig. 3).

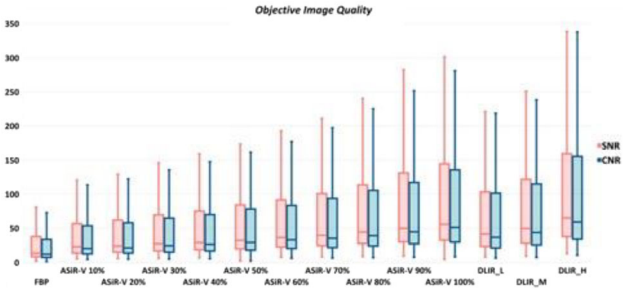


Box-and-whisker plots for objective image quality, with SNR and CNR comparable to ASiR-V 100% ($P = 0.139$ and 0.075, respectively). DLIR_M obtained comparable objective image quality with ASIR-V 80% and 90% ($P \geq 0.281$), while achieved the highest subjective image quality (4, IQR: 4 – 4; $P \leq 0.001$, Table 1).

| | Score | ASiR-V 50% | ASiR-V 100% | DLIR_M | DLIR_H |
|---|---|---|---|---|---|
| ASiR-V 50% | 3 | (3–3) | | 0.004 | 0.001 |
| 0.085 | | | | | |
| ASiR-V 100% | 2 | (2–3) | 0.004 | | 0.001 |
| < 0.001 | | | | | |
| DLIR_M | 4 | (4–4) | 0.001 | 0.001 | |
| < 0.001 | | | | | |
| DLIR_H | 3 | (3–4) | 0.085 | < 0.001 | < 0.001 |

Subjective image quality scores of ASiR-V and DLIR reconstructions, with related pairwise comparisons.

Sensitivity, specificity, and accuracy for DLIR and ASiR-V datasets were 100%, 94.9%, and 95.3%, respectively, with no significant differences ($P > 0.05$).

**Conclusion** DLIR_M significantly improves CCTA image quality and provides equal diagnostic accuracy compared to routinely applied ASIR-V 50% dataset.

## A-235

### Prognostic implications of CMR in Systemic Sclerosis patients: a pilot study about early diagnosis of cardiac complications

**L. Pugliese, G. Piccinni, T. Polidori, G. Tremamunno, M. Nicolai, D. De Santis, D. Caruso, A. Laghi**

AOU SANTA ANDREA, Department of Medical Surgical Sciences and Translational Medicine, ROMA, Italy.

**Purpose/Objectives** Cardiac involvement in systemic sclerosis (SS) consists of a range of manifestations resulting from microangiopathic, electrical and hemodynamic alterations, including myocarditis, pericarditis, myocardial and pericardial inflammation, arrhythmias, hypertensive pictures, and heart failure from the earliest stages of the disease. The aim of this study was to demonstrate that Cardiac Magnetic Resonance (CMR) has greater sensitivity in early characterization of myocardial damage than routine examinations that detect cardiac involvement only in more advanced cases.
**Methods & Materials** From October 2021 to May 2022, sixty SS patients all in the early stages of the disease, underwent 1.5 T CMR (Signa Voyager Magnetic Resonance, GE Healthcare) before and after contrast administration (Gd-DOTA, Dotarem). Exclusion criteria were severe motion artifacts and severe claustrophobia. Motility and FE% were evaluated by Cine SSFP sequences. Modified Look-Locker Inversion Recovery sequence (MOLLI) were performed before and after contrast administration; subsequently, using CIRCLE software, specific reconstructions were performed to derive T1 maps (pre- and post-contrast administration) and to calculate ECV (pathological $> 30\%$). Both allow quantification of left ventricular myocardial fibrosis. PSMDE sequences were performed 8–10 min after contrast injection to evaluate presence of late gadolinium enhancement (LGE), sign of irreversible myocardial damage.
**Results** A total of 66 participants with SS were enrolled; 5 patients were excluded for motion artifacts, one for claustrophobia. Final population comprised 60 patients (27F; average age 47 y.o.). No patients showed sign of LGE, while increased values of T1 mapping were found in 15/60 patients (25%) and ECV values in the same number of patients turn out to be slightly increased (with an average of about 33%). Although no patients showed LGE neither structural myocardial changes, 25% of them have increased T1 mapping values, which is why this value could be considered a good early predictor of myocardial damage.
**Conclusion** In our study, 25% of patients have increased T1 mapping values, as a consequence of edema and myocardial fibrosis, while being asymptomatic, but as pointed out by numerous studies, the presence of cardiac symptoms does not necessarily correlate with actual ultra-structural myocardial involvement and subsequent clinical severity. So the study of myocardial interstitial structural subversion by T1 mapping allows to intercept fibrosis early and change the patient's prognosis. CMR is the noninvasive diagnostic test of choice to follow the evolution of the pathology and intervene early therapeutically thanks to its higher sensitivity in diagnosing myocardial alterations from early stages.

## A-237

### Coronary computed tomography angiography as tool of secondary prevention: a monocenter prospective study

**C. Rucci, D. De Santis, T. Polidori, G. Tremamunno, G. Piccinni, D. Caruso, M. Zerunian, L. Pugliese, A. Laghi**

Sant'Andrea University Hospital, Department of Medical Surgical Sciences and Translational Medicine, Rome, Italy.

**Purpose/Objectives** The purpose of the study was to investigate the performances of coronary computed tomography angiography (CCTA) as a secondary prevention tool in the diagnosis of coronary artery disease (CAD).
**Methods & Materials** From January 2021 until September, 2021, consecutive asymptomatic patients stratified for cardiovascular risk according to the combined-SCORE were prospectively enrolled. All patients were pre-treated with sublingual nitrates (Trinitrine, 0.8 mg) to induce vasodilatation; intravenous beta blocker (Metoprolol, 5 mg) was administered to patients with heart rate $> 75$ bpm. All patients underwent a 128-slice CT (GE Revolution EVO CT Scanner, GE Medical Systems, Milwaukee, WI, USA), after the injection of 50 mL of Iomeprol 400 (Iomeron 400; Bracco Imaging, Italy) at fixed flow rate of 5 mL/sec. Exclusion criteria were symptoms of CAD, stenting or CABG, previous allergic reactions to iodinated contrast media, renal failure (eGFR $< 30$ mL/min), severe motion or misalignment artefact, or inadequate contrast enhancement. Two blinded radiologists with five and fifteen years of experience in cardiovascular imaging interpreted the CT scans. Coronary stenoses were assessed on a per-patient and per-segment basis, by means of a 3-point scale: absent, non-obstructive ($< 50\%$ lumen narrowing), and obstructive ($\geq 50\%$ lumen narrowing). Additionally, plaques were classified into non-calcified, calcified, and mixed. In case of detection of obstructive coronary stenoses, patients were addressed to invasive coronary angiography.
**Results** From an initial population of 161 individuals, 30 patients were excluded due to prence of symptoms (n = 20) and previous coronary stenting (n = 10). Thus, the final study population consisted of 131 patients (females: 48; mean age: $64 \pm 11$ years). On a per patient analysis, 60/131 patients (45%) showed healthy coronaries, 54/131 (41%) patients had non-obstructive CAD, while 17/131 (14%) had obstructive CAD, 11 non-calcified plaques, 4 calcified plaques and 1 mixed plaque. On a per segment analysis, a total of 2096 segments were analyzed, 265/2096 (12.6%) presented non-obstructive CAD, while 20/2096 (1%) segments presented obstructive CAD.
**Conclusion** Our results showed a prevalence of obstructive CAD of 14% in asymptomatic patients, involving 1% of coronary segments and mainly caused by non-calcified plaques. CAD was ruled-out in 45% of patient and 86.4% coronary segments.

## A-239

### CMR feature tracking and its correlation with traditional heart and liver parameters in patients with B Thalassemia Major: preliminary results

**T. Floros[1], A. Kallifatidis[2], E. Alexiou[1], K. Michailidis[3], M. Vlychou[4]**

[1]General Hospital Larisa, Radiology, Larisa, Greece, [2]St Lukes Hospital, Radiology, Thessaloniki, Greece, [3]Cardiac Intelligence, Ptolemaida, Greece, [4]University of Thessaly, Radiology, Larisa, Greece.

**Purpose/Objectives** Cardiomyopathy due to iron overload is a severe complication, in patients with thalassemia major. Although T2* is the gold standard in the diagnosis of severe iron overload, there is a subgroup of patients who will experience major cardiac events even though the T2* values are within normal limits. Therefore, additional biomarkers are needed to assist in the early detection, of those patients. Global longitudinal strain (GLS) derived from CMR feature

tracking, has been described in literature as a separate predicting factor, for severe cardiac events. The aim of our study is to assess for correlation between CMR GLS and other derived imaging parameters of left and right ventricle (EDV, ESV, SV, EF, LV Mass, LV T2*), as well as with Liver T2 * values.

**Methods & Materials.**

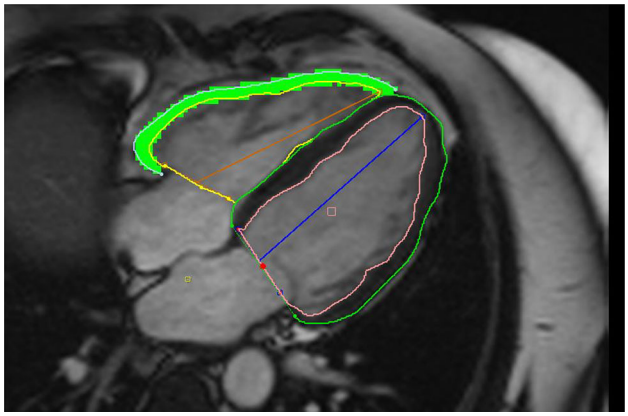

CMR feature tracking.

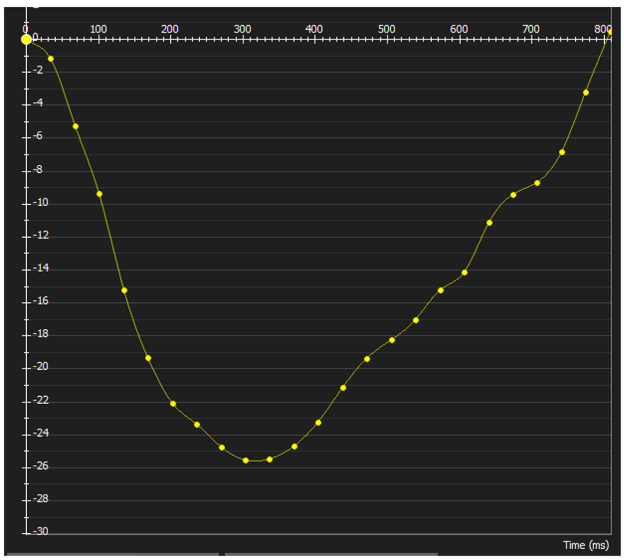


RV strain curve.

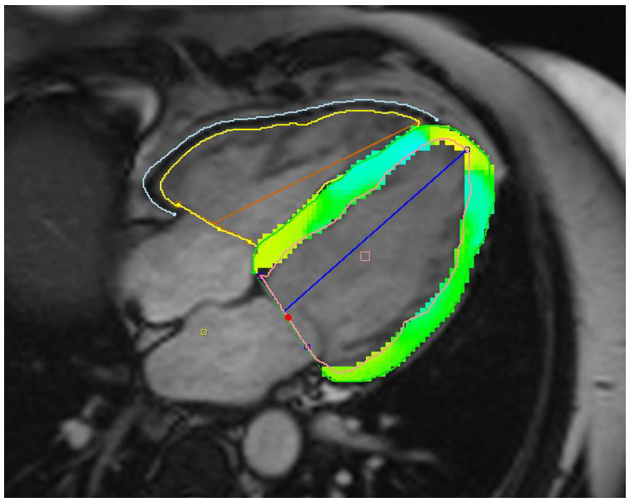

lv strain.

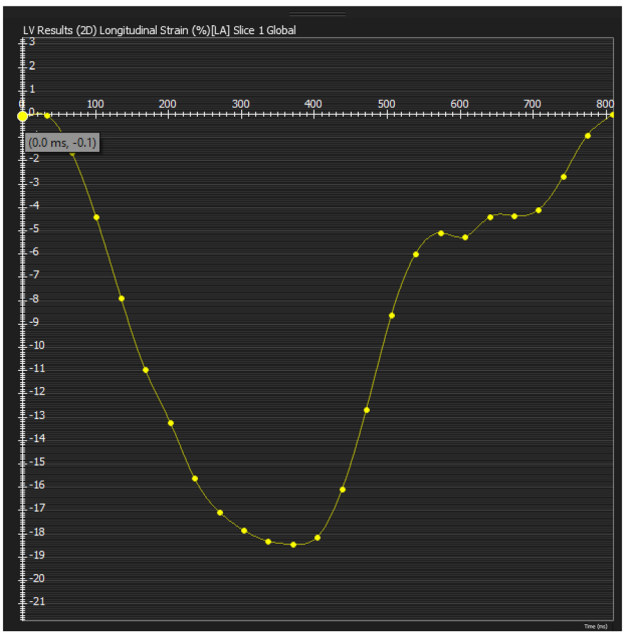


lvstrain curve.

Out of all consecutive patients with B thalassemia major that underwent Cardiac and Liver MRI (Siemens Avanto 1.5 T) in the General Hospital of Larisa between 2020–2022, we randomly extracted 50 patients, for preliminary analysis. In our cohort, Cardiac T2* values were within normal limits. Using dedicated software (Cvi 42, Circle Cardiovascular Imaging Inc.), biventricular volumes,

systolic function, global longitudinal strain (GLS) and T2* values of the left ventricle and T2* liver values, were calculated. Correlation between biventricular GLS with the respected biventricular EDV, ESV, SV, EF, LV mass, LV T2* and R2*values, as well as Liver T2* and R2* values, was assessed.

**Results** Fifty patients (mean age 46 years old, 22 females) underwent cardiac and liver MRI. Right ventricular GLS has significant statistical correlation with right ventricular EDV (r = -392, p = 0.005). However, there was no statistically significant association between LV GLS and LV EDV, LV mass and LV EF. Septal T2*and R2* showed significant statistical correlation with biventricular EDV (r = 0.442, p = 0,001 left, r = 0.483, p < 0,0 right) biventricular ESV (r = 0.355, p = 0,008 left, r = 0.394, p = 0,003 right) and with LV mass (r = 0.328, p = 0.015). Additionally, liver T2 * and R2* had significant correlation with the RV GLS (r = 0.280, p = 0.05).

**Conclusion** RV GLS is a potential biomarker of RV adaptation in patients with B thalassemia major. Liver T2*/R2* may serve as an additional biomarker, in the early diagnosis of cardiomyopathy in this category of patients, although further larger studies are required to support our results.

## A-240

### Effects of using oral nitroderivatives (NTG) in coronary computer tomography angiography (CCTA). Comparison between pre-medicated and naive patients: a prospective monocentric study

**G. Piccinni, T. Polidori, G. Tremamunno, C. Rucci, D. De Santis, D. Caruso, A. Laghi**

AOU SANTA ANDREA, Department of Medical Surgical Sciences and Translational Medicine, ROMA, Italy.

**Purpose/Objectives** The purpose of this prospective study was to evaluate the benefit of using nitroderivatives (NTG) in coronary computer tomography angiography (CCTA) in terms ofcoronary diameter, vessel attenuation, and number of evaluable coronary segments.

**Methods & Materials** Two hundred and four patients were prospectively enrolled from February to November 2021 and were randomly divided into two groups: Group A (114 patients) received NTG and Group B (90 patients) did not receive NTG. All patients underwent CCTA on a 128-slice CT (GE Revolution EVO CT Scanner, GE Medical Systems), after the injection of 60 mL of Iomeprol 400 (Iomeron 400; Bracco Imaging) at fixed flow rate of 5 mL/sec. Scanning parameters were the same in the two groups. Exclusion criteria were: elevated heart rate (HR > 90 bpm), severe motion artifacts, or contraindication to contrast administration. Two blinded radiologists, blinded to patients' assigned group, analyzed the images. The maximum diameter of the three main coronary arteries was measured and number of evaluable coronary segments were annotated. Regions of interest (ROIs) were also drawn in all coronary segments and vessel attenuation and image noise were recorded; thus, contrast-to-noise (CNR) and signal-to-noise ratio (SNR) were calculated, to assess objective image quality. Results were analyzed using nonparametric statistical tests for independent samples.

**Results** Group A showed significantly larger main coronary arteries diameters (3.38 mm vs 3.02 mm, $P < 0.001$) and a higher number of evaluable coronary segments (14.3 vs 12.4, $P < 0.01$) compared to Group B. No significant differences were reported between the two groups in terms of vessel attenuation, SNR, and CNR (all $P > 0.05$); Image 1.

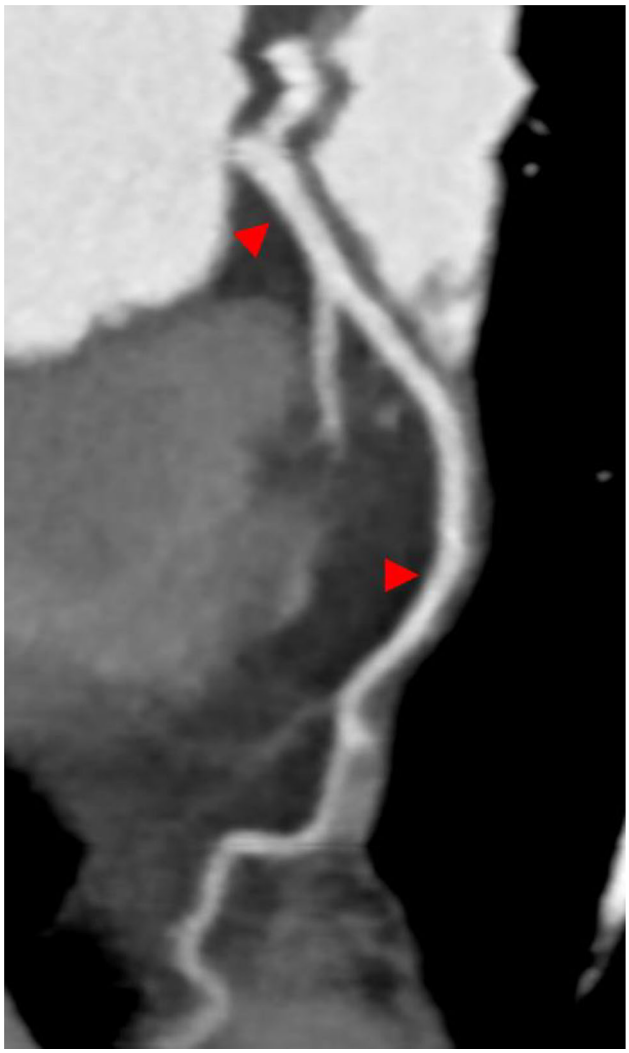

and image 2.

FIGURE B.

**Conclusion** NTG increase coronary artery diameter and improve the number of evaluable segments in patients undergoing CCTA, without affecting image quality.

## A-241

### Myocardial extracellular volume assessment at CT in Novel Coronavirus Disease (COVID-19) patients with regards to the presence of pulmonary embolism

**C. Monti[1], M. Zanardo[1], D. Capra[1], S. Schiaffino[2], F. Sardanelli[1,2], F. Secchi[1,2]**

[1]Università degli Studi di Milano, Biomedical Sciences for Health, Milan, Italy, [2]IRCCS Policlinico San Donato, Unit of Radiology, San Donato Milanese, Italy.

**Purpose/Objectives** To assess myocardial extracellular volume (ECV) in patients with novel coronavirus disease (COVID-19) with regards to the presence of pulmonary embolism (PE).

**Methods & Materials** After Ethical Comittee approval, we retrospectively reviewed consecutive patients who underwent contrast-enhanced computed tomography (CT) for the assessment of PE, and whose CT scans included at least one unenhanced and one venous phase acquisition performed at 1 min after contrast administration for evaluating the mediastinum. Included patients were also to have hematocrit values obtained at most one day from the CT scan. Regions of interest were placed in the myocardium and ventricular blood pool of both the unenhanced and venous phase scan, and ECV was subsequently calculated.

**Results** Our final population counted 94 patients, 63 (67%) of whom males, with a median age of 70 years (interquartile range (IQR), 56–76 years), 28 (30%) of whom with PE visible at CT. Median hematocrit was 39% (IQR 35–43%). Median overall ECV was 31% (IQR 26–35%), whereas median ECV in patients with PE was 34% (IQR 29–38%), significantly higher than in those without PE (30%, IQR 25–34%, p = 0.010).

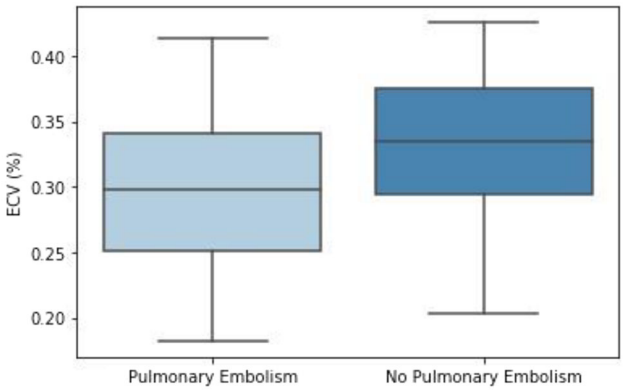


**Conclusion** Myocardial ECV is high in COVID-19 patients, possibly indicating a likelihood of underlying myocardial damage. The higher ECV in patients with PE may relate to the ventricular overload rising from subsequent pulmonary hypertension. CT-derived myocardial ECV could be used as a biomarker of cardiovascular involvement in COVID-19 patients, obtaining further data from an investigation that is already part of clinical workflows.

## A-242

### Validation of the accuracy of T1 mapping measurements of single vendor 1.5 T MRI integrated software

**L. Pugliese, T. Polidori, G. Piccinni, C. Rucci, G. Tremamunno, M. Nicolai, D. De Santis, D. Caruso, A. Laghi**

Sant'Andrea University Hospital, Department of Medical Surgical Sciences and Translational Medicine, Rome, Italy.

**Purpose/Objectives** The purpose of the current study was to develop and validate the accuracy of T1 mapping measurements of single vendor independent T1 mapping modules, comparing with commercially available clinical software cvi42 (Circle Cardiovascular Imaging, Calgary, Canada).

**Methods & Materials** From October 2021 to May 2022, all consecutive patients underwent 1.5 T Cardiac Magnetic Resonance (CMR, Signa Voyager Magnetic Resonance, GE Healthcare) using a 30-channel coil (body array and spine array), before and after contrast

administration (Gd-DOTA, Dotarem), were prospectively enrolled. Exclusion criteria were severe motion artifacts, severe claustrophobia and contraindication to contrast administration. Pre- and post-contrast Modified Look-Locker Inversion Recovery sequence (MOLLI, 5(3)3 variant) were performed to acquire three short-axis images (basal, midventricular and apical). Subsequently, T1 maps were derived with both the MRI integrated software (SIGNA$^{TM}$ Works, GE Healthcare) and with the software cvi42, commercially available for research and FDA approved for clinical applications. Two radiologists in consensus, with 4 and 8 years of experience in cardio-vascular imaging, respectively, performed the objective analysis: T1 measurements were performed by drawing endocardial and epicardial contour and by drawing four same size regions of interest (ROIs) on each one of the three short-axis images. Overall and ROIs-derived myocardial T1 relaxation times were collected and compared between the two mentioned software.

**Results** A total of 110 consecutive participants were enrolled; 6 patients were excluded for motion artifacts, 3 for contraindication to contrast administration, 1 for claustrophobia. Our final population comprised 100 patients (58 male; 63 ± 13y). The T1 measurements obtained with MRI T1 map reconstruction integrated software (SIGNA$^{TM}$ Works) were in close agreement with those obtained with cvi42 software ($p < 0.001$), confirming the accuracy of T1 measurements performed using SIGNA$^{TM}$ Works integrated T1 mapping modules.

**Conclusion** MRI T1 map reconstruction integrated software (SIGNA$^{TM}$ Works) was comparable to cvi42 T1 mapping application, thus enables accurate mapping of T1 relaxation times.

## A-243

### Viability and ischemia assessment in chronic coronary total occlusions according to collaterals distribution: a stress CMR study

**G. Pinto[1], M. Chiarito[1], G. Liccardo[1], S. Baggio[1], E. Bacci[1], G. Del Monaco[1], F. Fazzari[1], P. Rondi[2], F. Catapano[3], G. Gasparini[1], G. Stefanini[1], G. Condorelli[1], M. Francone[3], L. Monti.[3]**

[1]IRCCS Humanitas Research Hospital, Department of Biomedical Sciences, Humanitas University, Department Cardiology, Rozzano—Milan, Italy, [2]University of Brescia—Spedali Civili, Department of Radiology, Brescia, Italy, [3]IRCCS Humanitas Research Hospital, Department of Biomedical Sciences, Humanitas University, Department of Radiology, Rozzano—Milan, Italy.

**Purpose/Objectives** Well-developed collaterals are considered a marker of myocardial viability in CTO territory, but it remains questionable whether their presence should be considered protective from inducible ischemia. Viability and ischemia assessment may improve the selection of patients with chronic total occlusions (CTO) who could benefit from percutaneous coronary intervention (PCI).

**Methods & Materials** From a cohort of 749 patients referred to our centre between June 2010 and September 2020 with a diagnosis of CTO, we retrospectively analysed 131 patients who underwent Cardiac Magnetic Resonance (CMR): 111 of these also underwent an adenosine-stress CMR. Patients were divided in three groups according to collaterals distribution: totally developed (TD) collaterals (Rentrop grade = 3 AND collateral connection [CC] score = 2), well-developed (WD) collaterals (Rentrop = 3 OR CC score = 2) and poorly developed (PD) collaterals (neither Rentrop 3 or CC score 2 collaterals). The coronary collateralization status was used to analyse the amount of viable myocardium and inducible ischemia subtended by the CTO.

**Results** Patients with TD collaterals (n: 21) had a greater amount of inducible ischemia on CTO territory compared with patients with WD (n: 29) and PD (n: 81) collaterals (9.6% vs 6.4% vs 3.2% of the entire myocardial mass for inducible ischemia, $p = 0.031$) and of myocardial viability (100% vs 90% vs 80%). Only 30% of the global population showed an amount of ischemic myocardium > 10% of the LV mass.

**Conclusion** Patients with well-collateralized CTO show a greater amount of inducible ischemia in the CTO territory.

## A-244

### Evaluation of blood hematocrit levels using serial blood pool T1 mapping

**A. Tumenas[1], P. Bucius[2], G. Jureviciute[1], A. Banisauskaite[1], L. Pardervinskiene[1], J. Jureviciute[2], L. Kucinskas[1], A. Vaitiekiene[2], G. Stonciute[1], T. Lapinskas[2], A. Jankauskas.[1]**

[1]Hospital of Lithuanian University of Health Sciences Kauno Klinikos, Radiology, Kaunas, Lithuania, [2]Hospital of Lithuanian University of Health Sciences Kauno Klinikos, Cardiology, Kaunas, Lithuania.

**Purpose/Objectives** MRI derived extracellular volume fraction (ECV) is an important predictor of outcomes in various cardiovascular pathologies. Synthetic ECV has recently emerged as a convenient and relatively accurate alternative to classical ECV. Both the synthetic and classical ECV are dependent on correct estimation of T1 values of the blood pool. It is known that blood hematocrit (Htc) is posture dependent, therefore it might be important to standardize the timing of blood sample acquisitions for ECV estimations. We hypothesized that a change in the timing of T1 mapping acquisition during a routine scan could influence the mesaured T1 relaxation time of the blood pool.

**Methods & Materials** We acquired modified look-locker inversion recovery T1 mapping sequences using 3 T scanner at basal, middle and apical ventricular levels in 64 consecutive patients at two time points: at the beginning of the scan after scout sequences acquisition (early) and immediately before contrast injection (late). Blood pool and myocardium T1 map values were acquired by placing a region of interest of 1.0 – 2.5 $cm^2$ at the basal, middle and apical ventricular levels using Syngo.via software solution standard to our scanner. The measurements were then compared by using Paired samples t test and Wilcoxon signed rank test for normally and abnormally distributed data between early and late acquisitions. A referential synthetic Htc formula was used to determine the difference of synthetic Htc values at two timepoints.

**Results** The average time from the beginning of the scan to the early and late acquisitions was 9,6 ± 2,5 min and 29 ± 8,8 min, respectively. The T1 map values of the myocardium did not change significantly: at basal level – 1254 ± 80 ms (early) vs 1249 ± 80 ms (late); middle – 1240 ± 79 ms vs 1245 ± 120 ms; apical 1244 ± 89 ms vs 1255 ± 91 ms, overall 1246 ± 76 ms vs 1249 ± 82 ms, $p > 0,05$. T1 map values of blood pool significantly increased: 1852 ± 88 ms vs 1876 ± 89 ms; 1860 ± 91 ms vs 1883 ± 91 ms; 1886 ± 101 ms vs 1889 ± 132 ms; 1865 ± 90 ms vs 1882 ± 93 ms respectively, $p < 0,001$, yielding a total increasement from 0,2 to 1,3%. The biggest increase was observed at the basal level. Blood pool T1 map values of basal level were then plotted into a synthetic Htc formula providing 34,5% (early) vs 34,0% (late) synthetic Htc values, yelding 0,5% absolute difference, $p < 0,001$.

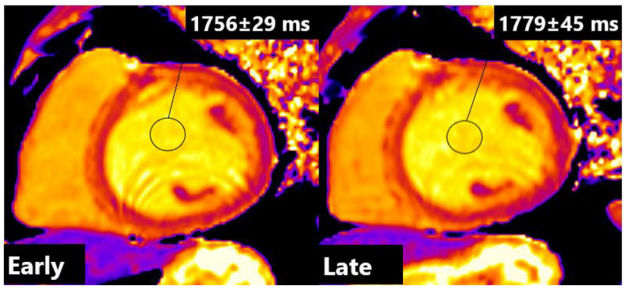


T1 map images at basal-ventricular level depicting the placement of Region of Interest (ROI) for blood pool T1 value measurements.

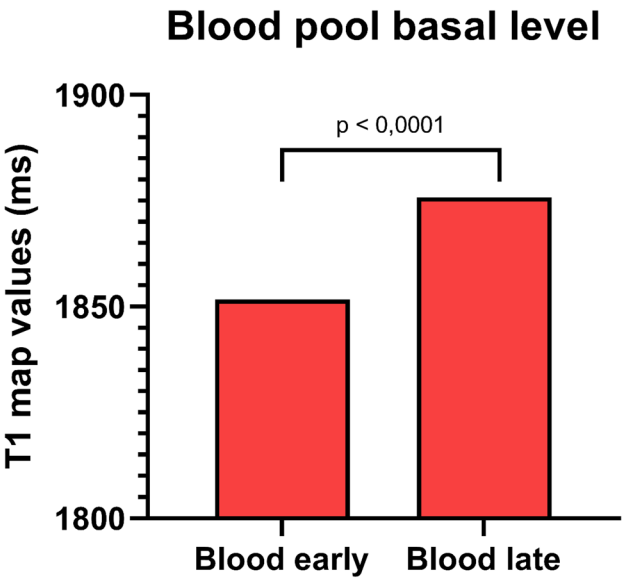


Bar graph depicting average changes of T1 map values of blood pool in early and late T1 map measurements at basal-ventricular level.

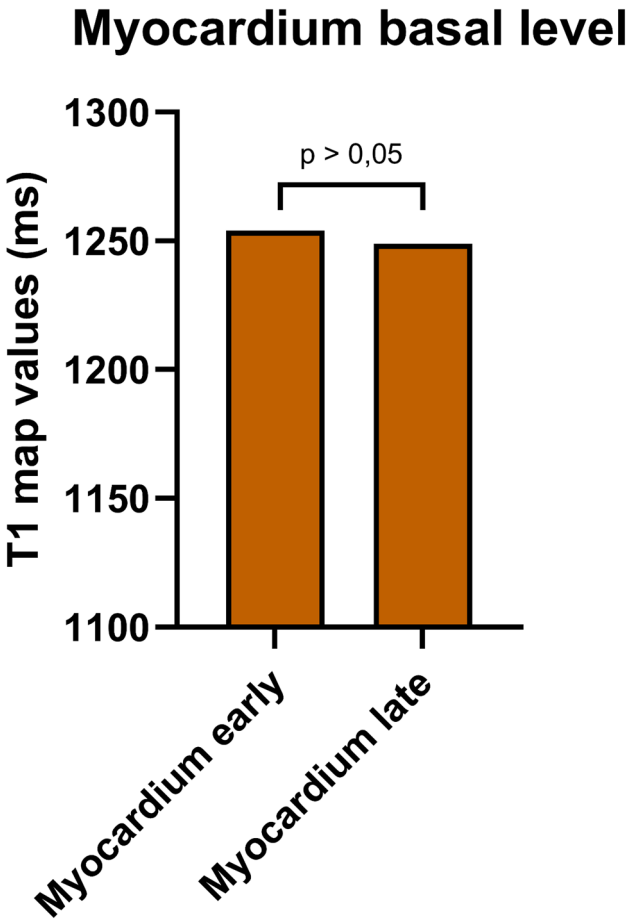


Bar graph depicting average changes of T1 map values of myocardium at early and late T1 map measurements at basal-ventricular level.

**Conclusion** We have demonstrated that there are small but statistically significant differences in native T1 map values of blood pool between early and late acquisitions of T1 mapping sequences. This difference could impact the accuracy of ECV calculations because T1 map value of blood pool is included in the MRI derived ECV formula itself and in synthetic Htc derivation.

## A-247

### Aliased flow signal planimetry by cardiovascular magnetic resonance imaging for grading aortic stenosis severity: a prospective pilot study

**V. Di Mascio[1], C. Mantini[1,2], M. Olivieri[1], L. Frattoloso[1], F. Ricci.[1]**

[1]"G. d'Annunzio" University of Chieti-Pescara, Department of Neuroscience, Imaging and Clinical Sciences, Chieti, Italy, [2]"G. d'Annunzio" University of Chieti-Pescara, Chieti, Italy., Chieti, Italy.

**Purpose/Objectives** Transthoracic echocardiography (TTE) is the standard technique for assessing aortic stenosis (AS), with effective orifice area (EOA) recommended for grading severity. EOA is operator-dependent, influenced by a number of pitfalls and requires

multiple measurements introducing independent and random sources of error. We tested the diagnostic accuracy and precision of aliased orifice area planimetry ($AOA_{cmr}$), a new, simple, non-invasive technique for grading of AS severity by low-VENC phase-contrast cardiovascular magnetic resonance (CMR) imaging.

**Methods & Materials** Twenty-two consecutive patients with mild, moderate, or severe AS and six age- and sex-matched healthy controls had TTE and CMR examinations on the same day. We performed analysis of agreement and correlation among (i) $AOA_{cmr}$; (ii) geometric orifice area ($GOA_{cmr}$) by direct CMR planimetry; (iii) $EOA_{echo}$ by TTE-continuity equation; and (iv) the "gold standard" multimodality EOA ($EOA_{hybrid}$) obtained by substituting CMR LVOT area into Doppler continuity equation.

**Results** There was excellent pairwise positive linear correlation among $AOA_{cmr}$, $EOA_{hybrid}$, $GOA_{cmr}$, and $EOA_{echo}$ ($p < 0.001$); $AOA_{cmr}$ had the highest correlation with $EOA_{hybrid}$ ($R^2 = 0.985$, $p < 0.001$). There was good agreement between methods, with the lowest bias (0.019) for the comparison between $AOA_{cmr}$ and $EOA_{hybrid}$. $AOA_{cmr}$ yielded excellent intra- and inter-rater reliability (intraclass correlation coefficient: 0.997 and 0.998, respectively).

**Conclusion** Aliased orifice area planimetry by 2D phase contrast imaging is a simple, reproducible, accurate "one-stop shop" CMR method for grading AS, potentially useful when echocardiographic severity assessment is inconclusive or discordant. Larger studies are warranted to confirm and validate these promising preliminary results.

## A-248

### Agreement and diagnostic efficacy of computed tomography (CT) half-dose aortic valve (AVCS) and coronary artery calcium scoring (CACS) acquisition protocol

C. Mantini[1,2], V. Di Mascio[2], M. Olivieri[2], L. Frattoloso.[2]

[1]"G. d'Annunzio" University of Chieti-Pescara, Chieti, Italy., Chieti, Italy, [2]"G. d'Annunzio" University of Chieti-Pescara, Department of Neuroscience, Imaging and Clinical Sciences, Chieti, Italy.

**Purpose/Objectives** To evaluate the agreement and the diagnostic efficacy of the CT half-dose protocol with the iterative reconstructions (SAFIRE) and without the iterative reconstructions (SAFIRE) for Aortic Valve Calcium Scoring (AVCS) and Coronary Artery Calcium Scoring (CACS) evaluation.

**Methods & Materials** We enrolled 101 patients (mean age 82.2 ± 4.9 y) eligible for Transcatheter Aortic Valve Implantation (TAVI) underwent prospective ECG-triggering unenhanced CT scan for coronary and aortic valve calcium score evaluation using standard protocol (120 kV, 20 mAS) and low dose protocol (120 kV, 10 mAS). The dataset obtained with the low dose protocol was reconstructed using both the standard filter (B35f) and the iterative reconstruction algorithm (SAFIRE; strength:3).

**Results** Half-dose protocol (10 mAs) with standard kernel filter (B35f) showed an excellent accuracy and precision both for the evaluation of CACS (CCC:0.99;95% CI:0.98–0.99; bias:-4.9) and AVCS (CCC:0.96; 95%CI:0.92–0.98; bias:54.3) compared with the standard protocol in both non-obese (BMI < 30 kg/m$^2$) and obese (BMI ≥ 30 kg/m$^2$) patients. The 10 mAs protocol showed significant reduction (47.5%) of the radiation exposures compared to the standard acquisition (8.5 ± 1.1 DLP Vs 17.9 ± 2.7 DLP). The application of SAFIRE has shown excellent accuracy and precision compared to the standard protocol in the evaluation of both calcium scores (CCC:0.98;95%CI:0.97–0.99;bias:-102).

**Conclusion** Compared to the standard protocol, the half tube current acquisition protocol (10 mAs Vs 20 mAs) allowed a significant dose reduction without significant changes in the coronary and aortic valve calcium score evaluation.

## A-249

### The added diagnostic role of first-pass rest-perfusion imaging in cardiac magnetic resonance (CMR) for the assessment of microvascular obstruction in patients with multi-vessel coronary artery disease (MVD) and left ventricular (LV) dysfunction

F. P. Sbordone, M. Cesareni, C. Cerimele, V. De Stasio, L. Pugliese, R. Floris, F. Garaci, M. Chiocchi

Policlinico Tor Vergata, ROME, Italy

**Purpose/Objectives** CMR plays a key role in patients with MVD, associated with evidence of total chronic occlusion (CTO), and LV dysfunction: specially the assessment of myocardial viability allows to establishing the best coronary revascularization strategy. Microvascular obstruction (MVO), also called "no-reflow phenomenon", a classic complication related primarly to reperfusion injury, represents an independent predictor of major adverse cardiovascular events and LV remodeling. Our purpose was to set up a standard protocol in this category of patients characterized by MVD who needed a study of myocardial viability to establish the subsequent therapeutic procedure: in particular by carrying out a "routine use" of the first-pass rest-perfusion sequences during the first minute of gadolinium-contrast agent (Gd) infusion to search MVO, to be confirmed in post-contrast delayed sequences (LGE), thus increasing diagnostic accuracy and allowing a better qualitative and semi-quantitative analysis by "combining" several post-contrast sequences.

**Methods & Materials** 12 patients in which coronary angiography study showing MVD, with associated LV dysfunction (ejection fraction < 40%), have been subjected to CMR with the perfusion study for the assessment of myocardial viability only at rest, i.e. during the first step of infusion of Gd, to evaluate the perfusion myocardial status.

**Results**

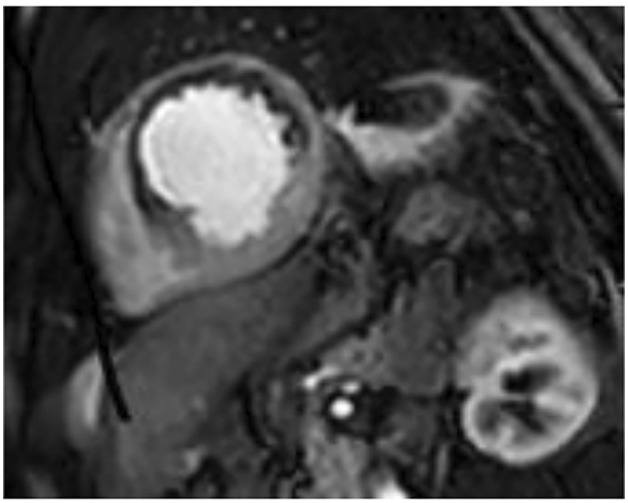

2 patients showed no signs of MVO;

2 patients treated with pPCI presented MVO at the level of the reperfused myocardial wall;

8 patients not treated, 6 with CTO in the anterior descending artery, showed an area of hypointensity, highlighted earlier in first-pass rest-perfusion images and then confirmed in the contest of transmural LGE, to be referred to MVO. So, they were all directed to the ICD implantation in primary prevention, and no indication was made for surgical coronary revascularization.

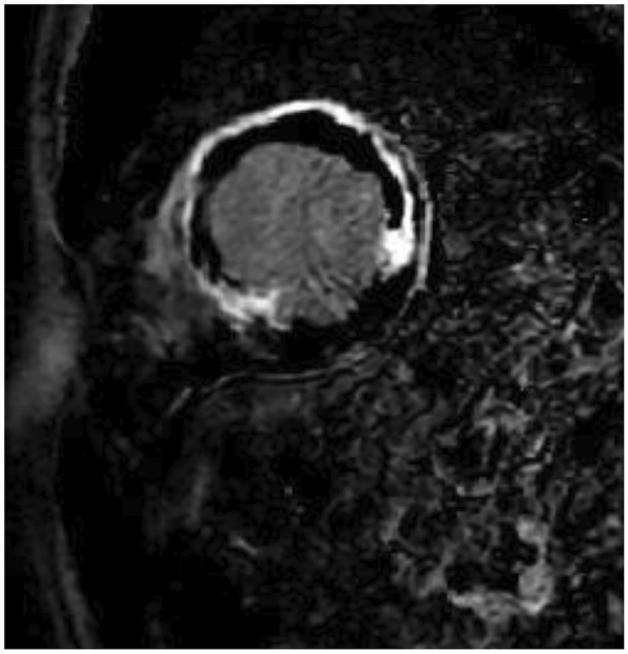

**Conclusion** In our series, a non-negligible percentage of patients presented MVO, which together with a transmural extension of the LGE area, has allowed to not subject these patients to surgical revascularization, but only to ICD implantation. In patients with CTO, the presence of MVO it could be due to the presence of a circulation collateral of hemodynamic compensation, which could have induced a possible chronic reperfusion injury in the infarcted area in a microcirculation already damaged. Therefore, in patients with MVD and LV dysfunction, in which a complete myocardial perfusion study (stress & rest) is contraindicated, the use of the only first-pass rest-perfusion sequences during the first minute of Gd infusion, which classically represents a "dead time", combined with the evaluation of the LGE, can increase the diagnostic accuracy of the qualitative and semi-quantitative analysis of MVO.

## A-251

### Evaluation of segmental T2 ratio in patients with acute myocarditis and its association with late gadolinium enhancement

**F. D'Errico, L. Pugliese, L. Benelli, F. P. Sbordone, M. Cesareni, M. Pasqualetto, F. Garaci, R. Floris, M. Chiocchi**

Fondazione Policlinico Tor Vergata, Rome, Italy.

**Purpose/Objectives** The aim of the study was to demonstrate the good diagnostic accuracy of segmental T2 ratio in predicting the presence of late gadolinium enhancement (LGE) in patients with suspected acute myocarditis undergoing cardiac magnetic resonance imaging (CMR) in order to reduce acquisition time while maintaining high diagnostic quality of the examination.

**Methods & Materials** 22 patients with clinical suspicion of acute myocarditis, who underwent CMR between 1 and 30 days after the acute onset of symptoms, were retrospectively evaluated by analyzing images in the STIR and PSIR sequences for LGE assessment. Two examiners measured the signal intensity in the STIR images in each of the 17 myocardial segments according to the ACC/AHA segmentation scheme. Similarly, the intensity of the visible skeletal muscle (serratus anterior, subscapularis, major and minor pectoralis) was assessed for each myocardial portion (basal, middle and apical). We obtained the segmental T2 ratio, i.e., myocardial signal intensity/skeletal muscle signal intensity. ROC curves were used to compare the diagnostic validity of T2 signal intensity and T2 ratio in predicting the presence of LGE in each myocardial segment.

**Results** The final analysis was performed in 326 segments. Signal intensity in STIR images showed an area under the curve (AUC) of 0.54 (95% CI: 0.44–0.63) for the first examiner and 0.53 (95% CI: 0.44–0.63) for the second examiner. The segmental T2 ratio showed an AUC of 0.8 (95% CI: 0.73–0.87) for the first examiner and 0.77 (95% CI: 0.71–0.84) for the second examiner.

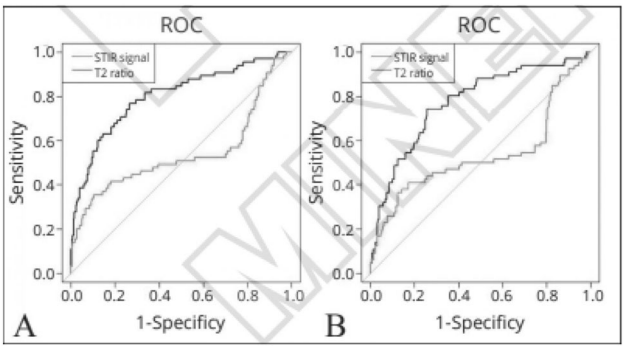


ROC curves analysis. Signal intensity in STIR images showed for both readers 1 (A) and 2 (B) an AUC of 0.54 (95% CI: 0.44–0.63) and 0.53 (95% CI: 0.44–0.63), and T2 ratio showed an AUC of 0.8 (95% CI: 0.73–0.87) and 0.77 (95% CI: 0.71–0.84) in discriminating myocardial segments with LGE. AUCs showed a statistically significant difference ($p < 0.001$).

Bland–Altman analysis showed good agreement for both T2 signal intensity (mean difference = -18.5 reader1 vs. reader 2 and 2SD = 247.3) and T2 ratio (mean difference = 0.03 vs. reader2 and 2SD = 0.9).

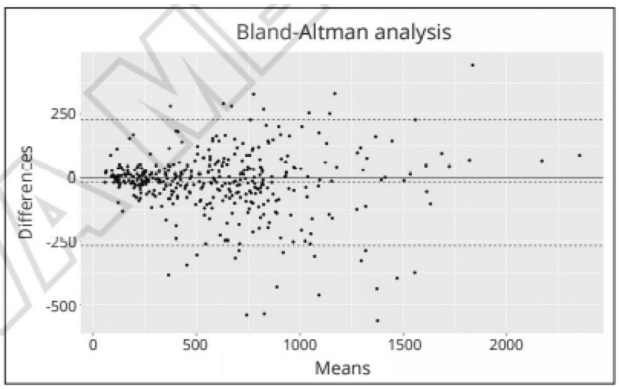

Bland Altman analysis for inter reader agreement for T2 signal intensity (mean difference = -18.5 reader 1 vs. reader 2 and 2SD = 247.3).

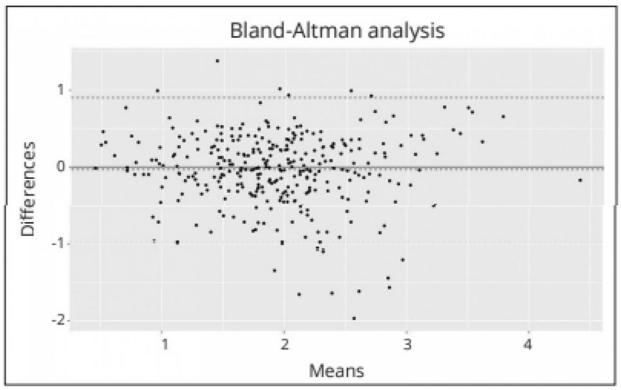


Bland Altman analysis for inter reader agreement for T2 ratio values (mean difference = 0.03 vs. reader 2 and 2SD = 0.9).

**Conclusion** Cardiac magnetic resonance is fundamental for reaching the final diagnosis in patients with suspected myocarditis and properly managing the patient. LGE is a valid diagnostic and prognostic marker in patients with myocarditis. However, evaluation of LGE is not always possible due to patient compliance. As reported in the recently updated Lake Louise criteria, regional high signal intensity in T2 weighted images are a good diagnostic marker of myocarditis and a global T2 ratio $> 2.0$ is considered diagnostic of myocardial inflammation if no focal hyperintensity is evident. In our experience, the segmental T2 ratio showed good diagnostic accuracy in predicting the presence of LGE in patients with clinical suspicion of acute myocarditis and might be useful in reducing scan times with no reduction in diagnostic accuracy.

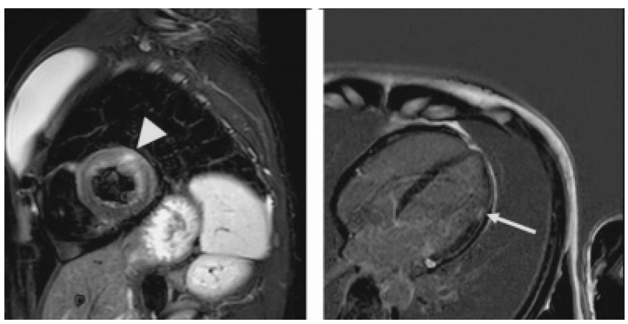

STIR short axis image of the mid ventricular segment in a patient with suspected myocarditis: a mesocardial hyperintense area is noted in the lateral wall (arrowhead). T2 ratio was 3.7 for reader 1 and 2.9 for reader 2. In PSIR images an LGE area with transmural distribution is noted in the same location (arrow).

Limitations are a small sample of patients and the retrospective design of the study.

## A-253

### Effectiveness of the automatic coronary analysis cardiac software in assisting inexperienced readers: comparison between two commercial vendors

**G. Tremamunno, D. De Santis, T. Polidori, R. Carlotta, M. Zerunian, D. Caruso, A. Laghi**

Sant'Andrea University Hospital, Department of Medical Surgical Sciences and Traslational Medicine, Roma, Italy.

**Purpose/Objectives** The purpose of our study was to compare the performances of two commercially available vendors' proprietary advanced cardiac software packages as support to inexperienced CCTA readers in the interpretation of CT coronary angiography (CCTA). We aimed at evaluating differences in terms of time of reconstruction and performances in vessels and segments identification.

**Methods & Materials** Datasets from consecutive patients undergoing clinically indicated routine CCTA were prospectively included from February 2021 to September 2021 and randomly assigned (1:1 ratio) into two groups: patients allocated in group 1 underwent CCTA on GE Revolution EVO CT Scanner (GE Medical Systems, Milwaukee, WI) and images were post-processed on vendor's proprietary software (CardIQ Xpress).

CardIQ Xpress software by GE Medical Systems, Milwaukee, WI.

Patients allocated in group 2 underwent CCTA on Brilliance iCT (Philips Healthcare, Cleveland, OH) and images were post-processed on vendor's proprietary software (Comp. Cardiac).

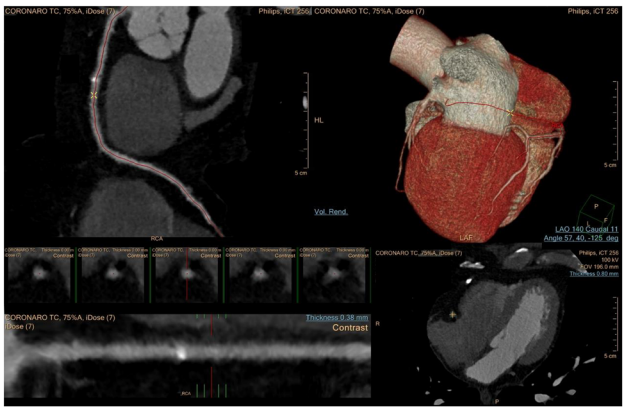

Comp. Cardiac software by Philips Healthcare, Cleveland, OH.

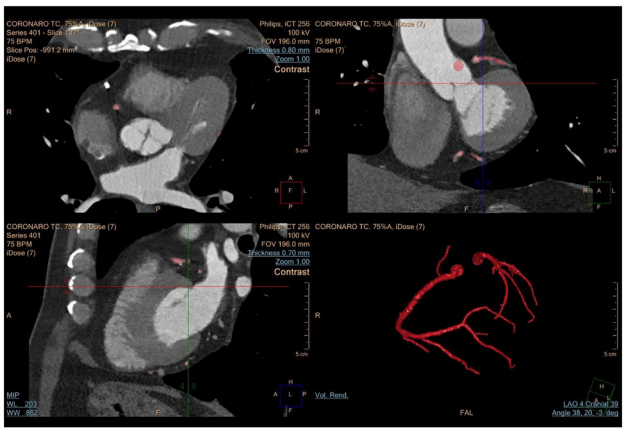

Comp. Cardiac software by Philips Healthcare, Cleveland, OH.

Post-processing included automatic detection of coronary vessels, curved Multiplanar Reformations (MPR), and Volume Rendering Techniques (VRT) reconstructions. We used a standardized approach to coronary vessel identification and segmentation, according to Society of Cardiovascular Computed Tomography guidelines.

Two inexperienced readers were trained in the use of the aforementioned software by a radiology with ten-year experience in cardiovascular imaging. For each software, the number of correctly identified coronary vessels, coronary segments, and the time required for automated coronary vessel selection were recorded. Additionally, readers evaluated whether the three main coronary vessels (RCA, Cx and LAD) were correctly nominated.

Chi-square and Wilcoxon tests were used for statistical evaluations.

**Results** The final study population consisted of 160 patients (96 males; mean age, 63 ± 11 years): 80 in group 1 and 80 in group 2. On a per-vessel basis, group 1 and group 2 software correctly identified 83% and 80% vessels, respectively ($P = 0.39$). Notably, group 1 software proved to be statistically better than group 2 in recognizing the Cx artery (80% versus 65%; $P = 0.03$), while no significant differences were recorded in the recognition of the other main coronary vessels ($P > 0.05$). On a per-segment basis, group 1 software outperformed group 2 software ($P = 0.01$), automatically detecting 938/1280 segments (73%), versus 801/1280 segments (63%). Average analysis time was significantly shorter for group 1 software compared with group 2 (13.8 s versus 21.9 s; $P < 0.001$).

**Conclusion** Group 1 software proved to be faster and more effective than group 2 software in detecting coronary segments, providing better support to unexperienced CCTA readers.

## A-254

### Cardiac Magnetic Resonance to Discriminate Chronic Myocarditis from Healed Myocarditis

**J. M. Brendel[1], J. Kübler[1], K. Klingel[2], K. Müller[3], F. Hagen[1], M. Gawaz[3], K. Nikolaou[1], S. Greulich[3], P. Krumm[1]**

[1]Universitätsklinikum Tübingen, Diagnostic and Interventional Radiology, Tuebingen, Germany, [2]Universitätsklinikum Tübingen, Cardiopathology, Tuebingen, Germany, [3]Universitätsklinikum Tübingen, Cardiology, Tuebingen, Germany.

**Purpose/Objectives** To non-invasively **1)** detect patients with ongoing chronic myocarditis and **2)** differentiate chronic from healed myocarditis.

**Methods & Materials** 50 patients (age 51 [41–61] years; 32% female) with biopsy-proven chronic myocarditis (n = 21, 42%) and healed myocarditis (n = 29, 58%) were consecutively included.

CMR protocol comprised current Lake Louise criteria (LLC) including late gadolinium enhancement imaging (LGE) and mapping ($T_1$, ECV, $T_2$), functional assessment, and strain.

**Results** (**1**) Chronic myocarditis showed higher elevated $T_2$ relaxation times with a median of 54 [52–57] ms vs. 50 [46–52] ms in healed, $p < 0.0001$ as well as more LGE with median 4 [3–5] % vs. 1 [0–4] % enhanced LV myocardial mass, p = 0.003. Both groups showed impaired global strain and LV-EF with significantly reduced functional parameters in chronic vs. healed myocarditis: Global radial strain 14 [7–26] % vs. 21 [14–27] %, p = 0.01; LV-EF 32 [20–48] % vs. 49 [37–56] %, p = 0.02. (2) In the differentiation of chronic from healed myocarditis, $T_2$ mapping yielded an area under the curve (AUC) of receiver-operating curve (0.89) followed by LGE (0.75), ECV (0.64) and $T_1$ (0.63).

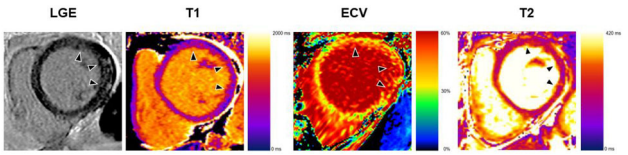


**Fig. 1** CMR findings. Typical appearance of chronic myocarditis

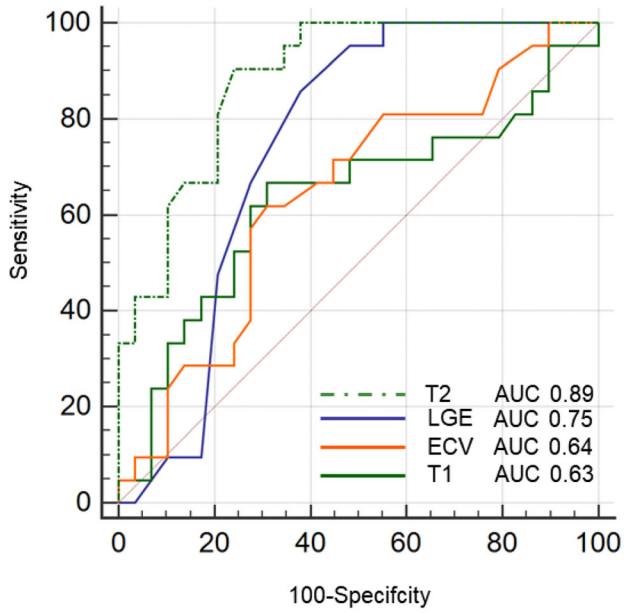


**Fig. 2** ROC curve of discrimination of chronic from healed myocarditis

**Conclusion** (1) Chronic myocarditis can be detected by elevated $T_2$ and higher percentage of LGE as well as a significantly further reduced global strain and LV-EF than in healed myocarditis. (2) The best differentiation of chronic and healed myocarditis was provided by $T_2$ mapping and LGE.

## A-255

### Relationship between risk of development of major arrhythmic complications after transcatheter valve implantation and septo-valvular angle

**L. Benelli[1], D. Francesca[2], M. Pasqualetto[1], S. Paolo[1], C. Marcello[1]**

[1]Università degli studi di Roma "Tor Vergata", Dipartimento di Biomedicina e Prevenzione, Roma, Italy, [2]Università degli studi di Roma, Dipartimento di Biomedicina e Prevenzione, Roma, Italy.

**Purpose/Objectives**

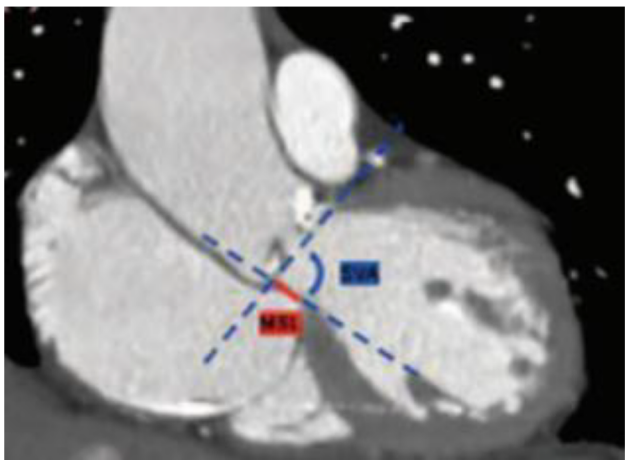


Septo-valvular angle.

Pre-TAVI CT has shown to be fundamental in the evaluation of pre and post procedural anatomical characteristics that predispose to major arrhythmic complications that require permanent pacemaker placement (PPM), secondary to the compressive effects caused by the implantation of the prosthesis on the conduction system at the level of the muscular crest and of the membranous septum of the interventricular septum. Our gues is that the width of the angle between the membranous septum and the aortic annulus (septo-valvular angle, SVA) may be a crucial factor for the impingement on the conduction system. Therefore, our study aims to establish whether the pre-TAVI assessment of the angle between the membranous septum and the aortic annulus (septo-valvular angle, SVA) might be a predictive factor for the onset of arrhythmias that requires PPM.

**Methods & Materials**

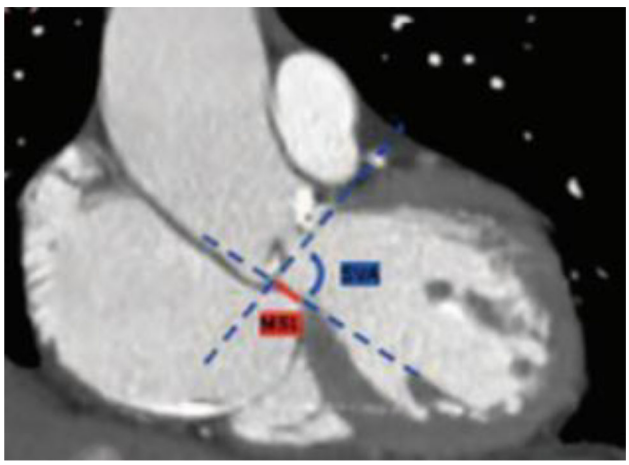


Septo-valvular angle.

Two cardiovascular specialist radiologists retrospectively and double blind evaluated a randomized list of pre-procedural CT of 85 patients who underwent TAVI from April 2020 to January 2021. Two anatomical features were measured by readers: membranous septum length (MSL) and width of the septum-valve angle (SVA).

**Results**

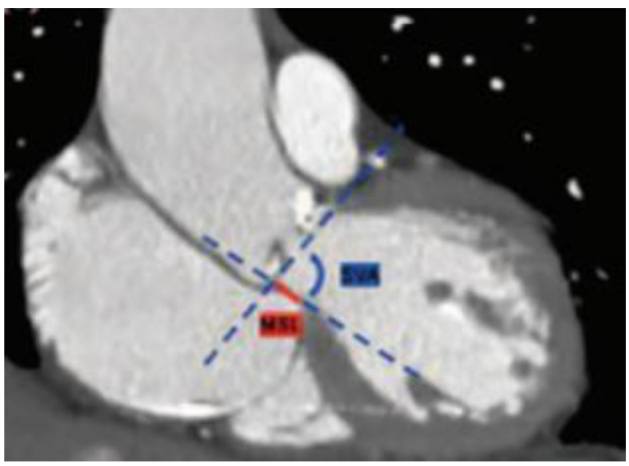


Septo-valvular angle

A PPM was implanted in 25 patients (31%) after the procedure. Receiver-operating characteristic curves (ROC) performed for both measurements have documented: for the ASV sensitivity 94% and VPN 96% (AUC: 0.77 (95% CI: 0.66–0.90)). There was no significant difference in the anatomical measurements performed between the two observers, regarding both anatomical measurements (ICC was 0,754 for the MSL and 0,922 for the SVAThe MSL ROC was not significant. The mean SVA value stratified for patients who did not undergo PPM implantation and patients who did resulted significant (p < 0,005).

**Conclusion**

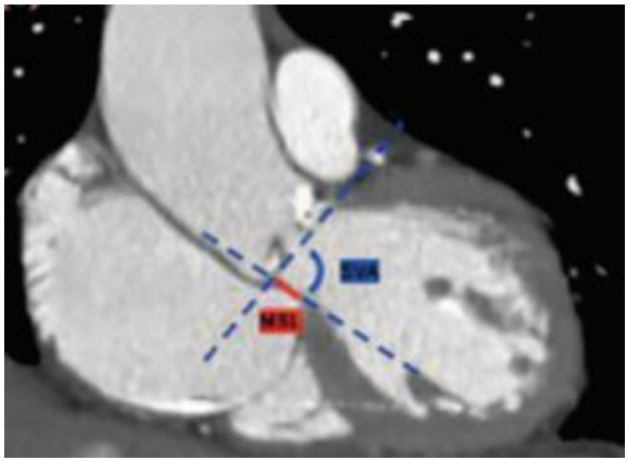


Septo-valvular angle

Evaluation of the SVA measured in preprocedural CT scans has shown to be related to the onset of major arrhythmias after TAVI requiring permanent pacemaker implantation.

## A-256

### Role of transcatheter aortic valve implantation in patients with an associated unruptured aortic root pseudoaneurysm detected at preprocedural cardiac computed tomography angiography

**F. D'Errico, M. Pasqualetto, L. Benelli, M. Cesareni, C. Cerimele, F. Grimaldi, L. Pugliese, F. Garaci, R. Floris, M. Chiocchi**

Fondazione Policlinico Tor Vergata, Rome, Italy.

**Purpose/Objectives** Unruptured aortic root pseudoaneurysm (UARP) is a rare complication often related to aortic valve endocarditis. Infectious spread to the valvular annulus or myocardium can lead to septic complications such as wall thickening and abscess, the spontaneous drainage of which leads to pseudoaneurysm formation. We report for the first time a patient series in which transcatheter aortic valve implantation (TAVI), using a single valve, resolved aortic valvulopathy associated with UARP.

**Methods & Materials** At our center, from December 2017 to October 2019, we studied 138 patients who underwent TAVI for aortic valve stenosis and/or regurgitation, in 20 of whom (12 female patients, 8 male patients) we found an associated incidental UARP in echocardiography or cardiac computed tomography angiography (CCTA) pre-TAVI. The average age of these 20 patients with UARP was 76.9 W 5.2 years. All patients were assessed using preprocedural and postprocedural multimodality imaging, including transthoracic echocardiography (TTE), transesophageal echocardiography (TEE), and CCTA.

**Results** In all patients with UARP underwent TAVI, the final angiographic examination showed correct valve positioning with complete coverage of the false aneurysm, with total or subtotal UARP thrombosis documented in post-TAVI CCTA images. The mean follow-up period was 17.5 months (12–23 months). During follow-up, CCTA and TEE showed normal prosthetic valve function with no leakage (trace or mild), and complete UARP exclusion in all patients, without any complications.

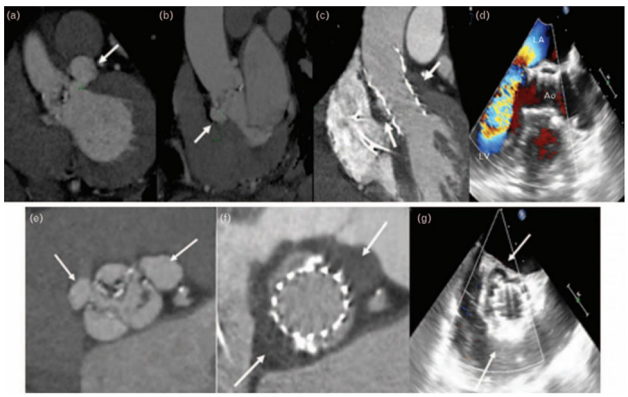


Pre-TAVI CT shows left unruptured aortic root pseudoaneurysm and right unruptured aortic root pseudoaneurysm (a, b and e). After procedure CCTA shows complete thrombosis of pseudoaneurysm(c and f); the TEE shows optimal prosthesis position, absence of residual aortic regurgitation and complete exclusion of the UARP (d and g).

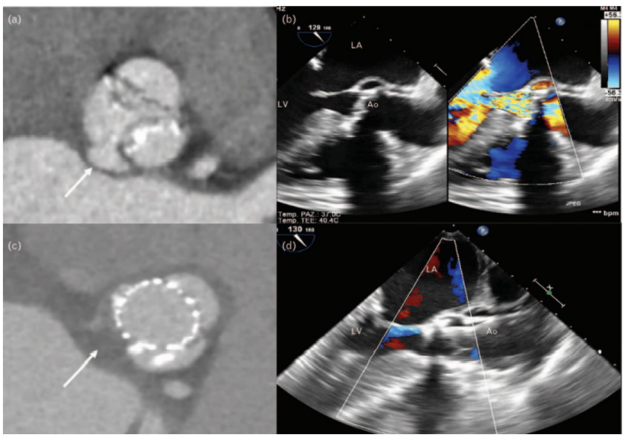


Pre-TAVI CT in axial view shows PMAIVF (a). Pre (TAVI) transesophageal LVOT view shows PMAIVF partially collapsed in diastole and severe aortic regurgitation (b). Postprocedural CCTA shows PMAIVF thrombosis (c); Postprocedural TEE shows correct position of the aortic prosthesis, exclusion of the PMAIVF and trivial aortic regurgitation (d).

**Conclusion** In conclusion, CCTA assessment is essential not only for the planning of the TAVI procedure but even for the identification of possible incidental post-infectious pseudoaneurysms and assessment of their complications. We have shown how percutaneous valve

positioning can simultaneously solve pseudoaneurysm complications by excluding the sac and promoting thrombosis, avoiding surgery of the pseudoaneurysm. In our experience, pseudoaneurysm does not increase the complexity of the TAVI procedure and the choice of the prosthesis must not only be made on the basis of annulus measurements, but also as a function of radial force, which must be high to exclude the collar of the bag. We used just Corevalve as it has scaffolding properties because of the long stent frame.

## A-257

### The role of Cardiac Magnetic Resonance in post-COVID19 patients in the absence of clinical-laboratory suspicion of myopericarditis: a diagnostic overuse?

**F. P. Sbordone, F. Grimaldi, A. Luciano, V. De Stasio, L. Pugliese, R. Floris, F. Garaci, M. Chiocchi**

Policlinico Tor Vergata, ROME, Italy.

**Purpose/Objectives** Identify and characterize cardiac involvement following Sars-Cov-2 infection, in young-adult patients who have experienced a pauci-asymptomatic form of respiratory disease, in the absence of clinical and laboratory signs of myo-pericardial involvement.

**Methods & Materials** 25 patients aged between 25 and 50 years, who presented a pauci-asymptomatic form of Sars-Cov-2 related respiratory disease, were evaluated retrospectively at least 3 months after infection. The exclusion criteria were a history of previous myo-pericarditis, the presence of other known cardiac pathologies and the presence of clinical-laboratory signs of myo-pericardial involvement during the infection. Patients underwent Cardiac Magnetic Resonance (CMR) to study ventricular volumes and function and to highlight any signs of myocardial damage.

**Results**

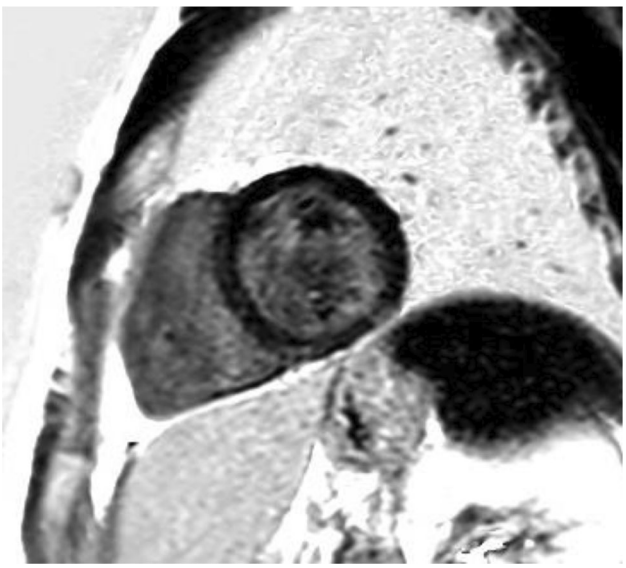

Four patients (16%) had signs of mild myocardial injury in the sequences for the LGE study (PSIR sequences). In particular three patients presented a focal sub-epicardial LGE at mild-basal inferior-lateral segments. Only one patient presented evidence of meso-cardial LGE at mild-apical inferior-septal wall. Post-processing myocardial segmentation demonstred in these four patients a rather preserved ventricular function. All four patients had Left Ventricular Ejection Fraction (LVEF) with minimally reduced values (mean: 57%). They also had a slightly increased end-systolic volume (ESV), in particular the BSA-identified volume. A mild pericardial effusion was found in 6 patients (24%) in the absence of any signs of inflammation. No patient presented significant changes in ventricular function.

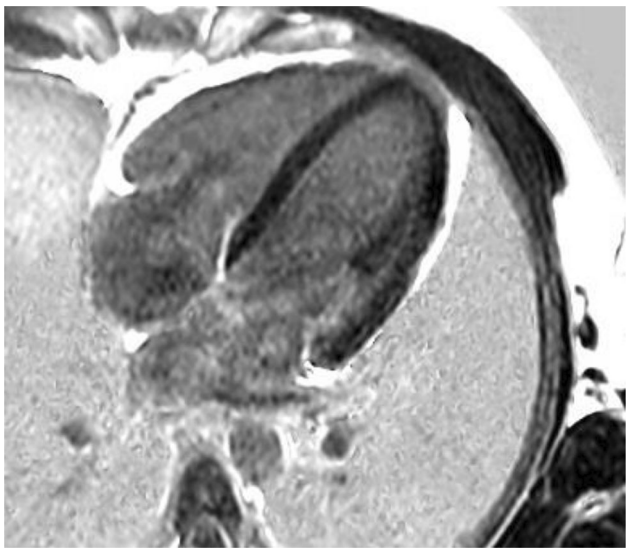

**Conclusion** A non-negligible percentage of pauci-asymptomatic patients during Sars-CoV-2 infection showed mild signs of myo-pericardial involvement at the CMR, in the absence of significant alterations in ventricular function and / or volumes. Further studies are needed to interpret the reported findings, and in particular to follow the clinical and / or radiological evolution over time.

## A-258

### Coronary CT angiography with myocardial Late Contrast Enhancement in patients with acute chest pain syndrome and mild troponin rise

**D. Vignale, A. Palmisano, C. Colantoni, V. Nicoletti, L. Brunetti, M. Slavich, M. Montorfano, A. Esposito**

IRCCS San Raffaele Scientific Institute, Milano, Italy.

**Purpose/Objectives** Acute chest pain syndrome with mild troponin rise, being caused by a variety of etiologies, represents a diagnostic conundrum in the emergency department. A recent study (doi:10.1148/radiol.211288) published by out gropus has demonstrated the incremental diagnostic value of adding a late contrast enhancement (LCE) scan, in addition to coronary CT angiography (cCTA), in patients without coronary artery disease (CAD) or with non-osbstructive CAD. However, the additional value of LCE in patients with obstructive CAD remained undetermined. Thus, our objective was to explore the value of the LCE scan in patients presenting to the emergency department with acute chest pain syndrome and mild troponine rise and with osbstructive CAD at cCTA.

**Methods & Materials** This was a prospective study performed on 36 patients (men = 20 [58%], median age 64 [IQR 48–77] years) presenting to emergency department with acute chest pain or anginal equivalent, without diagnostic criteria for acute myocardial infarction, with mild troponin rise (median 154 [IQR 45–510] ng/L), undergoing cCTA to evaluate CAD status and wall motion abnormalities followed by the LCE scan to assess presence and extent of myocardial necrosis/scar.

**Results** Fourteen (39%) patients had negative cCTA: among these, 9 (64%) had LCE suggestive of myocarditis, 2 (14%) of myocardial infarction with non-obstructed coronary arteries, and 3 (21%) had abnormal wal motion and absence of LCE suggesting Takotsubo. Twenty-two (61%) patients had obstructive CAD (stenosis > 50%), involving one vessel in 16 (73%) and two and three vessels in 3 (13.5%) patients each. Among these, 12 (55%) had ischemic LCE, mostly with transmural distribution (10 [83%]) involving a median of 4 [IQR3-5] segments, with microvascular obstruction (MVO) in 3 (30%). Two (17%) patients had subendocardial LCE involving two segments. LCE was always in the territory of an obstructive lesion in one-vessel CAD (9 [75%]) and in the territory of worse stenosis in multi-vessel CAD (3 [25%]) (IMAGE01). Ten (45%) patients with obstructive CAD had preserved wall thickness and no LCE, with hypokinesia in 6 (60%), and were diagnosed with non-ST elevation myocardial infarction.

**Conclusion** In this study, we have confirmed the additional diagnostic value of the LCE scan in patients without CAD or with non-obstructive CAD ad cCTA. Furthermore, in patients with obstructive CAD, the LCE scan can detect loss of viable myocardium and can identify well-known predictors of worse prognosis (i.e., MVO and transmurality) and helps in identifying the culprit lesion, especially in multivessel CAD, thus guiding revascularization. The main limitations of this study is the small sample size.

## A-259

### Coronary stent image quality with a spectral photon counting CT: first results in humans

**S. Boccalini[1], S. Si-Mohamed[2], H. Lacombe[3], M. Villien[4], L. Boussel[2], P. Douek[2]**

[1]Hospices Civils de Lyon, Radiology, Lyon, France, [2]Hospices Civils de Lyon, Lyon, France, [3]Creatis, Villeurbanne, France, [4]Philips, Suresne, France.

**Purpose/Objectives** The aim of this study is to compare the image quality (IQ) of *in-vivo* coronary stents between an energy-integrating detectors dual-layer CT (EID-DLCT) and a clinical prototype of spectral photon counting CT (SPCCT).

**Methods & Materials** In January-June 2021 consecutive patients with coronary stents were prospectively enrolled to undergo a coronary CT with an EID-DLCT and a SPCCT. The study was approved by the local ethical committee and patients signed an informed consent. A retrospectively ECG-gated acquisition was performed with optimized matching parameters and identical injection protocol on the two scanners. Images were reconstructed with slice thickness of 0.67 mm, 512 matrix, XCD kernel, iDose 3 for EID-DLCT and 0.25 mm slice thickness, 1024 matrix, Sharp kernel and iDose 6 for SPCCT. The difference (ΔS-C) between ROIs drawn inside the stent and the adjacent coronary artery was calculated. Measures of the outer and inner diameters of the stents were used to quantify blooming artefacts. For subjective IQ, 3 experienced observers graded different parameters with a 4-point scale: coronary wall before stents, stent lumen, stent structure, calcifications surrounding stents, beam hardening artefacts.

**Results** Eight patients (age: 68 (IQ = 8); all males; BMI: 26.2 (IQ = 4.2)) with 16 stents were scanned. Five stents were not evaluable due to motion artefacts on the SPCCT and were excluded from further analysis. Radiation dose was lower for SPCCT (fixed $CTDI_{vol}$ = 25.7 mGy vs $CTDI_{vol}$ = 35.7 mGy(IQ = 13.6); p = 0.02). With SPCCT, external diameters were smaller, internal diameters were larger and, consequently, blooming artefacts were reduced ($p < 0.05$). The ΔS-C was lower for SPCCT as compared to EID-DLCT-XCD ($p < 0.05$) translating a reduction of intra-stent artefacts. SPCCT received higher IQ subjective scores than EID-DLCT for all scored parameters (all $p \leq 0.05$).

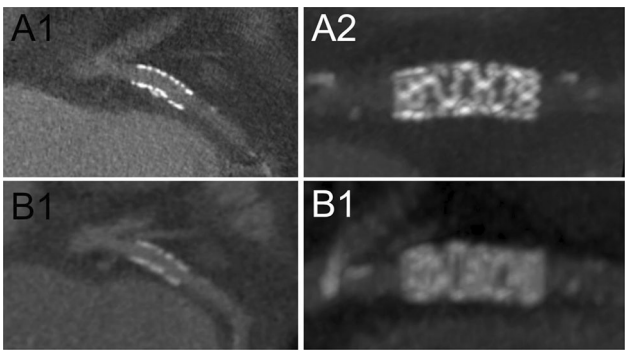


In panels A, an example of a stent imaged with SPCCT on multiplanar (A1) and MIP (A2) reconstructions. In panels B, corresponding images on DECT. To be noticed the small calcification adjacent to the posterior wall of the stent well depicted on SPCCT images in A1 and not detectable on DECT images.

**Conclusion** SPCCT demonstrated improved objective and subjective image quality as compared to EID-DLCT for the evaluation of coronary stents with a lower radiation dose.

## A-260

### Cardiovascular magnetic resonance in chronic-phase myocarditis: role of parametric mapping to solve the challenging diagnosis between active and healing myocarditis

**R. Zurrida, A. Palmisano, E. Bruno, C. Gnasso, D. Vignale, A. Esposito**

IRCCS Ospedale San Raffaele, Milano, Italy.

**Purpose/Objectives** Myocarditis is an inflammatory injury of the myocardium and it's an important cause of cardiac morbidity and mortality in young adults. The identification of subtle chronic inflammation is challenging. Cardiac magnetic resonance (CMR) has the capability to non-invasively characterize myocardial injury in an accurate way; 2009 Lake Louise Criteria (LLC) showed suboptimal performances in the identification of myocarditis, especially in convalescent and chronic phase. The introduction of parametric mapping opened to the possibility to characterize the myocardial inflammation in a quantitative way, with increased sensitivity, and they were included in the updated diagnostic criteria (2018 LLC). Despite a lot of literature is available about the performance of 2018 LLC in the setting of acute injury, data on chronic myocarditis are sparse and conflicting. The aim of the present study was to compare the diagnostic performance of 2018 LLC versus the original LLC in the identification of chronic active myocarditis in patients with clinical suspicion of active chronic inflammation, also related to the clinical pattern presentation.

**Methods & Materials** This is a single-center retrospective study enrolling 149 consecutive patients with clinical suspicion of convalescent or chronic myocarditis (> 3 months before) who underwent CMR from July 2018 to March 2022 with a multi-parametric protocol for the assessment of 2009 and 2028 LLC. 31 patients have been excluded for acute presentation and 23 for other underlying cardiac disease; the final cohort included 95 patients with clinical suspicion of convalescent or chronic active myocarditis.

**Results** Enrolled patients were mainly men (64%) with median age of 48 years [IQR 32–55]; 47(49%) were symptomatic (36% arrhythmia, 16% infarct-like presentation, 6% heart failure symptoms and 2% fever or flu-like presentation). According to 2018 LLC, 75(79%) patients were positive for active myocarditis, while only 29 (30%) had positivity of 2009 LLC. Out of the remaining 20 patients (21%), 14(15%) were classified as negative at 2018 LLC and 6(6%) as unclassifiable for non-assessable T2-mapping. Patients with active versus healed myocarditis differed in term of mapping parameters (segments with altered T2 mapping: 50%[12–90] vs 17%[7–25]; $p < 0.0001$; native-T1 segments 50%[17–81] vs 16%[6–52]; $p = 0.032$; ECV 56%[38–82] vs 16%[0–55]; $p = 0.022$), while no significant differences were found in the number of segments with focal edema at STIR images (0[0–2] vs 0[0–0]; p = 0,0548) and in percentage of late gadolinium enhancement (LGE), (2,6%[1,5–5] vs 2,2%[0,6–3,8]; p = 0,343).

**Conclusion** Mapping parameters significantly improved the detection of subtle inflammation in patients with chronic myocarditis.

## A-263

### Aortic dissection from A to Z – a pictorial review

**R. M. Popa[1], R. E. Bîrlă-Coroiu[1], T. Matei[1], R. M. Manea[1,2]**

[1]Clinical Emergency County Hospital of Braşov, Romania, Department of Radiology and Medical Imaging, Braşov, Romania, [2]Faculty of Medicine, "Transilvania" University of Braşov, Romania, Radiology, Braşov, Romania.

**Purpose/Objectives** Aortic Dissection is the prototype and most common form of acute aortic syndromes. It occurs when blood enters the medial layer of the aortic wall through a tear or penetrating ulcer in the intima and tracks longitudinally along with the media, forming a second blood-filled channel, also known as false lumen, within the vessel wall. The incidence of aortic dissection is reported to be approximately 5 to 30 cases per 1 million people per year. Aortic dissection still carries a very high mortality rate (ranges from 20 to 30%), at least 30% of patients die after reaching the Emergency Department, therefore, the aim of this pictorial review is to clearly outline the imaging features of this life-threatening pathology, representing helpful and important aspects for radiologists.

**Methods & Materials** This pictorial review includes 27 patients, who were admitted to the Emergency Department of Clinical Emergency County Hospital Braşov, Romania, between 01.01.2019 – 20.05.2022, who had immediately performed a contrast enhanced CT scan on admission and CT acquisitions illustrate aortic dissection. Cases were investigated with a GE Optima660 128-slice CT scanner, with different scanning protocols including unenhanced, arterial and venous phase, imaging the aorta.

**Results** The selected cases were classified based on the Stanford Classification (type A – surgical management or type B – medical management) and DeBakey Classification, noting the imaging particularities of each case of aortic dissection and the pathophysiological impact. Multiple images acquired from contrast enhanced CT scans were included in this pictorial review along with their detailed imagistic description, including the identification of the true lumen and the false lumen and tips and tricks on how to quickly identify them are also richly illustrated. Moreover, the predisposing high-risk factors for non-traumatic aortic dissection and the etiology of each case were also noted, representing important aspects for further management.

**Conclusion** All aspects taken into account, the MDCT is an indispensable and valuable imaging tool for the accurate diagnosis of aortic dissection. Because there is a wide spectrum of major complications, that can occur such as, dissection and occlusion of branch vessels, aortic rupture, ischemic stroke, paraplegia (involvement of artery of Adamkiewicz), distal thromboembolism, aneurysmal dilatation, aortic incompetence, coronary artery occlusion, rupture into the pericardial sac causing hemopericardium resulting cardiac tamponade etc., correct knowledge of this life-threatening pathology is at the utmost importance in order to obtain an accurate diagnosis immediately, which can significantly lower morbidity, as well as reduce mortality regarding this pathology.

## A-264

### Prediction of outcome using relative versus absolute change in cardiac MRI measurements in patients with pulmonary arterial hypertension

**S. Alabed[1,2], P. Garg[3], K. Dwivedi[1,2], F. Alandejani[1], A. Maiter[1,2], K. Karunasaagarar[1,2], S. Rajaram[1,2], C. Hill[2], S. Thomas[1,2], M. Sharkey[1], M. Mamalakis[1], J. M. Wild[1], H. Lu[4], R. Condliffe[1,5], D. G. Kiely[1,5], A. J. Swift[1]**

[1]University of Sheffield, Department of Infection, Immunity & Cardiovascular Disease, Sheffield, United Kingdom, [2]Sheffield Teaching Hospitals, Department of Clinical Radiology, Sheffield, United Kingdom, [3]University of East Anglia, Norwich Medical School, Norwich, United Kingdom, [4]University of Sheffield, Department of Computer Science, Sheffield, United Kingdom, [5]Sheffield Teaching Hospitals, Sheffield Pulmonary Vascular Disease Unit, Sheffield, United Kingdom.

**Purpose/Objectives** Cardiac MRI is an important prognostic modality in pulmonary arterial hypertension (PAH)[1]. As a monitoring tool cardiac MRI can assess right ventricle (RV) adaptation to increased pulmonary pressure and is sensitive to RV changes resulting from initiating or escalating therapy[2][3][4][5]. Previous studies have suggested absolute change in RV function and volumes as markers of disease progression[6]. While absolute differences in cardiac MRI parameters give an idea of whether the RV is improving or worsening, it does not account for the quantity of change compared

to the initial state of the RV. Our study compares the prognostic value of relative compared to absolute change in RV measurements between baseline and follow-up cardiac MRI scans.

**Methods & Materials** All treatment-naive PAH patients between 2007 and 2021 who had two cardiac MRI scans (at baseline and at 12–24 months follow-up) were identified from the ASPIRE registry. All patients were followed up for additional 12 months after the second scan. For both scans, cardiac measurements were obtained from a validated automatic segmentation tool to obtain RV measurements from both scans, including ejection fraction (RVEF), end-diastolic volume (RVEDV) and end-systolic volume (RVESV) and stroke volume (RVSV). For each metric, the absolute (follow-up minus baseline measurement) and relative differences (ratio of the absolute difference to baseline measurement) were compared using Cox proportional hazard regression and Kaplan–Meier analysis of one-year mortality. Previously published thresholds of absolute changes of 3% in RVEF and 10 ml in RV volumes were compared to a 10% relative change in each of the RV measurements.

**Results** 239 patients were included in this retrospective study (53 ± 13 years, 79% female, 82% WHO functional class 3). 42% had PAH associated with connective tissue disease, 37% had idiopathic PAH and 21% had other types of PAH. The mean relative and absolute differences in RVEF, RVESV, RVEDV and RVSV are shown in Table 1.

| | Baseline | Follow-up | Absolute difference | Relative difference (%) |
|---|---|---|---|---|
| RVEF (%) | 34 ± 11 | 41 ± 11 | 7 (1 to 13) | 20 (2 to 44) |
| RVESV (ml) | 139 ± 62 | 119 ± 58 | -14 (-41 to 1) | -12 (-29 to 1) |
| RVEDV (ml) | 205 ± 70 | 195 ± 71 | -4 (-32 to 16) | -2 (-14 to 10) |
| RVSV (ml) | 66 ± 24 | 76 ± 28 | 9 (-4 to 23) | 14 (-5 to 39) |

Baseline and follow-up cardiac MRI measurements in 239 patients with pulmonary arterial hypertension. Measurements are shown in mean ± standard deviation. Differences are shown in median (interquartile range).

Relative changes of RV parameters were significantly associated with one-year mortality, while only using the absolute difference in RVEDV had predictive value (Table 2).

| Parameter | Change | Absolute Difference Hazard ratio, [95% CI] | P | Change | Relative Difference Hazard ratio, [95% CI] | P |
|---|---|---|---|---|---|---|
| RVEF | 3% | 2.44, [1.00, 6.00] | 0.05 | 10% | 3.02, [1.23, 7.40] | 0.02 |
| RVESV | 10 ml | 1.49, [0.91, 2.45] | 0.12 | 10% | 1.55, [1.02, 2.37] | 0.04 |
| RVEDV | 10 ml | 1.77, [1.07, 2.93] | 0.03 | 10% | 1.80, [1.12, 2.87] | 0.01 |
| RVSV | 10 ml | 1.04, [0.58, 1.84] | 0.90 | 10% | 0.98, [0.63, 1.53] | 0.93 |

Cox proportional hazard regression results assessing change in RV ejection fraction and volumes to predict 1-year mortality.

Kaplan–Meier survival curves showed better differentiation into improved, stable and worsened patient status with relative change in RV measurements compared to absolute change (Fig. 1).

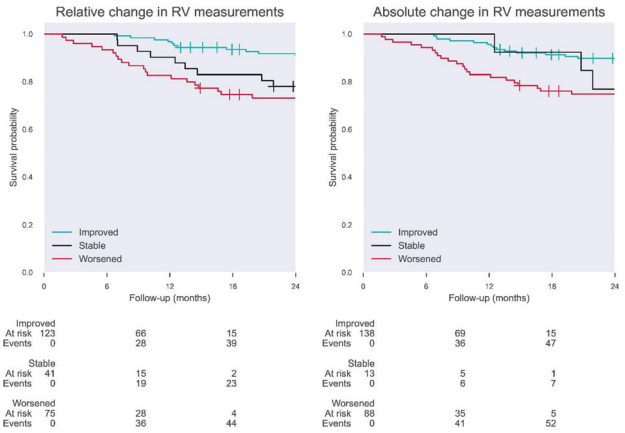


Kaplan–Meier plot comparing survival prediction of relative (left panel) and absolute (right panel) change in RV measurements.

**Conclusion** In patients with PAH, relative differences in RV measurements between two MRI scans reflect the risk of one-year mortality more accurately than absolute differences.

**Literature**

[1] Alabed, Samer, Yousef Shahin, Pankaj Garg, Faisal Alandejani, Christopher S. Johns, Robert A. Lewis, Robin Condliffe, James M. Wild, David G. Kiely, and Andrew J. Swift., (2021), "Cardiac-MRI Predicts Clinical Worsening and Mortality in Pulmonary Arterial Hypertension: A Systematic Review and Meta-Analysis.", JACC. Cardiovascular Imaging, 931–42, 14, https://doi.org/10.1016/j.jcmg.2020.08.013

[2] Swift, Andrew J., Frederick Wilson, Marcella Cogliano, Lindsay Kendall, Faisal Alandejani, Samer Alabed, Paul Hughes, Yousef Shahin, Laura Saunders, Charlotte Oram, David Capener, Alex Rothman, Pankaj Garg, Christopher Johns, Matthew Austin, Alistair Macdonald, Jo Pickworth, Peter Hickey, Robin Condliffe, Anthony Cahn, Allan Lawrie, Jim M Wild, David G Kiely, (2021), "Repeatability and Sensitivity to Change of Non-Invasive End Points in PAH: The RESPIRE Study.", Thorax, 1032–1035, 76, https://doi.org/10.1136/thoraxjnl-2020-216078.

[3] Goh, Ze Ming, Samer Alabed, Yousef Shahin, Alexander M. K. Rothman, Pankaj Garg, Allan Lawrie, David Capener, Roger Thompson, Faisal Alandejani, Christopher S Johns, Robert A Lewis, Krit Dwivedi, James M Wild, Robin Condliffe, David G Kiely, Andrew J Swift, (2021), "Right Ventricular Adaptation Assessed Using Cardiac Magnetic Resonance Predicts Survival in Pulmonary Arterial Hypertension.", JACC. Cardiovascular Imaging, 1271–72, 14, https://doi.org/10.1016/j.jcmg.2020.10.008

[4] Goh, Ze Ming, Nithin Balasubramanian, Samer Alabed, Krit Dwivedi, Yousef Shahin, Alexander M. K. Rothman, Pankaj Garg, Allan Lawrie, David Capener, Roger Thompson, Faisal Alandejani, Jim M Wild, Christopher S Johns, Robert A Lewis, Rebecca Gosling, Michael Sharkey, Robin Condliffe, David G Kiely, Andrew J Swift, (2022), "Right Ventricular Remodelling in Pulmonary Arterial Hypertension Predicts Treatment Response.", Heart, https://doi.org/10.1136/heartjnl-2021-320733

[5] Kiely, David G., David Levin, Paul Hassoun, David D. Ivy, Pei-Ni Jone, Jumaa Bwika, Steven M. Kawut, Jim Lordan, Angela Lungu, Jeremy A. Mazurek, Shahin Moledina, Horst Olschewski, Andrew J. Peacock, G.D. Puri, Farbod N. Rahaghi, Michal Schafer,

Mark Schiebler, Nicholas Screaton, Merryn Tawhai, Edwin J.R. van Beek, Anton Vonk-Noordegraaf, Rebecca Vandepool, Stephen J. Wort, Lan Zhao, Jim M. Wild, Jens Vogel-Claussen, Andrew J. Swift, (2019), "EXPRESS: Statement on Imaging and Pulmonary Hypertension from the Pulmonary Vascular Research Institute (PVRI).", Pulmonary Circulation, 9, https://doi.org/10.1177/2045894019841990

[6] Bradlow WM, Hughes ML, Keenan NG, Bucciarelli-Ducci C, Assomull R, Gibbs JS, Mohiaddin RH., (2010), "Measuring the heart in pulmonary arterial hypertension (PAH): implications for trial study size.", Journal of Magnetic Resonance Imaging, 117–24, 31.

## A-266

### Biatrial volumetric assessment by non-ECG gated CTPA correlated with transthoracic echocardiography in patients with normal diastology

**D. Gopalan[1], J. Riley[2], K. Leong[3], S. Alsanjari[4], B. Ariff[5], S. Nyrén[6], W. Auger[7], P. Lindholm[8]**

[1]Karolinska Insitutet, Department of Physiology and Pharmacology, Stockholm, Sweden, [2]Monash Health, Department of Diagnostic Imaging, Melbourne, Australia, [3]Royal Melbourne Hospital, Department of Cardiology, Melbourne, Australia, [4]Imperial College Hospital NHS Trust, Radiology, London, United Kingdom, [5]Imperial College Hosptial NHS Trust, Radiology, London, United Kingdom, [6]Karolinska Institutet, Department of Molecular Medicine and Surgery, Stockholm, Sweden, [7]University of California, San Diego, United States of America, [8]University of California, Department of Emergency Medicine, San Diego, United States of America.

**Purpose/Objectives** Atrial size can be useful for prediction of cardiovascular mortality [1][2]. Non-ECG gated CTPA is a common test for cardiopulmonary evaluation but there is no data regarding normative CTPA values for biatrial volumes. We examined feasibility and reproducibility of deriving CT normative biatrial volumes using manual contouring and automated segmentation with comparative transthoracic echocardiography (TTE) to confirm normal diastology.
**Methods & Materials** Radiology Information System and echocardiography databases scrutinised from Jan 2017 to Dec 2019 to select 35 consecutive cases in sinus rhythm with no history of cardiovascular, renal, or pulmonary disease, normal diastolic function on TTE and no thromboembolic disease on contemporaneous CTPA.

| | Normal diastology (n = 35) |
|---|---|
| Age (years) | 45 (34–50) |
| Gender | 18 M (51%), 17 F (49%) |
| BMI | 27.0 (23.5–32.0) |
| BSA | 1.95 + 0.25 |
| CTPA-TTE time interval (days) | 44 (11–113) |

Baseline characteristics of the thirty-five cases.

TTE atrial volumes measured using atrial length method as per established guidelines [3].

| | Normal diastology cohort (n = 35) |
|---|---|
| Simpson's biplane LVEF (%) | 61 + 4 |
| Transmitral E (cm/s) | 84 (63–96) |
| Transmitral A (cm/s) | 65 (53–73) |
| E/A | 1.29 + 0.24 |
| Medial mitral e' (cm/s) | 11 (9–12) |
| Lateral mitral e' (cm/s) | 14 (12–15) |
| E/medial e' | 7.9 + 2.0 |
| E/lateral e' | 5.9 + 1.4 |
| TR Vmax (m/s) (n = 15) | 2.3 + 0.2 |

Transthoracic echocardiography (TTE) measures of normal diastology.

CT manual planimetry performed by 2 radiologists using Vitrea Advanced Visualization multimodal platform, creating CT 2 and 4 chamber planes analogous to TTE with exclusion of pulmonary veins and atrial appendages. LA volume estimated by: [0.85 × area 1 (2 chamber) x area 2 (4 chamber)] ÷ shortest LA long axis length and RA volume by: [0.85 X (RA 4 chamber area)$^2$] ÷ RA long axis length. Automated measurements recorded using commercially available software (Circle Cardiovascular Imaging V5.12.1). Time to complete analyses was recorded.

**Results** TTE and CTPA derived normal LAVi and RAVi were 27 + 5 & 20 + 6 mL/m$^2$ and 30 + 8 & 29 + 9 mL/m$^2$ respectively. Bland–Altman analysis revealed underestimation of biatrial volumes by TTE.

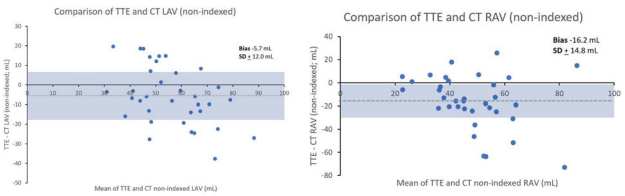


Bland–Altman comparison of normal transthoracic echocardiography (TTE) and CT (non-indexed) LA & RA volume measurements.

TTE- CT mean biases for (non-indexed) LAV and RAV were -5.7 + 12.0 mL and -16.2 + 14.8 mL respectively. CT intraclass correlation coefficient (ICC 95% CI) 0.99 (0.96–1.00) and 0.96 (0.76–0.99) for LA and RA volumes respectively. There was excellent correlation between automated and manual measurement for LA (r 0.99, 95% CI 0.98–0.99; p < 0.001) and RA (r 0.99, 95% CI 0.99–1.00; p < 0.001).

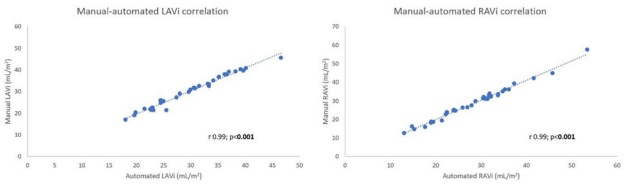


CT manual and automated atrial volume correlation.

Automated measurement was systematically smaller (LA bias -0.2 + 1.2 mL/m$^2$; RA bias -0.4 + 1.1 mL/m$^2$) but bias magnitude

was not clinically relevant. Mean analysis time 12 and 6 min respectively for manual and automated measurement.

**Conclusion** Knowledge of normative atrial volumes is required to differentiate pathological conditions from normal state. Our study proves that CT atrial volumetric assessment is easy and reproducible and can provide additional metric in cardiopulmonary assessment. The finding of TTE volumetric underestimation is similar to previous studies comparing TTE with ECG gated CT [4][5][6]. Manual and automated measurements had excellent correlation but latter is quicker to perform. Although our cohort is small, this is the only study with corroborative TTE in all cases to ensure normal diastology.

**Literature**

[1] Hoit BD, (2014), Left atrial size and function: role in prognosis, J Am Coll Cardiol.2014 Feb 18;63(6):493–505.

[2] Lerchbaumer MH, Ebner M, Ritter CO, Steimke L, Rogge NIJ, Sentler C, Thielmann A, Hobohm L, Keller K, Lotz J, Hasenfuß G, Wachter R, Hamm B, Konstantinides SV, Aviram G, Lankeit M, (2021), Prognostic value of right atrial dilation in patients with pulmonary embolism, ERJ Open Res.2021 May 24;7(2):00,414–2020.

[3] Lang RM, Badano LP, Mor-Avi V, Afilalo J, Armstrong A, Ernande L, Flachskampf FA, Foster E, Goldstein SA, Kuznetsova T, Lancellotti P, Muraru D, Picard MH, Rietzschel ER, Rudski L, Spencer KT, Tsang W, Voigt J-U, (2015), Recommendations for cardiac chamber quantification by echocardiography in adults: an update from the American Society of Echocardiography and the European Association of Cardiovascular Imaging, J Am Soc Echocardiogr. 2015 Mar;16(3):233–70.

[4] Koka AR, Yau J, Van Why C, Cohen IS, Halpern EJ., (2010), Underestimation of left atrial size measured with transthoracic echocardiography compared with 3D MDCT, Am J Roentgenol. 2010 May;194(5):W375-381.

[5] Koka AR, Gould SD, Owen AN, Halpern EJ, (2012), Left atrial volume: comparison of 2D and 3D transthoracic echocardiography with ECG-gated CT angiography, Acad Radiol. 2012 Jan;19(1):62–8.

[6] Kataoka A, Funabashi N, Takahashi A, Yajima R, Takahashi M, Uehara M, Takaoka H, Saito M, Yamaguchi C, Lee K, Nomura F, Komuro I, (2011), Quantitative evaluation of left atrial volumes and ejection fraction by 320-slice computed-tomography in comparison with three- and two-dimensional echocardiography: a single-center retrospective-study in 22 subjects, Int J Cardiol. 2011 Nov 17;153(1):47–54.

## A-267

### T1, T2, and ECV mapping derived from a single-slice measurements is often non-inferior compared to mean of mutiple views in diagnosing myocarditis: insights from the MyoRacer Trial

**C. Lücke[1], C. Wirsing[2], W. Rutschke[3], B. Foldyna[4], P. Seitz[1], K.-P. Rommel[5], R. Gohmann[1], K. Klingel[6], P. Lurz[5], M. Gutberlet.[1]**

[1]Heart Center Leipzig, Diagnostic and Interventional Radiology, Leipzig, Germany, [2]Klinikum Ludwigsburg, Institute for Diagnostic and Interventional Radiology, Ludwigsburg, Germany, [3]Klinikum St. Georg, Interdisciplinary Cental Emergency Room, Leipzig, Germany, [4]Heart Center Leipzig, Cardiovascular Imaging Research Center, Boston, United States of America, [5]Heart Center Leipzig, Clinic for Internal Medicine/Cardiology—University Hospital, Leipzig, Germany, [6]Universitätsklinikum Tübingen, Department for Pathology and Neuropathology, Tübingen, Germany.

**Purpose/Objectives** Parametric mapping aids the detection of myocarditis on cardiac magnetic resonance imaging (MRI) and is recommended by the revised Lake-Louise-Criteria [1]. We compared the diagnostic performance of single slice T1, ECV, and T2 mapping vs. mean of three separate measurements performed in two-chamber- (2CH), four-chamber- (4CH) views and midventricular short-axis-orientation (SA). Second aim was to find the slice orientation with the best diagnostic performance compared to endomyocardial biopsy (EMB).

**Methods & Materials** This study is a sub study of the prospective MyoRacer trial [2]. We selected patients with complete and excellent-image-quality datasets. Cardiac MRI was obtained using a 1.5 Tesla MRI scanner and standard imaging protocols including parametric mapping. The mapping sequences included native free-breathing navigator-gated multi-echo T2 mapping and T1 mapping, performed with a modified Look-Locker inversion recovery sequence (MOLLI) using a 3(3)5 scheme before and 15 min after contrast application (0.15 mmol/kg Gadobutrol). Mapping was acquired as single slices in 2CH, 4CH and SA orientations and measured on a dedicated cardiovascular MRI workstation (cmr42, version 5.1.0). The readers were blinded to the biopsy results. We compared the discriminative capacity of individual single-slice mapping measures with the means of multi-slice measures using ROC analysis and biopsy as standard of reference. Diagnostic performance was examined by using ROC analysis, comparison of the AUCs was performed by the DeLong method.

**Results** Among 88 included patients (20 (32%) women; 43 ± 12 years of age) 62 (70,4%) were EMB positive for myocarditis. For all T1, T2 and ECV measurements, areas under the curve (AUC) of the mean were always greater than the median, but no significant differences could be observed.

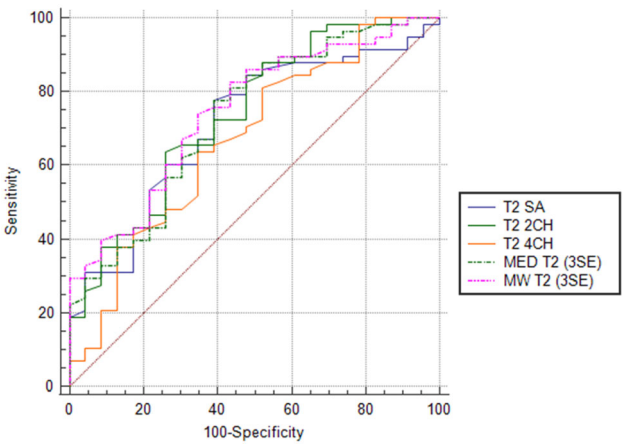


T2 ROC Analysis.

AUC for T2 mapping were 0.696 for the mean, 0.693 for SA, 0.671 for 2CH and 0.62 for 4CH and did not differ significantly $p > 0.125$.

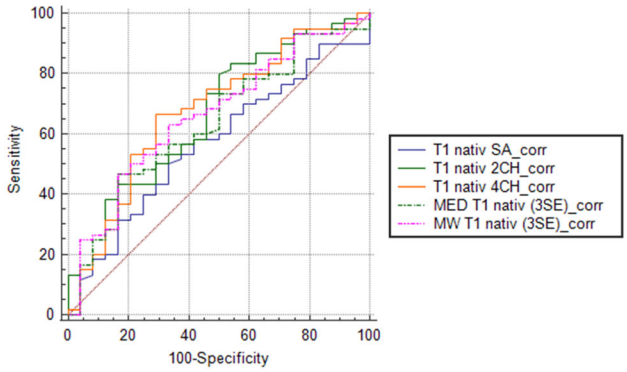


T1 native ROC Analysis.

AUC for T1 mapping were 0.667 for the mean, 0.667 for 4CH, 0.662 for the 2CH and 0.583 for the SA orientation. The difference between mean and SA was statistically significant p = 0.0256 (other differences p > 0.19).

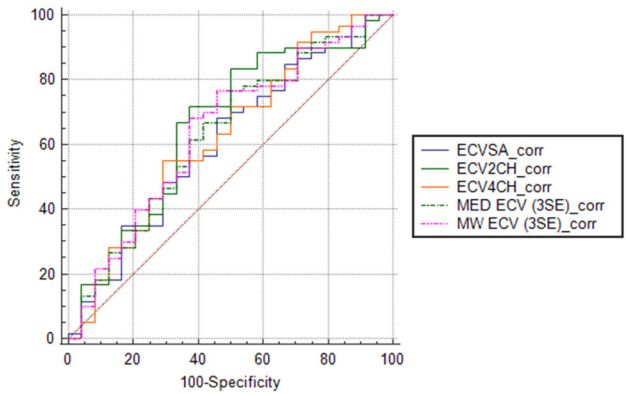


ROC Analysis of Extracellular volume (ECV).

AUC for ECV calculation were 0.667 for the mean, 0.635 for SA, 0.679 for 2CH and 0.629 for 4CH, not statistically significant (p > 0.18).

**Conclusion** Although the mean of three measurements performed in 2CH, 4CH and SA orientation shows the best diagnostic performance, even a single slice of native T1 or T2 Mapping or ECV-analysis delivers similar diagnostic accuracy in patients with suspected myocarditis. Long axis T1 mapping can however outperform a single slice T1 mapping in midventricular short axis orientation.

**Literature**

1. Vanessa M Ferreira, Jeanette Schulz-Menger, Godtfred Holmvang, Christopher M Kramer, Iacopo Carbone, Udo Sechtem, Ingrid Kindermann, Matthias Gutberlet, Leslie T Cooper, Peter Liu, Matthias G Friedrich, (2018), Cardiovascular Magnetic Resonance in Nonischemic Myocardial Inflammation: Expert Recommendations, J Am Coll Cardiol, 3158–3176, Dec 18;72(24), https://doi.org/10.1016/j.jacc.2018.09.072

2. Philipp Lurz, Christian Luecke, Ingo Eitel, Felix Föhrenbach, Clara Frank, Matthias Grothoff, Suzanne de Waha, Karl-Philipp Rommel, Julia Anna Lurz, Karin Klingel, Reinhard Kandolf, Gerhard Schuler, Holger Thiele, Matthias Gutberlet, (2016), Comprehensive Cardiac Magnetic Resonance Imaging in Patients With Suspected Myocarditis: The MyoRacer-Trial, J Am Coll Cardiol, 1800–1811, Apr 19;67(15), https://doi.org/10.1016/j.jacc.2016.02.013

## A-269

### Mind the arch: congenital abnormalities and malformations of the aortic arch

**F. Ramon Company[1], A. Arias Medina[1], E. R. Amador González[1], M. Gassió Riu[1], J. Roldán Busto[1], A. B. Marín Quiles[1], M. Á. Martín Martín[2]**

[1]Hospital Universitario Son Espases, Palma de Mallorca, Spain, [2]Clínica Rotger Quirónsalud, Palma de Mallorca, Spain.

**Purpose/Objectives** -To review cross-sectional imaging techniques used in the evaluation of the aortic arch. -To explain the different congenital arch anomalies and malformations we can find on a daily-basis, illustrating the most common ones and their clinical implications.—To emphasize the importance of diagnosing mediastinal vascular rings.


Mind the arch: Congenital abnormalities and malformations of the aortic arch.

**Methods & Materials** Carry out an educational review of the congenital arch anomalies focusing on MR angiography and CT angiography as the most important diagnostic tools. Show a pictorial review of the most frequent and clinically relevant congenital arch anomalies studied by our institution.

**Results** Abnormal development of the embryological arch system results in congenital aortic arch abnormalities [1]. Recognizing them is crucial for the radiologist since they can be associated with congenital heart disease as well as with chromosomal abnormalities.

They can also produce vascular rings in the mediastinum which are often misdiagnosed [2].
Cross-sectional imaging allows to perform high quality multiplanar reconstructions, helping clinicians and surgeons decide the best treatment option [3] [4].

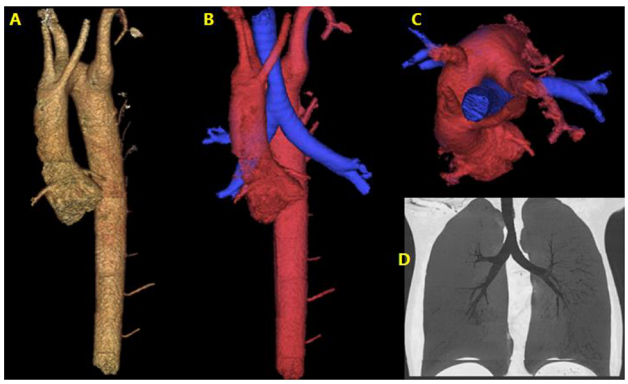


Asymptomatic 13-year-old boy with mild dyspnea, with known congenital anomaly of the aortic arch and interventricular communication. Volume-rendering (VR) CT angiography images (A, B and C) showed a right aortic arch, aberrant left subclavian artery and diverticulum of Kommerell. MinIP reconstructions (D) reveal tracheal compression.

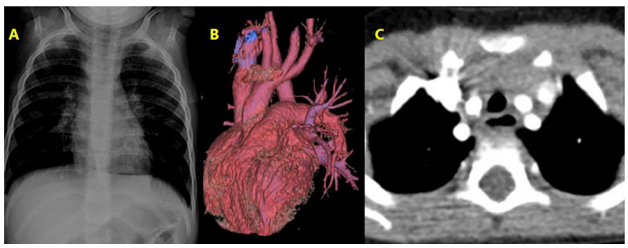


2-year-old girl. RX (A) incidentally revealed an abnormal mediastinal silhouette. CT angiography (B and C) demonstrated a right aortic arch with mirror image branching.

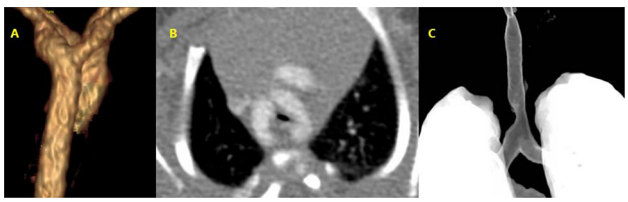


8-days-old newborn arrived to the emergency room with stridor. CT angiogram axial images (B) and volumetric reconstructions (A and C) showed a double aortic arch which was causing a vascular ring with an important tracheal compression.

**Conclusion** Congenital arch anomalies represent a diagnostic and therapeutic challenge, being CT-angiography the modality of choice for its diagnosis, classification and management.

**Literature**

1. Hanneman, Kate, Beverley Newman, and Frandics Chan, (2017), Congenital variants and anomalies of the aortic arch, Radiographics.

2. Gould SW, Rigsby CK, Donnelly LF, McCulloch M, Pizarro C, Epelman M., (2015), Useful signs for the assessment of vascular rings on cross-sectional imaging, Pediatr Radiol.

3. Ramos-Duran L, Nance JWJ Jr, Schoepf UJ, Henzler T, Apfaltrer P, Hlavacek AM, (2012), Developmental aortic arch anomalies in infants and children assessed with CT angiography, AJR.

4. Edward Y. Lee, Marilyn J. Siegel, Charles F. Hildebolt, Fernando R. Gutierrez, Sanjeev Bhalla and Juliet H. Fallah, (2004), MDCT Evaluation of Thoracic Aortic Anomalies in Pediatric Patients and Young Adults: Comparison of Axial, Multiplanar, and 3D Images, AJR.

## A-273

### Pulmonary atresia imaging: what to look for?

**A. Coutinho Santos[1], D. Martins[2], C. Saraiva[1]**

[1]Centro Hospitalar de Lisboa Ocidental, Radiology, Lisbon, Portugal, [2]Centro Hospitalar de Lisboa Ocidental, Pediatric Cardiology, Lisbon, Portugal.

**Purpose/Objectives**—To define and characterize pulmonary atresia, describing the spectrum of the condition and its associations.—To assess treatment options and potential complications of the disease.—To depict the main imaging features of pulmonary atresia variants and treatment procedures, focusing on the role of cardiac CT angiography and cardiac MR in the evaluation of these patients.
**Methods & Materials** Review of the literature and search in our imaging department database for pediatric and adult patients with the diagnosis of pulmonary atresia and related conditions, from 2015 to present.
**Results** Pulmonary atresia corresponds to absence of a communication between the right ventricle and the main pulmonary artery. It is a complex congenital heart disease with highly variable presentations and outcomes. It can be either isolated or in association with other congenital heart conditions and syndromes and is mainly divided in two entities, based on the presence or absence of a ventricular septal defect. These range of possibilities affect the prognosis and treatment strategies, which include catheter-based interventions and/or surgery correction. Although the initial diagnosis is made with echocardiography and the hemodynamic assessment through cardiac catheterization, cross-sectional imaging techniques provide important information for treatment planning and follow-up. The most relevant data include the evaluation of anatomy and size of pulmonary arteries (normal, hypoplastic, absent), the presence and distribution of major aortopulmonary collateral arteries (MAPCAs), cardiac chambers (namely the right ventricle and interventricular septum), patency of ductus arteriosus, and coronary arteries circulation. Cardiac CT angiography has an important role in this context as a non-invasive diagnostic tool for detailed characterization of the condition due to its high spatial resolution. It allows multiplanar and volumetric reconstructions, especially useful before surgery, and the study of lung parenchyma and congenital airway anomalies. MR is particularly helpful for the evaluation of ventricular volumes and function, flow quantification as well as for vascular anatomy through MR angiography. Both techniques can be used postoperatively, including for shunt and conduit patency assessment, but MR is preferred due to the absence of ionizing radiation.
**Conclusion** Pulmonary atresia includes a diverse spectrum of entities with different grades of complexity. Cardiac CT and MR are useful for characterization of pulmonary arteries and MAPCAs and to evaluate intra and extracardiac associated anomalies. Imaging

findings depend on each presentation; therefore, their knowledge is crucial to the description of results that support the decision making and treatment of each patient.

## A-278

### MRI assessment of the systemic right ventricle deformation: a cross-sectional study

M. Hrabak Paar[1,2], A. Gregov[2]

[1]University Hospital Center Zagreb, Department of Diagnostic and Interventional Radiology, Zagreb, Croatia, [2]University of Zagreb School of Medicine, Zagreb, Croatia.

**Purpose/Objectives** To compare the right ventricle (RV) strain parameters between patients with systemic RV (SRV) and individuals without structural heart disease.

**Methods & Materials** Cine steady-state free precession cardiac MRI sequences were acquired using a 1,5 T scanner in short- and long-axis views in 25 patients with SRV (16 with atrial switch repair for D-transposition of great arteries (TGA) and 9 with congenitally corrected TGA; age range 19–68, 13 males). The control group consisted of 25 individuals without structural heart disease (age range 10–73, 14 males). After performing routine RV MRI volumetry, mean longitudinal RV strain was measured on a 4-chamber view and mean circumferential RV strain from three short-axis images (basal, midventricular, and apical) based on feature tracking using Segment software (Medviso AB, Sweden). The strain parameters between patients with SRV and the control group were compared using an independent samples T-test.

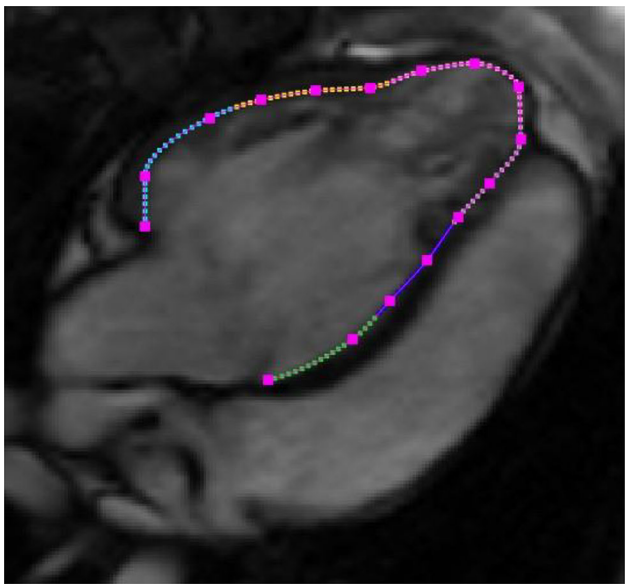

RV segmentation in a patient after atrial switch for TGA.

**Results** Patients with SRV, compared to the control group, had significantly higher RV indexed enddiastolic volume (122 ± 40 ml/m2 vs. 70 ± 9 ml/m2, $p < 0.001$), lower RV ejection fraction (EF, 45 ± 12% vs. 62 ± 6%, $p < 0.001$), and reduced mean longitudinal RV strain (-13.7 ± 3.6% vs. -21.6 ± 2.7%, $p < 0.001$).

| | SRV | Control group | p-value |
|---|---|---|---|
| Number of patients | 25 | 25 | |
| Age (years) | 33 ± 11 | 37 ± 21 | 0.404 |
| Gender (males/females) | 13/12 | 14/11 | 0.777 |
| RV EF (%) | 45 ± 12 | 62 ± 6 | < 0.001 |
| RV EDVi (ml/m2) | 122 ± 40 | 70 ± 9 | < 0.001 |
| RV mean longitudinal strain (%) | − 13.7 ± 3.6 | − 21.6 ± 2.7 | < 0.001 |
| RV basal circumferential strain (%) | − 13.1 ± 3.4 | − 14.2 ± 2.8 | 0.210 |
| RV midventricular circumferential strain (%) | − 12.6 ± 4.5 | − 14.9 ± 4.2 | 0.074 |
| RV apical circumferential strain (%) | − 12.0 ± 6.1 | − 17.9 ± 5.6 | < 0.001 |

Comparison between patients with systemic right ventricle and individuals from the control group without structural heart disease.

There was no relevant difference between mean circumferential SRV strain in the basal and midventricular plane, however in patients with SRV mean circumferential strain was reduced at the apical level (-12.0 ± 6.1% vs. -17.9 ± 5.6%, $p < 0.001$). Mean longitudinal RV strain was reduced in patients with preserved SRV EF (-16.0 ± 2.5%) as compared to the control group (-21.6 ± 2.7%) but was better than in patients with reduced SRV EF (-11.6 ± 3.3%, $p < 0.001$). The mean circumferential RV strain was significantly lower in patients with reduced SRV EF (-9.5 ± 2.3%) compared to those with preserved SRV EF (-15.2 ± 3.6%) and compared to the control group (-15.5 ± 3.2%), but it was not different between patients with preserved SRV EF and controls ($p < 0.001$).

**Conclusion** In patients with SRV, RV is enlarged and has decreased function compared to control subjects. Unlike mean circumferential RV strain, mean longitudinal RV strain is reduced even in patients with preserved SRV EF, so mean longitudinal RV strain could be an early indicator of SRV impairment and should be measured in patients with SRV.

## A-280

### Cardiac magnetic resonance in suspected acute COVID-19 myocarditis

E. Detorakis[1], C. Skiadas[2]

[1]University Hospital of Heraklion, Radiology, Department of Computed Tomography and Magnetic Resonance Imaging, Heraklion Crete, Greece, [2]University Hospital of Heraklion, Department of Computed Tompgraphy and Magnetic Resonance Imaging, Heraklion Crete, Greece.

**Purpose/Objectives** The aim of the present study is to underline the role of basic cardiac magnetic resonance (CMR) sequences in the evaluation of patients with suspected COVID-19 myocarditis.

**Methods & Materials** 46 patients with COVID-19 infection and suspected acute myocarditis were retrospectively included in the present study, including 36 males and 10 females of mean age 38 years. They all exhibit chest pain/discomfort with elevated levels of serum troponin. CMR study was performed within 8–20 days after acute onset of cardiac symptoms, in a1.5 T MR scanner (Siemens Magnetom 1.5 T). Image analysis was based on STIR, cineSSFP and late gadolinium enhancement (LGE) sequences. The extent of myocardial oedema and LGE was visually calculated. Statistical

analysis was performed using Student-t test and Chi-square test and a $p$ value of $< 0.05$ was considered statistically significant.

**Results** All 46 patients had elevated troponin levels ranging 0.04–0.42 ng/mL that returned to normal levels within 4–7 days after symptoms onset. CMR study revealed areas of myocardial oedema in 26/46 patients while LGE was detected in 32 patients. Inferior and inferolateral segments were involved in 24/32 (Fig. 1) and septal segments in 8 patients (Fig. 2) with subepicardial localization, while in 12 patients a concomitant mesocardial involvement was recorded (Fig. 3).

**Conclusion** Even in centers where the evaluation of extracellular volume (ECV), T1 and T2 mapping is impossible, STIR, cineSSFP and LGE sequences may safely depict myocardial involvement in COVID-19 myocarditis. Inferior, inferolateral and septal segments were mostly involved.

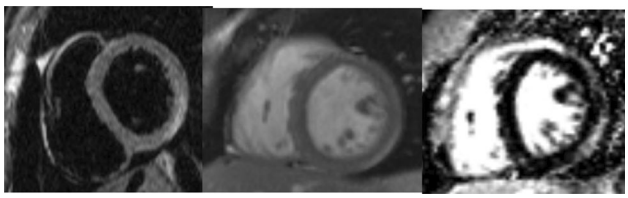

Subepicardial involvement of inferior and inferoseptal segments. (Left) Stir sequence showing myocardial oedema, (Middle) cine SSFP after i.v gadolinium administration depicting an area of high intensity signal, (Right) LGE revealing a myocardial scar, findings attributed to COVID-19 myocarditis.

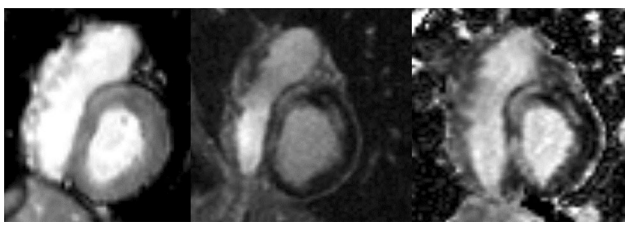

(Left) cineSSFP showing high intensity subepicardial to mesocardial region involving septal segments, (Middle) LGE involving septal segments and (Right) PSIR image depicting septal segments involvement of LGE.

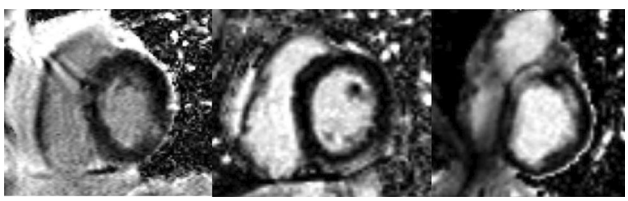

Three different patients having LGE in subepicardial to mesocardial distribution, attributed to COVID-19 myocarditis.

## A-283

### Anomalous solitary left coronary artery: a case report

**T. Nadarević[1], L. Bastijančić[2], I. Žuža[1], S. Kovačić[1], D. Miletić[1]**

[1]Clinical Hospital Center Rijeka, Department of Radiology, Rijeka, Croatia, [2]Clinical Hospital Center Rijeka, Department of Cardiology, Rijeka, Croatia.

**Purpose/Objectives** Coronary artery anomalies represent an uncommon finding of anomalous origin, course or termination of coronary arteries [1]. Their prevalence in general population is low, and clinically patients are asymptomatic or present with chest pain, dyspnea, arrhytmias, syncope, myocardial infarction or sudden death [2]. Computed tomography (CT) and invasive coronary angiography are the modalies of choice for their direct visualization and characterization [3]. We hereby present a case of an anomalous solitary left coronary artery detected by invasive coronarography and further characterized by CT coronary angiography.

**Methods & Materials** A 63-year old male with previous arterial hypertension suffered an out-of-hospital cardiorespiratory arest due to ventricular fibrilation and was succesfully reanimated. At emergency department admission, he was hemodinamically stable without chest pain. Electrocardiogram showed mild ST depression in lateral leads. An urgent invasive coronary angiography was performed which excluded obstructive coronary artery disease. However, an anomalous origin of the left coronary artery with atypical course was detected.

Atypical course of left coronary artery (arrows).

Right coronary artery (RCA) was dominant, without significant stenosis. Transthoracic echocardiogram showed preserved left ventricular ejection fraction and borderline interventricular septum thickness. In order to further evaluate the coronary anomaly, CT coronarography was performed.

**Results** Calcium scoring showed significant atherosclerotic burden (Ca score 1770, RCA alone 1580). RCA as a dominant artery showed normal anatomical origin and course, without significant stenosis. The left coronary artery originated from the right coronary sinus separately from RCA, and showed longitudinal intramyocardial course in the basal interventricular septum (IVS).

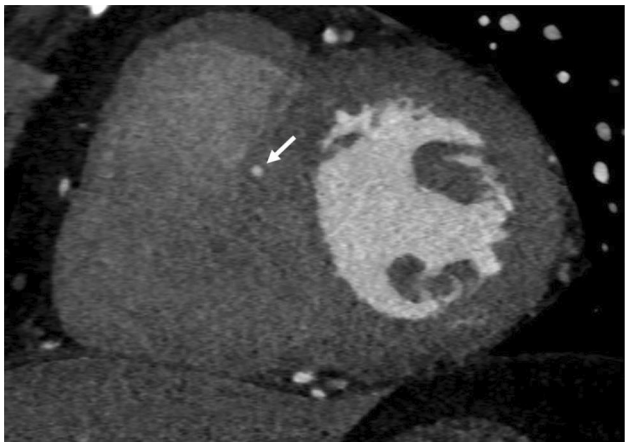

Intramyocardial course of solitary left coronary artery (white arrow).

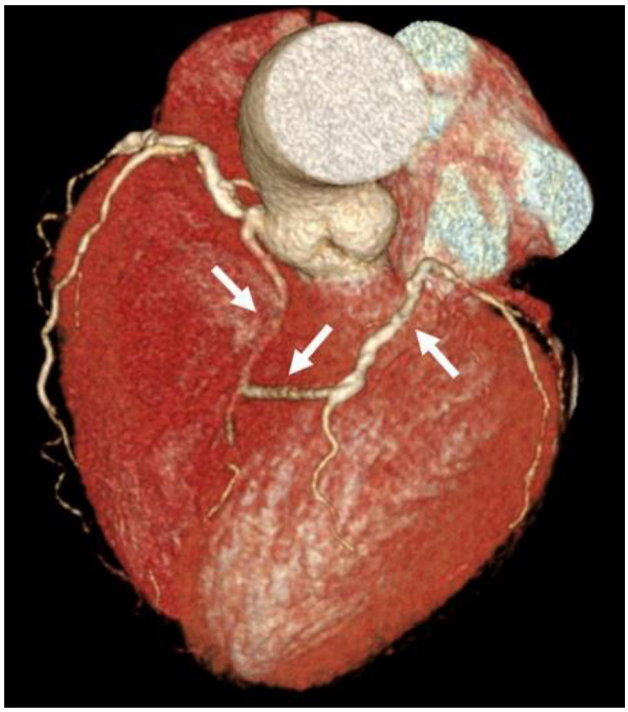

Solitary left coronary artery (white arrows).

In the mid IVS segment the artery angulated and coursed upwards to epicardial fat in the anterior interventricular groove. The artery continued to course through the basal third of the anterior interventricular groove and continued to the left atrioventricular groove.

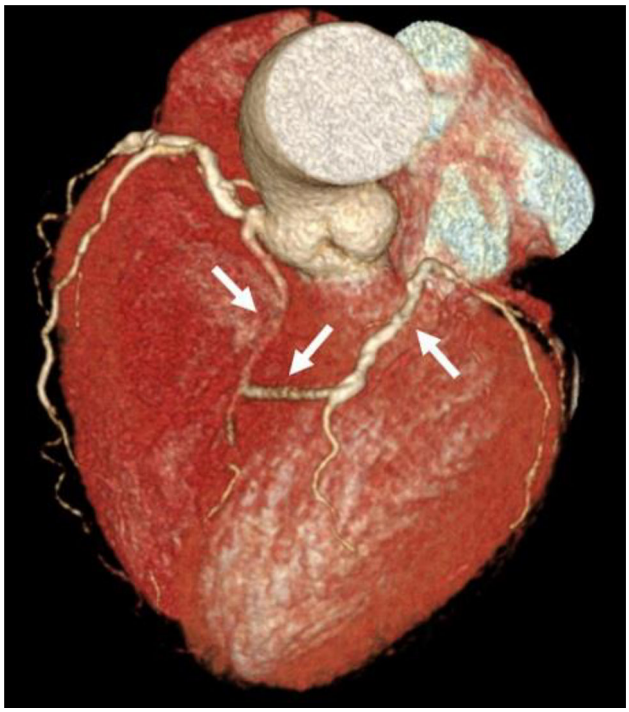

Solitary left coronary artery (white arrows).

No significant stenosis or occlusions were found. Following the definitive diagnosis, a cardioverter defibrilator was implanted as a measure of secondary sudden cardiac death prevention with optimal medical therapy. After discharge, patient was followed-up at 1 and 3 months and was clinically stable without episodes of arrhythmias or ICD activation.

**Conclusion** This case presents an uncommon coronary artery anomaly and shows the benefit of CT coronary angiography in its detailed anatomical evaluation.

**Literature**

1. Gentile F, Castiglione V, De Caterina R, (2021), Coronary Artery Anomalies, Circulation, 983–996.

2. Ali M, Hanley A, McFadden EP, et al., (2011), Coronary artery anomalies: a practical approach to diagnosis and management, Heart Asia, 8–12.

3. Frommelt P, Lopez L, Dimas VV, et al., (2022), Recommendations for Multimodality Assessment of Congenital Coronary Anomalies: A Guide from the American Society of Echocardiography: Developed in Collaboration with the Society for Cardiovascular Angiography and Interventions, Japanese Society of Ec, Journal of the American Society of Echocardiography, 259–294.

## A-285

### Investigation of the degree of coronary artery stenosis severity in individuals with zero coronary artery calcium

**T. Floros[1], E. Delaveridou[2], G. Tsiaousis[3], O. Furmaga[2], A. Kallifatidis[4], E. Alexiou[1], K. Michailidis[5], M. Vlychou[6]**

[1]General Hospital Larisa, Radiology, Larisa, Greece, [2]Papanikolaou General hospital, Radiology, Thessaloniki, Greece, [3]Private Cardiology Practice, Cardiology, Kastoria, Greece, [4]St Lukes Hospital, Radiology, Thessaloniki, Greece, [5]Cardiac Intelligence, Ptolemaida, Greece, [6]University of Thessaly, Radiology, Larisa, Greece.

**Purpose/Objectives** Coronary artery calcium (CAC) score has a well established predictive value for cardiovascular disease and zero CAC score is considered the best single predictor of prognostic factor of a low overall risk for severe atherosclerosis. The aim of our study was to investigate the negative prognostic value of zero CAC score both separately and compared to other CAC score subgroups.

**Methods & Materials** Individuals with zero CAC, included in a cohort of approximately 4,000 patients undergoing Cardiac Computed Tomography Angiography (CCTA) in our institution, were prospectively studied. Both asymptomatic and symptomatic patients (I.e., atypical angina, uncertain stress test result) were enrolled. Zero CAC score population was checked for the presence and the severity of coronary artery stenosis, symptoms, medical history.

**Results** Zero CAC individuals formed a study sample of 1525 and were predominantly male (56,6%), and 52,78 ± 11,2 years of age. Half of them were asymptomatic, while another 39% had atypical chest complaints. Only 7 participants (0,5%) had a critical coronary stenosis (CADRADS 4 and above) and 32 (2,2%) had a moderate stenosis. Among zero CAC population, a history of diabetes mellitus ($p < 0,001$, 95,0% CI 0,101–0,277) and smoking ($p = 0,03$, 95,0% CI 0,006–0,113) independently predicted and with statistical significance, the advancing degree of coronary stenosis. Additionally, diabetes ($p = 0,001$, 95,0% CI 3,348–142,656) and an abnormal treadmill stress test ($p = 0,008$, 95,0% CI 2,598 -647,090) predicted independently the presence of a critical stenosis.

**Conclusion** Our results further support the current knowledge of low overall cardiovascular risk in the zero CAC group, without, however, completely excluding the presence of critical stenosis. Diabetes, smoking, and an abnormal treadmill stress test show a significant predictive value for the presence and the severity of coronary stenosis in this subgroup, although additional large scale studies are required to corroborate our results.